



**NTNU – Trondheim**  
Norwegian University of  
Science and Technology

# Simulation Program for Stability Analysis of Hydropower Plants

**Simen Nordre Vogt-Svendsen**

Product Design and Manufacturing

Submission date: June 2012

Supervisor: Torbjørn Kristian Nielsen, EPT

Norwegian University of Science and Technology  
Department of Energy and Process Engineering



EPT-M-2012-92

**MASTER THESIS**

for

Stud.techn. Simen Vogt-Svendsen

Spring 2012

**Simulation program for Stability Analysis of hydro power plants***Simuleringsprogram for stabilitetsanalyser av vannkraftverk***Background and objective**

Norwegian hydro power plants are subjected to thorough analyses with respect to governor stability. There are several methods for performing simulations of governor stability. During his project work, the student has established a model based on the Matrix Method where the conduit system, turbine and governor are represented. The Master thesis will be a continuance and refinement of the code established in the project work.

Topics to be addressed are turbine characteristics, alternative governor algorithms and frictional damping.

**The following tasks are to be considered:**

- 1 Incorporate a complete turbine model where the turbine characteristics are better represented
- 2 Investigate alternative schemes for representing alternative frequency governors
- 3 Formulate and include a more precise friction model to better reflect the actual frictional damping
- 4 Develop the program code for more general conduit system geometry representation

-- " --

Within 14 days of receiving the written text on the master thesis, the candidate shall submit a research plan for his project to the department.

When the thesis is evaluated, emphasis is put on processing of the results, and that they are presented in tabular and/or graphic form in a clear manner, and that they are analyzed carefully.

The thesis should be formulated as a research report with summary both in English and Norwegian, conclusion, literature references, table of contents etc. During the preparation of the text, the candidate should make an effort to produce a well-structured and easily readable report. In order to ease the evaluation of the thesis, it is important that the cross-references are correct. In the making of the report, strong emphasis should be placed on both a thorough discussion of the results and an orderly presentation.


The candidate is requested to initiate and keep close contact with his/her academic supervisor(s) throughout the working period. The candidate must follow the rules and regulations of NTNU as well as passive directions given by the Department of Energy and Process Engineering.

Risk assessment of the candidate's work shall be carried out according to the department's procedures. The risk assessment must be documented and included as part of the final report. Events related to the candidate's work adversely affecting the health, safety or security, must be documented and included as part of the final report.

Pursuant to "Regulations concerning the supplementary provisions to the technology study program/Master of Science" at NTNU §20, the Department reserves the permission to utilize all the results and data for teaching and research purposes as well as in future publications.


The final report is to be submitted digitally in DAIM. An executive summary of the thesis including title, student's name, supervisor's name, year, department name, and NTNU's logo and name, shall be submitted to the department as a separate pdf file. Based on an agreement with the supervisor, the final report and other material and documents may be given to the supervisor in digital format.

Department of Energy and Process Engineering, 10. January 2012



---

Olav Bolland  
Department Head



---

Torbjørn K. Nielsen  
Academic Supervisor

## **Preface**

This master thesis has been written at the Waterpower Laboratory, Department of Energy and Process Engineering at the University of Science and Technology during the spring of 2012. The aim of the project has been to develop a simulation program for stability analysis of hydropower systems.

I wish to acknowledge the help and inspiration from my supervisor, professor Torbjørn Nielsen. I am also indebted to Post Doc Pål-Tore Storli for readily being available to help me tackle some of the challenges of hydro power system stability.

It is also my duty to record my thankfulness to the students at the Hydropower laboratory for good discussion and advises throughout this project. Finally, I take this opportunity to acknowledge the great environment for learning and inspiration that exist among the students, Phd-candidates, professors and staff at the Waterpower Laboratory. This master thesis concludes my engineering studies at NTNU, a period of life I truly have enjoyed!

Simen Vogt-Svendsen  
Trondheim, June 7, 2012



## **Abstract**

Over the last few years Norway has seen an increasing number of hours where the grid frequency exceeds the required limits (49.9-50.1Hz). To improve this situation one alternative is to implement hydropower governing with quicker response time. However, long conduits and oscillatory flow set strict requirements to the hydropower system stability and turbo set governing. This thesis establishes a simulation program based on the structure matrix method for stability analysis of hydropower systems.

The method is implemented in a Matlab program to study the oscillatory flow in the frequency domain. Implementation of frictional influence, turbine characteristics, and alternative governing has been given special attention. The program is validated through comparison with measurements and previous analysis at Kongsvinger and Tafjord power plants. The program simulations generally compare well with physical dynamics of the two systems. Further a stability analysis of speed governing at Aldal power plant has been performed. Finally some alternative control systems are discussed.

## Sammendrag

I de senere årene har det norske elektriske nettet operert med et økende antall timer utenfor det tillatte frekvensområdet (49.9-50.1Hz). For å forbedre denne situasjonen kan regulerings-systemer for vannkraft med raskere responstid implementeres. Lange vannveier og oscillerende strømninger setter strenge krav til stabilitet og turbinregulering. Denne hovedoppgaven etablerer et simuleringsprogram basert på strukturmatisemetoden for stabilitetsanalyser.

Metoden er implementert i Matlab for å undersøke oscillerende strømninger i frekvensplanet. Implementeringen av friksjonsinnvirkning, turbinkarakteristikker, samt alternative reguleringsformer er viet spesiell oppmerksomhet. Programmet er validert gjennom sammenligning av målinger og tidligere analyser av vannkraftanleggene Kongsvinger og Tafjord. Simuleringsprogrammet samsvarer generelt godt med den fysiske dynamikken i de to systemene. Videre er forholdene ved det foreslåtte vannkraftverket Aldal undersøkt ved å anvende simuleringsprogrammet og generelle stabilitetskriterier. Noen alternative former for regulering er avslutningsvis diskutert.



# Table of Contents

Preface.....	I
Abstract.....	III
Sammendrag.....	IV
Table of Contents.....	V
List of Figures.....	VII
List of Tables.....	VIII
Nomenclature.....	IX
1 Introduction.....	1
2 Hydropower model.....	2
2.1 Governing equations.....	2
2.2 Analytical approach.....	5
3 The Structure Matrix Method.....	8
3.1 The governing element matrices.....	8
3.1.1 Pipes and tunnels.....	9
3.1.2 Throttles and valves.....	10
3.1.3 Surge shafts.....	11
3.1.4 PID governor.....	11
3.1.5 Generator system.....	13
3.1.6 Permanent speed droop.....	13
3.1.7 Turbine self-governing.....	14
3.2 Turbine.....	14
3.2.1 The turbine characteristics algorithm.....	18
4 Matlab program.....	20
4.1 General description.....	20
4.1.1 Input.....	20
4.1.2 Output.....	21
4.2 System stability.....	23
4.2.1 System stability criteria.....	24
4.2.2 Transfer function program.....	25
5 The frictional damping factor.....	26

5.1	Browns Model.....	27
5.2	Brekkes model .....	28
5.3	The frictional subroutine.....	29
6	Program Validation.....	31
6.1	Kongsvinger hydro power plant.....	31
6.2	Tafjord hydropower plant .....	37
6.2.1	The damping factor .....	41
7	Model Application .....	43
7.1	Aldal powerplant .....	43
8	Hydropower governor control.....	49
8.1	Classical control approach.....	49
8.1.1	Water column compensator .....	50
8.1.2	Pressure compensator .....	51
8.2	Optimal control (LQR og MPC).....	53
9	Discussion .....	56
10	Conclusion .....	57
11	Further work.....	58
12	Bibliography.....	59
	Appendix A Hydropower model.....	62
	Appendix B General Matrix Representation.....	78
	Appendix C Turbine Characteristics.....	80
	Appendix D Stability plots .....	82
	Appendix E Transfer functions.....	84
	Appendix F Full size plots.....	88

## List of Figures

Figure 2.1 A basic hydropower system.....	2
Figure 3.1 Modified Kværner PI-governor.....	11
Figure 3.2 Block diagram representation of a parallel PID-governor.....	12
Figure 3.3 Turbine characteristics diagram (Xinxin & Brekke, 1988).....	16
Figure 3.4 Turbine characteristics routine.....	18
Figure 3.5 Surface plot, $Y = 5-6\text{deg}$ .....	19
Figure 4.1 General hydropower system.....	20
Figure 4.2 Matlab program flowchart.....	22
Figure 4.3 Block diagram of a hydropower system with feedback.....	23
Figure 4.4 Simplified block diagram representation.....	24
Figure 5.1 The ratio $C$ .....	27
Figure 5.2 Simulation flowchart for determining system damping.....	30
Figure 6.1 Kongsvinger power plant layout.....	31
Figure 6.2 $p/y$ plot and measurements for Kongsvinger.....	33
Figure 6.3 The frictional damping constants in the draft tube gate shaft.....	34
Figure 6.4 $p/y$ plot including the Brown friction model.....	35
Figure 6.5 $n/n_{\text{ref}}$ stability analysis.....	35
Figure 6.6 $n/n_{\text{ref}}$ stability analysis.....	36
Figure 6.7 Tafjord power plant layout.....	37
Figure 6.8 $h/y$ response with Brown friction model.....	39
Figure 6.9 Friction damping, $K$ (surge shaft).....	40
Figure 6.10 $n/n_{\text{ref}}$ stability analysis.....	40
Figure 6.11 Influence of friction model scaling.....	42
Figure 7.1 Simplified system layout of Aldal.....	43
Figure 7.2 Bode diagram based on transfer function.....	45
Figure 7.3 $b_t$ and $T_d$ envelope (ref. Appendix E).....	45
Figure 7.4 Aldal $n/n_{\text{ref}}$ stability study.....	48
Figure 7.5 $n/P_{\text{gen}}$ response for Aldal.....	48
Figure 8.1 Water column compensator.....	50

Figure 8.2 Effect of water level governor on Aldal .....	51
Figure 8.3 Governor with integrated compensator.....	52
Figure 8.4 Effect of pressure compensator on Aldal.....	53
Figure 8.5 Model Predictive Control (Imsland, 2010).....	54

## List of Tables

Table 2.1 Governing system equations.....	5
Table 3.1 Turbine Characteristics .....	15
Table 6.1 Main dimensions according to Figure 6.1 .....	32
Table 6.2 Turbine and governor settings.....	32
Table 6.3 Geometrical data related to Figure 6.7 .....	37
Table 6.4 Tafjord turbine and governor characteristics .....	38
Table 7.1 Turbine characteristics (Jørundland) and governing of Aldal .....	46

## Nomenclature

$A$	cross sectional area [m]	$T_d$	integrating time constant [s]
$A_{eqv}$	free surface area [m]	$T_w$	hydraulic inertial time constant for the water conduit [s]
$a$	wave propagation speed [m/s]	$T_{ws}$	capacity time constant of surge shaft [s]
$b_p$	permanent speed droop	$T_{wt}$	water starting time constant of the tunnel [s]
$b_s$	turbine self-regulation constant	$t$	time [s]
$b_t$	temporary speed droop	$v$	mean fluid velocity [m/s]
$D$	Pipe diameter [m]	$x$	length-wise position [m]
$f$	Darcy-Weisbach friction factor	$y$	relative valve movement, $\Delta Y/Y_0$
$g$	gravitational constant [9.81 m/s <sup>2</sup> ]	$z$	LaPlace flow identity
$H$	head [m]	$\mu_y$	flow coefficient
$H_0$	mean reference head at turbine [m]	$\lambda$	friction factor
$h$	relative head deviation, $\Delta H/H_0$	$\omega$	frequency/angular speed of the turbine [rad/s]
$h_w$	Allievis constant, $aQ_0/(2gH_0A)$		
$K$	frictional damping coefficient		
$K_{comp}$	Modulus of compressibility [Pa]		
$K_D$	derivative constant, governor		
$K_I$	integral constant, governor		
$K_P$	proportionality constant, governor		
$L$	pipe length [m]		
$M$	Manning's number		
$n$	relative turbine speed, $\Delta\omega/\omega_0$		
$n_{ref}$	incremental reference speed setting		
$P_{ref}$	incremental reference power setting		
$Q_t$	flow rate in regarded pipe [m <sup>3</sup> /s]		
$Q_0$	mean reference flow rate at turbine [m <sup>3</sup> /s]		
$q$	relative flow deviation, $\Delta Q/Q_0$		
$s$	Laplace operator		
$T_a$	mechanical inertial time constant of the rotating masses [s]		



# 1 Introduction

Over the last decade the Norwegian electrical power system has seen increasing fluctuations in grid frequency (Lindeberg, 2010). A changing energy mix in Europe increase the need of Norway's vast energy capacity stored in hydropower systems. Thus a closer connection to the european electrical grid is expected in the future. Grid frequency fluctuations will as a consequence likely continue to give rise to concern (Eek, et al., 2006). Hydropower systems balance the grid power requirement and the available hydraulic power while maintaining the rotational speed synchronous. Hydropower systems provide quick power regulations on demand, but may often have complex and long conduits. Oscillatory flow and resonance in the conduits set strict requirements to the system stability analysis and turbo set governing.

To address this challenge a strong demand is placed on accurate mathematical modeling of the physical system dynamics. This thesis is a continuance of the authors project thesis (Vogt-Svendsen, 2011). The aim of this thesis is to develop and refine a simulation program to investigate the dynamics and governing of hydropower systems. The simulation program is based on the structure matrix model. The following approach is taken:

## **Governing system equations - *chapter 2***

The equations describing the various sections of the system are established.

## **System model - *chapter 3 and 4***

Mathematical implementation of hydropower systems by the structure matrix method in Matlab is outlined.

## **Modeling turbine and friction - *chapter 4 and 5***

Challenges related to including the turbine characteristics and system friction are addressed.

## **Validation - *chapter 6***

The simulation results have been compared to measurements at the Kongsvinger and Tafjord hydropower systems to validate the Matlab simulation program.

## **Application - *chapter 7***

A proposed hydropower system at Aldal is investigated with respect to layout and frequency stability.

## **Alternative control strategies - *chapter 8***

Pressure compensator, water column compensator and Model Predictive Control have been investigated as examples of alternative control strategies.

## 2 Hydropower model

A stability analysis of hydropower systems is based on the governing equations of the system. Equilibrium balance equations based on principles of hydraulic continuity and motion characterize the water conduits. Along with power transmission and inertial equations for the power conversion, the systems physics are captured. In the following are derivations of the differential and LaPlace transformed equations of the system structures. Some analytical equations are presented before the structure matrix model is established and discussed in the subsequent chapter.

### 2.1 Governing equations

A study of dynamic hydro power systems can briefly be divided into four major units: tunnels, surge shafts, turbine unit and governor. Each of these elements can be described by individual characteristic equations. A simplified representation of a hydropower system is displayed in figure 2.1 below. In the subsequent paragraphs the differential equations for each element will be specified (Nielsen, 1990).

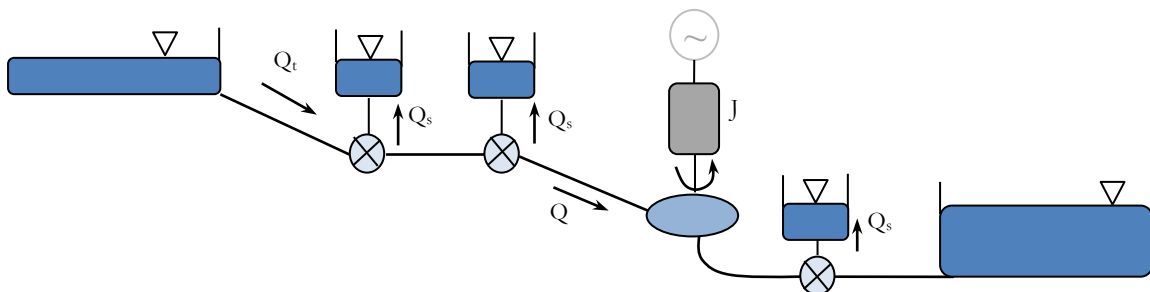


Figure 2.1 A basic hydropower system

If the height is defined as the hydraulic head and position relative to a reference, the pipe flow can be described by the continuity equation and the equation of motion:

$$\frac{\partial H}{\partial t} + \frac{a^2}{g} \frac{\partial v}{\partial x} = 0 \quad 2.1$$

$$g \frac{\partial H}{\partial x} + \frac{\partial v}{\partial t} + \lambda \frac{v \cdot |v|}{2D} = 0 \quad 2.2$$

The speed of sound is an elementary quantity in the modeling of an elastic hydropower system. The wave propagation speed is defined by  $a = \sqrt{K/\rho}$  where  $K$  is the modulus of



compressibility and  $\rho$  is the mass density of water. A force applied to a section of water will result in a compression analogous to a spring-mass system (elastic hydraulic system).

The model for hydraulic losses along the pipe is related to the volumetric flow rate squared ( $Q^2$ ). Due to this relation the frictional damping vanishes close to stationary flow conditions. This model also assumes fully developed, turbulent flow profile. This assumption does not necessarily reflect the real water conduits and in general this approach will underestimate the damping effect from the frictional forces. The tunnel hydraulics take the equilibrium balance:

$$\frac{L_t}{gA_t} \frac{dQ_t}{dt} + \Delta H + \frac{fL_t Q_t^2}{2gDA_t^2} = 0 \quad 2.3$$

To simplify the equation, the variables can be non-dimensionalized or scaled:

$$T_{wt} = \frac{L_t}{gA_t} \quad h = \frac{\Delta H}{H_0} \quad q = \frac{\Delta Q}{Q_0} \quad K_t = \frac{fL_t v_0^2}{2gDH_0}$$

Applying the simplified entities above to the tunnel in equation 2.3 :

$$T_{wt} \frac{dq_t}{dt} + h + K_t q_t = 0 \quad 2.4$$

Similarly, for the penstock:

$$T_w \frac{dq_t}{dt} + h - h_s + K_{pr} q = 0 \quad 2.5$$

The continuity equation connecting the pipe and the surge shaft is mathematically given by:

$$Q = q + Q_s = q + A_s \frac{dz}{dt} = q + A_s \frac{1}{A_s} (Q - q) \quad 2.6$$

Further, if the time constant is defined by:

$$T_{ws} = \frac{A_s H_0}{Q_0}$$

Then equation 2.6 becomes:

$$T_{ws} \frac{dh_s}{dt} = q_s = q_t - q \quad 2.7$$

The equilibrium balance of the surge shaft can be represented by a differential equation in a similar manner as the tunnel and penstock above:

$$T_{ws} \frac{dq_s}{dt} + h_s + K_s q_s = 0 \quad 2.8$$

If  $T_{ws} \ll 1$  is assumed, the first term can be neglected. Equation 2.4, 2.5, 2.7 and 2.8 define the entire water conduit system. The turbine converts the hydraulic power it is exposed to into rotating mechanical power. The hydraulic power is converted to electrical power, acceleration of the rotating masses and losses arising from the energy conversion:

$$J\omega \frac{d\omega}{dt} = P_h - P_N - loss \quad 2.9$$

If the generator unit is included in the basic differential equation for turbine operation, the power produced by a turbine is (Wylie & Streeter, 1993):

$$P = \eta \rho g Q H = I\omega \frac{d\omega}{dt} + P_G \quad 2.10$$

Where  $\eta$  is the turbine efficiency,  $I$  is the polar moment of inertia ( $I = WR_g^2/g$ ),  $\omega$  is the rotational speed of the turbine and  $P_G$  is the power absorbed by the generator. If  $E_n$  is set to represent the statics of the generator, then the differential equation of the generator is:

$$T_a \frac{dn}{dt} + E_n \cdot n = P \quad 2.11$$

The governor controls the hydraulic system so that the rotational speed is maintained at synchronous speed regardless of the grid power requirement. In order to efficiently control the hydropower system a PID-governor can be applied. The intake valve opening is controlled by a proportional, differential and integral term according to the PID-equation (Nielsen, 1990):

$$\frac{dY}{dt} = -K_P \frac{dn}{dt} + \frac{K_D}{T_d} (n_{ref} - n) - K_I T_N \frac{d^2n}{dt^2} \quad 2.12$$

Where  $Y$  is the opening,  $n$  is the rotational speed,  $K_P$  is the proportionality constant,  $T_d$  is the time constant for the integral term,  $T_N$  is the time constant for the derivative term. The latter term must also be limited by a filter constant,  $T_f$ . However, in classical governing of hydro power systems the derivative term is normally not included.

The differential equations for each section of the system are summarized in Table 2.1. If the systems differential equations are Laplace transformed the equations in the right

column of the table are obtained. The subscript i has been introduced to indicate that the equations are applied to multiple individual sections of a system. The Laplace transformed equations facilitate construction of transfer functions for the dynamic system.

*Table 2.1 Governing system equations*

Section	Eqn	Differential equation	Laplace transformed equation
Tunnel	2.4	$T_w \frac{dq_t}{dt} + h - h_s + K_{pr}q = 0$	$T_{wti}q_{ti} \cdot s + h_{si} + K_{ti}q_{ti} = 0$
Penstock	2.5	$T_w \frac{dq_t}{dt} + h - h_s + K_{pr}q = 0$	$T_wq \cdot s + h - h_s + K_{pr}q = 0$
Surge shaft	2.7	$T_s \frac{dh_s}{dt} - q_s = 0$	$T_{si}h_{si} \cdot s + q_{ti} - q = 0$
Surge shaft inertia	2.8	$T_{ws} \frac{dq_s}{dt} + h_s + K_s q_s = 0$	$T_{ws}q_{si} \cdot s + K_{si}q_{si} + h_{si} = 0$
Generator	2.11	$T_a \frac{dn}{dt} + E_n \cdot n = P$	$\mu = \frac{\Delta n}{n} = \frac{\Delta P}{P_0} \frac{1}{T_a s + E_n}$
Governor	2.12	$\frac{dY}{dt} = -K_p \frac{dn}{dt} + \frac{K_D}{T_d} (n_{ref} - n) - K_I T_N \frac{d^2n}{dt^2}$	$y = K_p + \frac{K_I}{s} + K_D s = \frac{1 + T_d \cdot s}{b_t T_d \cdot s} \mu$

## 2.2 Analytical approach

During initial planning of hydro power systems, analytical equations are often applied in order to study the system behavior. Some rules of thumb have been developed along with the regarded equations. A selection of the most relevant approaches are presented in the following section, which is based on references by Nielsen (1990) and Brekke (1999).

The time constant of the water conduit is an important quantity, which considers the elements between two free water surfaces according to the relation:

$$T_w = \frac{Q_0}{gH_0} \sum \frac{L}{A} \quad 2.13$$

The inertia of the rotating masses (primarily turbine and generator) acts as a dampening element to alternating water flows. Thus for stable operation of the system, the inertial time constant of the rotating masses ( $T_a$ ) should be significantly larger than the time constant of the water conduit ( $T_w$ ):

$$\frac{T_a}{T_w} > 6 \quad 2.14$$

If the ratio of the rotating masses to water conduit time constant is not achieved either the pipes' length-to-cross sectional area ratio can be altered or surge shafts introduced. Of the two options the latter is generally the only practically feasible solution. When surge shafts are introduced the water surface must fulfill the Thoma criterion, which is defined as:

$$A_T = 0.0083 \cdot \frac{M^2 A^{5/3}}{H_0} \quad 2.15$$

This identity is based on Newton's second law, continuity and ideal governing<sup>1</sup>. In order to ensure dampened oscillations between shaft and reservoir, a minimum free water surface area in the surge shaft is required. The surge shafts free water surface has to be at least equal to the Thoma-area for stable u-pipe oscillations<sup>2</sup>. The amplitude and frequency of the u-pipe oscillations can be estimated by the following formulas:

$$\Delta z = \Delta Q \sqrt{\frac{\sum \frac{L}{A}}{gA_s}} \quad 2.16$$

$$\omega = \sqrt{\frac{g}{A_s \sum \frac{L}{A}}} \quad 2.17$$

The frequency-value of the u-tube oscillations will be estimated and compared with the simulations as they often appear in the Bode diagrams of hydropower systems. The maximum pressure rise directly upstream the turbine can be estimated by equation 2.18.

---

<sup>1</sup> Derived in (Brekke, 1999, p. 52)

<sup>2</sup> Usually  $1.5 \cdot A_T$  is set as a guiding criterion

$$\Delta h = \frac{a\Delta c}{g} \cdot \frac{T_r}{T_L} \quad 2.18$$

Where  $T_r$  is the reflection time for the first harmonic defined by:

$$T_r = \frac{4L}{a} \quad 2.19$$

These approximations are applied to validate some of the computational results.

### 3 The Structure Matrix Method

The structure matrix method was first introduced into hydropower system stability studies by Brekke (Brekke, 1984). The method was later popularized and generalized by Li Xinxin (Xinxin, 1988). This section is mainly based on these two references. Finally the construction of complete system geometries is developed in order to illustrate the approach and establish a numerical model.

The method is a mathematical model for stability study of hydro power systems. The structure matrix approach has its origin in solid structural analysis. The method differs only organizationally to the transfer or impedance method, but its computer-oriented procedure is simpler. Matrix equations describing the individual components of the system can with little effort be interconnected as the flow direction is defined out of each component. Thus this building block arrangement has its obvious advantages in the data structure for a computer assisted analysis.

The structure matrices involve element matrices, representing the individual valves, pipes, surge shafts, turbines etc. Element matrices may be combined and interconnected into a representation of a group of elements. This is known as a local structure matrix. By incorporating the element and local structure matrices one can obtain the global structure matrix, which represents the complete hydropower system. The element, local and global matrices are represented by the system matrix  $A$  in the matrix equation on general form:

$$\mathbf{A}(s) \cdot \mathbf{h} = \mathbf{q} \quad 3.1$$

Where  $\mathbf{A}$  is a matrix ( $m$  by  $n$ ) and  $\mathbf{h}$  ( $n \times 1$ ) and  $\mathbf{q}$  ( $m \times 1$ ) are vectors of length  $n$  and  $m$  respectively. In this equation  $\mathbf{h}$  is the “pressure head vector” and  $\mathbf{q}$  the “flow vector”. Chapter 3.1 will address how the governing equations are formulated and included into these matrices.

#### 3.1 The governing element matrices

In order to construct the global structure matrix each element and local structure in the system must be established. In this section the element matrices are derived and then approximations of some of the physical behaviors are explained. The following section is based on the theoretical derivation from Xinxin (1988) (1989) and Brekke (1999) (1984). The element and local structure matrices will take the form of the differential equation and are based on the governing equations of the relevant element.

### 3.1.1 Pipes and tunnels

The equation of motion and the continuity equation can be organized as follows:

$$\frac{\partial h}{\partial x} = \frac{Q_0}{H_0 A g} (s + K) q \quad 3.2$$

$$\frac{\partial q}{\partial x} = \frac{H_0 A g}{Q_0 a^2} s h \quad 3.3$$

The damping coefficient,  $K$ , is linearized at steady state and defined as:

$$K = gA \left( \frac{dh_f(Q)}{dQ} \right)_0 \quad 3.4$$

It should be noted that a range of challenges arise due to the modeling of the damping term  $K$ . These challenges will be studied closer in chapter 5. The identity  $z = (s^2 + Ks)^{1/2}$  can now be introduced to obtain the differential equation :

$$\frac{\partial^2 h}{\partial x^2} - \frac{z^2}{a^2} h = 0 \quad 3.5$$

The general solutions of  $h$  and  $q$  then become:

$$h = \alpha_1 e^{\frac{x}{a} z} + \alpha_2 e^{-\frac{x}{a} z} \quad 3.6$$

$$q = \frac{1}{2h_w} \frac{s}{z} \left( \alpha_1 e^{\frac{x}{a} z} - \alpha_2 e^{-\frac{x}{a} z} \right) \quad 3.7$$

Where  $h_w = Q_0 a / 2A g H_0$ , known as Allievis' constant. The most common element matrix is based on the equations for a pipeline section. If the boundary conditions for a pipe section are set to specific pressure and flow values at both ends the matrix equation describing the section can be expressed as:

$$\begin{bmatrix} -T & S \\ S & -T \end{bmatrix} \cdot \begin{bmatrix} h_L \\ h_R \end{bmatrix} = \begin{bmatrix} q_L \\ q_R \end{bmatrix} \quad 3.8$$

Where the flow is defined out of the pipe section and:

$$T = \frac{s}{2h_w s \tanh\left(\frac{L}{z} a\right)} \quad 3.9$$

$$S = \frac{s}{2h_w s \sinh\left(\frac{L}{z} a\right)} \quad 3.10$$

### 3.1.2 Throttles and valves

The matrix representation of the pressure and flow across a point element, such as a throttle, is:

$$\begin{bmatrix} -\frac{1}{K_p} & \frac{1}{K_p} \\ \frac{1}{K_p} & -\frac{1}{K_p} \end{bmatrix} \cdot \begin{bmatrix} h_L \\ h_R \end{bmatrix} = \begin{bmatrix} q_L \\ q_R \end{bmatrix} \quad 3.11$$

$K_p$  is a function of the loss constant, steady state flow as well as the smaller and larger area of the throttling point. This equation should typically be included for pipe intersections and rapid changes in cross-sectional area. However this term will dampen the oscillations and neglecting these throttling points will give a conservative stability simulation. The throttling element equation is analogous to a locked valve. On the other hand the complete valve matrix becomes somewhat more complex. The flow through the valve is:

$$Q = \mu(Y)(2gH)^{0.5} \quad 3.12$$

Where  $Y$  is the valve opening,  $\mu$  the flow coefficient and  $H$  is the pressure difference over the valve ( $H_R - H_L$ ). If a Taylor expansion of  $Q$  is performed at  $Q_0$  and the second and higher order terms are neglected equation 3.13 is left.

$$\begin{aligned} \Delta Q &= \left( \frac{\partial Q}{\partial H} \right)_0 \Delta H + \left( \frac{\partial Q}{\partial \mu} \frac{\partial \mu}{\partial Y} \right)_0 \Delta Y = 0.5\mu Y_0 \left( \frac{2g}{H_0} \right)^{0.5} \Delta H + (2gH_0)^{0.5} \frac{\partial \mu}{\partial Y} \Delta Y \\ &= 0.5(h_L - h_R) + \frac{\partial \mu}{\partial Y} y \end{aligned} \quad 3.13$$

By establishing the relationship  $K_q = y/y_{ex}$  and using the notation  $q_L = -q_R = q$  the local structure matrix for an oscillating valve becomes:

$$\begin{bmatrix} -\frac{1}{2} & -\frac{\partial \mu}{\partial Y} & \frac{1}{2} \\ 0 & \frac{1}{k_q} & 0 \\ \frac{1}{2} & \frac{\partial \mu}{\partial Y} & -\frac{1}{2} \end{bmatrix} \cdot \begin{bmatrix} h_L \\ y \\ h_R \end{bmatrix} = \begin{bmatrix} q_L \\ y_{ex} \\ q_R \end{bmatrix} \quad 3.14$$

When the power and rotating speed outputs are not of interest this equation is also valid for an open-loop excited Pelton turbine.



### 3.1.3 Surge shafts

Surge shafts are often essential elements in a hydro power plant in order to ensure stable operation. An element matrix representing a surge shaft can be expressed by the matrix equation below:

$$\begin{bmatrix} 1 & 0 \\ 0 & -\frac{sH_0A_{eqv}}{Q_0} \end{bmatrix} \cdot \begin{bmatrix} h_L \\ h_R \end{bmatrix} = \begin{bmatrix} q_L \\ q_R \end{bmatrix} \quad 3.15$$

This equation also holds for enclosed surge shafts with enclosed air pockets, so called air accumulators.  $A_{eqv} = A$  for a free surface surge shaft, whereas in an air accumulator the gas behavior has to be taken into account (Brekke, 1984).

$$A_{eqv} = \left[ \frac{1}{A_w} + \frac{nH_a}{V_0} \right] \quad 3.16$$

Where  $n$  is the polytropic compression constant,  $H_a$  is the accumulator pressure head and  $V_0$  is the air volume.

### 3.1.4 PID governor

PID-governors can be represented by various block diagrams. One representation introduced by Kvaerner in the 70s is displayed in Figure 3.1 (Xinxin, 1988).

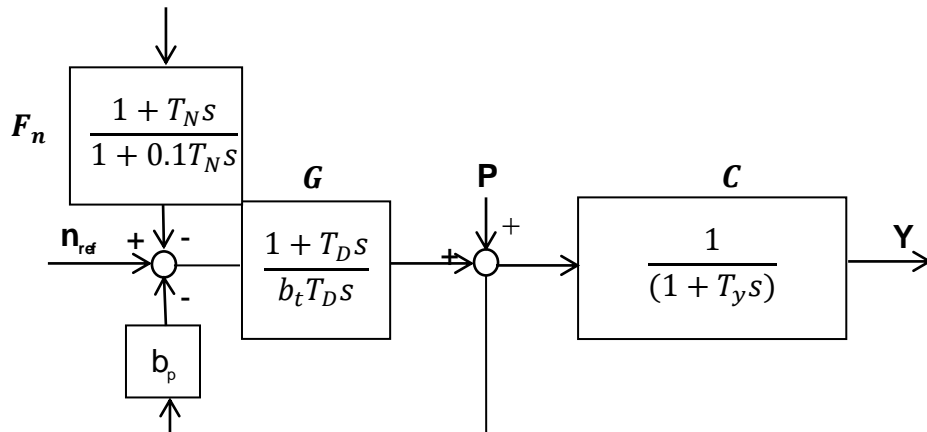


Figure 3.1 Modified Kvaerner PI-governor

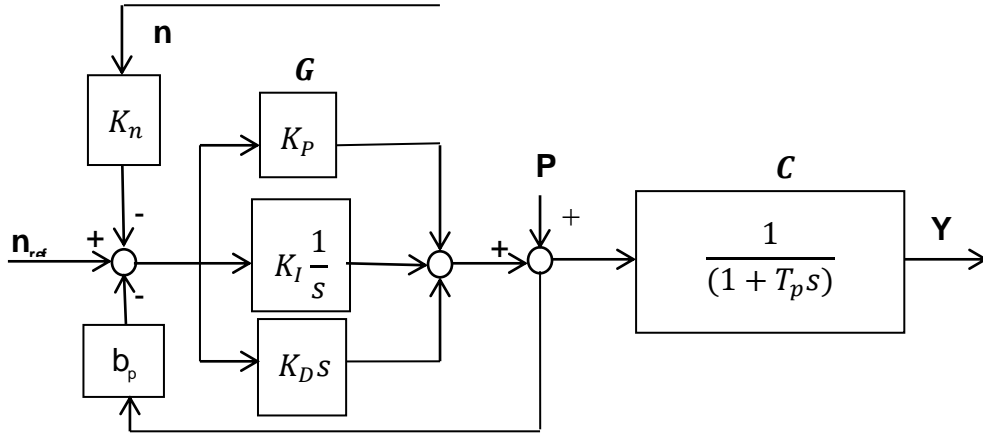


Figure 3.2 Block diagram representation of a parallel PID-governor

From the block diagrams in Figure 3.1 and Figure 3.2 the two equations below are obtained.

$$n_{ref} - nK_n + \left(P_r - \frac{y}{C}\right) b_p = \frac{y}{CG} - \frac{P_r}{G} \quad 3.17$$

$$n_{ref} = nK_n - \left(b_p + \frac{1}{G}\right) P_r + \frac{Gb_p + 1}{GC} \quad 3.18$$

Note that if the derivative block is neglected the two figures are identical. This is made apparent by the simplified governing block:

$$G = K_p + \frac{K_I}{s} = \frac{1}{b_t} + \frac{K_p}{T_d s} = \frac{T_d s + 1}{b_t T_d s} \quad 3.19$$

The configurations above can thus be described by the following governor structure matrix equation:

$$\begin{bmatrix} K_n & -(b_p + \frac{1}{G}) & \frac{Gb_p + 1}{GC} \\ 0 & 1 & 0 \end{bmatrix} \cdot \begin{bmatrix} n \\ p_r \\ y \end{bmatrix} = \begin{bmatrix} n_{ref} \\ p_{ref} \end{bmatrix} \quad 3.20$$

Here  $K_n$  is a constant that is used to include feed-back signal of the rotational speed. Thus  $K_n=1$  for feed-back and  $K_n = 0$  for an open-loop system.  $T_p$  is the time constant of the electric hydraulic amplifier. Note that  $p_{ref}$  is often neglected as its responses are of less importance as those to speed setting and load disturbances. When  $p_{ref}$  is neglected in the PI-governor equation the second row and column are reduced.

### 3.1.5 Generator system

For the design of single machine generator systems two assumptions can often be made:

- The turbine and generator are the only rotational masses so that the electric load is purely resistive.
- The transients of the hydropower system are much slower than the electric system transient, rendering the latter negligible.

With these assumptions and neglecting generator power loss, the equation of motion (eqn 2.9) in dimensional matrix form becomes:

$$[1 \quad -T_a s] \cdot \begin{bmatrix} p \\ n \end{bmatrix} = [p_g] \quad 3.21$$

The electric power load of the generator,  $p_g$ , must not be confused with the reference power setting  $p_{ref}$  used in the PID matrix equation. The generator and governor matrices will later be incorporated into the turbine equation. First the governing equations characterizing the turbine will be established.

### 3.1.6 Permanent speed droop

The permanent speed droop  $b_p$  is often an important property of the turbine governing. The permanent speed droop defines the change in frequency per change in turbine power output, and is defined by (Nielsen, 1990):

$$b_s = \frac{1}{Y} \left( \frac{\Delta n}{n_{ref}} \right) \quad 3.22$$

When turbines are connected in a common grid, the frequency is the same for all power plants, thus the load is determined by the permanent speed droop. However, if one governor is set to  $b_p=0$ , the associated turbine must accept all load variations. If multiple machines in the same grid are set to zero permanent speed droop load variations might lead to power fluctuations between the turbines.

### 3.1.7 Turbine self-governing

For reaction turbines the rotational speed influences the volumetric flow rate through the turbine. This relation affects the regulation of the dynamic system. The self-regulation adds stability in the case of a Francis turbine, since the flow rate decreases when the rotational speed increases. The self-regulation time constant  $b_s$  is defined as:

$$b_s = \frac{1}{P_0} \left( \frac{\Delta P}{\Delta \omega} \right) \quad 3.23$$

$b_s$  is negative and thus adds stability for Francis turbines, while it is positive for Kaplan turbines.

## 3.2 Turbine

Involvement of turbine characteristics is essential for realistic modeling of hydropower systems. The physics of hydropower turbines add complexity to the overall hydropower system. Based on an analytical approach the following matrix equation can be established<sup>3</sup>:

$$\begin{bmatrix} -B & -Q & 0 & -C & 0 & 0 & B \\ 0 & D & -E & F & 0 & 0 & 0 \\ 0 & 0 & 1 & 0 & 0 & H & 0 \\ J & K & 0 & L & M & 0 & -J \\ 0 & N & 0 & 0 & 1 & 0 & 0 \\ 0 & 0 & 0 & 0 & 0 & 1 & 0 \\ B & Q & 0 & C & 0 & 0 & -B \end{bmatrix} \cdot \begin{bmatrix} h_R \\ n \\ p_I \\ y \\ p \\ h_w \\ h_L \end{bmatrix} = \begin{bmatrix} q_R \\ n_{ref} \\ p_{ref} \\ 0 \\ p_g \\ h_{ref} \\ q_L \end{bmatrix} \quad 3.24$$

---

<sup>3</sup> See reference (Brekke, 1984, p. 79) for full derivation

Table 3.1 Turbine Characteristics

Turbine Characteristic	Definition	Turbine Characteristic	Definition
B	$0.5(1 - Q_n)$	K	$\frac{Q_n + E_n}{1 + E_q}$
C	$Q_y$	L	$Q_y$
J	$\frac{3 - E_n - (1 + E_q) \cdot Q_n}{2 \cdot (1 + E_q)}$	M	$-\frac{1}{(1 + E_q)}$

The turbine characteristics are presented in Table 3.1. These turbine characteristics have to be established from the turbine characteristic/hill diagram for the relevant turbine. The static turbine characteristics are assumed to be valid in the region from 0.005-6.0 rad/s, which is a typical range for hydropower governing analysis (Brekke, 1984). Thus the characteristics ( $Q_n$ ,  $Q_y$ ,  $E_n$  and  $E_q$ ) of the matrix equation can be found by their respective linearized equations<sup>4</sup>.

$$Q_n = \frac{^*Qn_0}{Q_0 \ ^*n} \left( \frac{\partial \underline{Q} / \ ^*Q}{\partial \underline{n} / \ ^*n} \right)_0 \quad 3.25$$

$$Q_y = \frac{^*QY_0}{Q_0 \ ^*Y} \left( \frac{\partial \underline{Q} / \ ^*Q}{\partial \underline{Y} / \ ^*Y} \right)_0 \quad 3.26$$

$$E_q = \frac{Q_0 \sqrt{^*H}}{\sqrt{H_0} \ ^*Q} \left( \frac{\partial \eta / \ ^*\eta}{\partial \underline{Q} / \ ^*Q} \right)_0 \quad 3.27$$

$$E_n = \frac{n_0 \sqrt{^*H}}{\sqrt{H_0} \ ^*n} \left( \frac{\partial \eta / \ ^*\eta}{\partial \underline{n} / \ ^*n} \right)_0 \quad 3.28$$

Note that in some literature the two last equations are also multiplied by the efficiency relation. The author has not included this ratio as it complicates the model and will have little influence on the overall results (Brekke, 1984). Figure 3.3 illustrates how these values can be extracted from the characteristic diagram of the turbine.

<sup>4</sup> From reference (Sand, 1999). The subscript “\*” denotes best efficiency condition and the “0” subscript imply the respective steady state values.

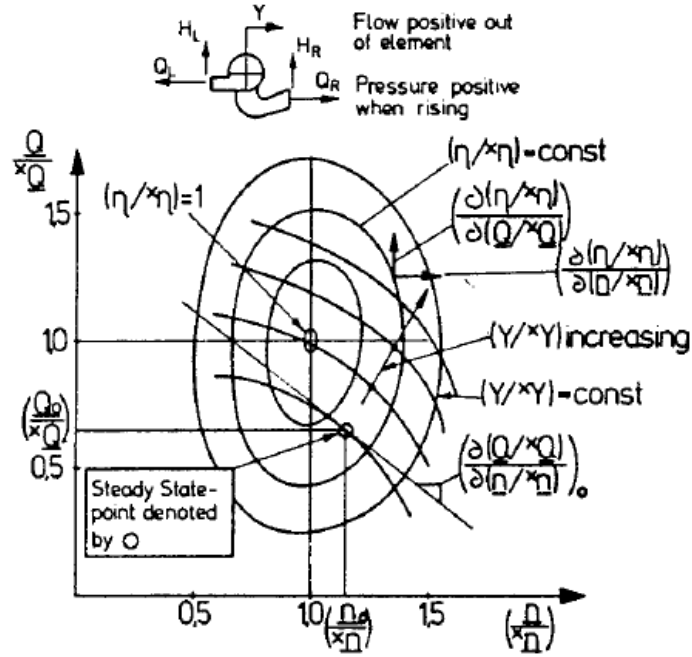


Figure 3.3 Turbine characteristics diagram (Xinxin & Brekke, 1988)

The primary task involves the linearization and extraction of the differentials in the characteristic equations. The hill diagram displays the dimensionless quantities  $n_{ED}$  and  $Q_{ED}$ , which are defined as follows:

$$n_{ED} = \frac{n \cdot D}{\sqrt{g \cdot H}} \quad 3.29$$

$$Q_{ED} = \frac{Q}{D^2 \cdot \sqrt{g \cdot H}} \quad 3.30$$

However, in the characteristic equations  $\underline{Q} = Q/\sqrt{H}$ , thus due to the fractions, the constants will cancel. For valves and Pelton turbines  $Q_n = 0$ . It should be noted that when  $E_n = E_q = 0$  and the relation  $K_q = y/y_{ex}$  is included, the turbine equation (3.24) becomes equal to the valve equation (3.14). If the turbine guide vanes or valve is locked ( $y=0$ ), the central row and column of the matrix is cancelled, leaving only the throttling equation (3.11) with  $K_p=2$ . Based on these considerations it is obvious that the turbine equation can be regarded as a complete representation of any linearized point obstacle in pipe flow.

Pelton turbines and valves with atmospheric pressure on one side have a flow rate downstream that in principle is equivalent to water pouring into a surge shaft pond. If  $q_n$  represents the flow into the “pond” and the outflow of the Pelton equation  $h_R = 0$  (zero

pressure downstream), then the last column of the turbine/valve matrix must be zero. Further, by flow continuity, the turbine inflow must equal the flow rate out of the turbine,  $q_L = -q_r$ . If the surge shaft equation (eqn. 3.15) is included the flow rate out of the pond becomes:

$$-\frac{1}{2}h_L - \frac{\partial\mu}{\partial Y}y - \frac{sH_0A_{eqv}}{Q_0}h_R = q_R \quad 3.31$$

Thus the matrix for a Pelton or valve with an atmospheric downstream pressure can be represented by the local structure matrix equation (Brekke, 1984):

$$\begin{bmatrix} -\frac{1}{2} & -\frac{\partial\mu}{\partial Y} & 0 \\ 0 & \frac{1}{k_q} & 0 \\ \frac{1}{2} & \frac{\partial\mu}{\partial Y} & -\frac{sH_0A_{eqv}}{Q_0} \end{bmatrix} \cdot \begin{bmatrix} h_L \\ y \\ h_R \end{bmatrix} = \begin{bmatrix} q_L \\ y_{ex} \\ q_R \end{bmatrix} \quad 3.32$$

The equations for the turbine, governor and generator were established in equation 3.24, 3.20 and 3.21 respectively. These can be integrated into one matrix equation. This local system structure is composed of six nodes, which can be integrated in one structure matrix (Xinxin, 1988):

$$\begin{bmatrix} -B & -Q & 0 & -C & 0 & B \\ 0 & K_n & E & F & 0 & 0 \\ 0 & 0 & 1 & 0 & 0 & 0 \\ J & K & 0 & L & M & -J \\ 0 & -T_a s & 0 & 0 & 1 & 0 \\ B & Q & 0 & -C & 0 & B \end{bmatrix} \cdot \begin{bmatrix} h_r \\ n \\ p_r \\ y \\ p \\ h_L \end{bmatrix} = \begin{bmatrix} q_r \\ n_{ref} \\ p_{ref} \\ 0 \\ p_g \\ q_L \end{bmatrix} \quad 3.33$$

If an ideal turbine is considered and  $P_{ref}$ -adjustments are neglected the equation is reduced to:

$$\begin{bmatrix} -B & -Q & -C & 0 & B \\ 0 & K_n & F & 0 & 0 \\ J & K & L & M & -J \\ 0 & -T_a s & 0 & 1 & 0 \\ B & Q & -C & 0 & B \end{bmatrix} \cdot \begin{bmatrix} h_r \\ n \\ y \\ p \\ h_L \end{bmatrix} = \begin{bmatrix} q_r \\ n_{ref} \\ 0 \\ p_g \\ q_L \end{bmatrix} \quad 3.34$$

The turbine characteristics applied are taken from best point measurements. For completeness automatically updated linearized values from a turbine hill diagram should be included in the simulations program.

### 3.2.1 The turbine characteristics algorithm

The turbine characteristics ( $Q_n$ ,  $Q_y$ ,  $E_n$  and  $E_q$ ) must be determined in order to properly represent the system behavior. To the authors knowledge graphical methods are generally applied in order to extract empirical values for these characteristics. The graphical method is illustrated in Figure 3.3 for the mentioned characteristics. The operating point of the turbine is partially linearized to determine the constants. This process requires extensive data on the relevant turbine in addition to a manual procedure for each operating point.

An algorithm has been designed in order to extract the turbine characteristics more efficiently. The algorithm is designed to take field or laboratory measurements and plot a hill diagram before differentiating the surface with respect to various directions. Finally the differentials at the steady state condition are determined. The procedure will now be explained in further detail and it is displayed on the flowchart in Figure 3.4.

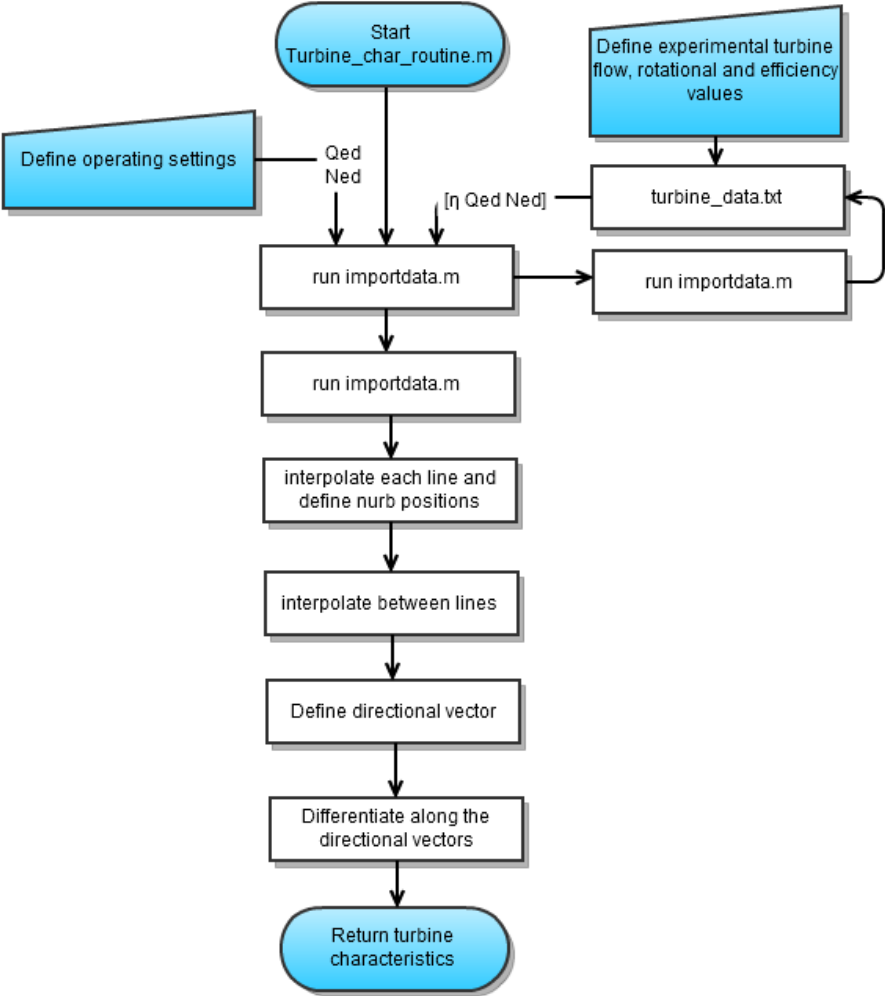


Figure 3.4 Turbine characteristics routine



A text-file with turbine data for rotational speed ( $N_{ed}$ ), ( $Q_{ed}$ ) and hydraulic efficiency ( $\eta_{hyd}$ ), at a range of guide vane openings ( $Y$ ), is produced from turbine tests. A Matlab file then incorporates this data into a set of matrices. The three dimensional lines are interpolated and stored in the Matlab format for “Non-Uniform Rational B-Splines” (NURBS). The routine applied for creating and manipulating the surfaces is named “Turbine\_char\_routine.m” and is supplied in Appendix C.

The routine interpolates the measured points and creates surfaces between the various constant guide-vane-angle lines. The plot of the surface between two guide vane angles is shown in Figure 3.5. Since the interpolated characteristics are stored in nurb-format the directional derivatives anywhere on the surfaces can be determined. The inputs are values for  $N_{ed}$  and  $Q_{ed}$  points to the position on the surface for each differential direction. Vectors in the direction along each axis are then defined and the angle between the vector and the derivative at the point is generated. The directional derivate for  $Q_n$ ,  $E_n$  and  $E_q$  can then be determined. The author did not succeed in developing a consistent procedure to define the derivative along different guide vane angles. The identity  $Q_y$  is for that reason not determined automatically with the current procedure. For the analysis in this thesis turbine identities were available and application of the turbine characteristics routine was not required.

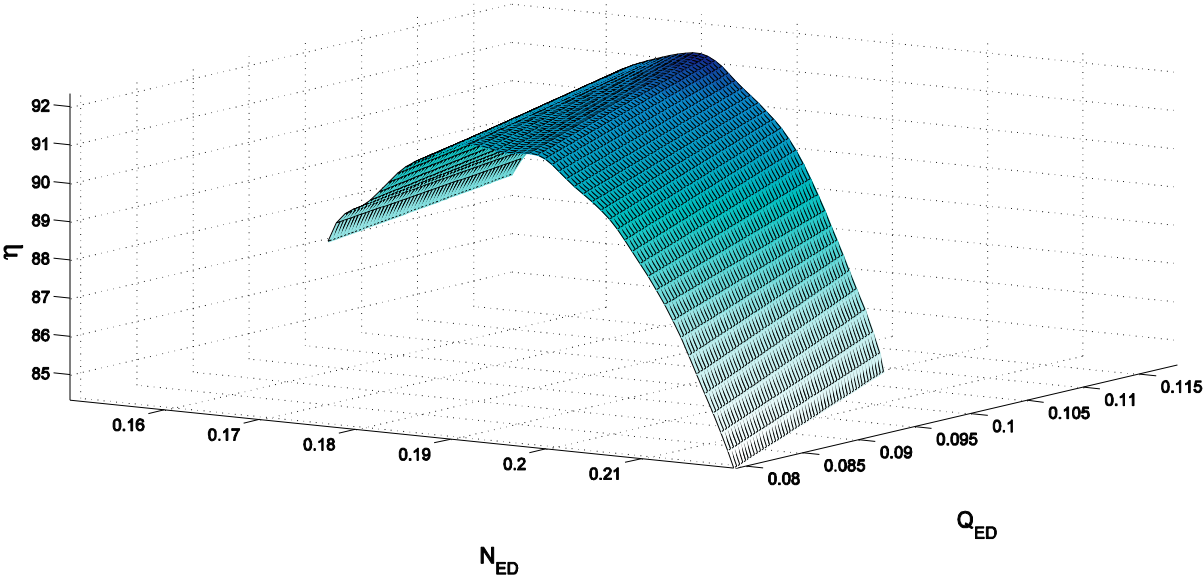


Figure 3.5 Surface plot,  $Y = 5-6deg$

## 4 Matlab program

A Matlab program was developed according to the structure matrix theory presented in chapter 3. The algorithm layout is presented by the flowchart in Figure 4.2. The general hydropower system modeled by the algorithm is shown in Figure 4.1 below.

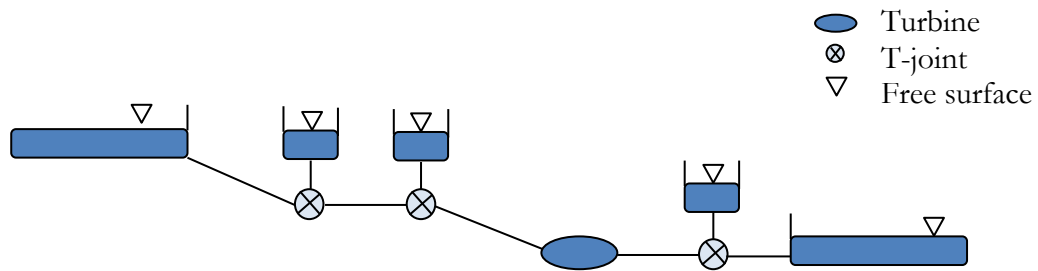


Figure 4.1 General hydropower system

### 4.1 General description

The program is general with respect to the system geometry. The response is plotted at discrete frequencies throughout the spectrum relevant for hydropower systems (i.e. 0.001-10 rad/s). In order to capture all details and create a continuous plot of the frequency responses, ten thousand logarithmically spaced and discrete frequency disturbances are simulated. This high number of discrete points was selected in order to avoid step adaption or acceptance criteria in the friction routine (chapter 5). The overall simulation algorithm is presented in Figure 4.2 and the inner loop determining the friction is presented in Figure 5.2.

#### 4.1.1 Input

The user has the option of including zero, one or two surge shafts upstream and zero or one surge shafts downstream the turbine. Throttles can also be simulated at common locations in the system. Dimensions and parameters of all elements must be entered prior to running the program. However the geometry, turbine parameters and governor settings of some hydropower systems are already included. These are initialized by the program switches “system geometry” and “Turbine type”<sup>5</sup>. The response type and friction model

---

<sup>5</sup> Governor settings are included in the latter

also have to be selected prior to initializing the program routine. For reasons that will be discussed later inputs for adjustments of angles are also available for the user.

The disturbance amplitudes were chosen to be 5% of the nominal values of the flow rate in order to justify the linear assumption in the frictional terms. This was implemented by setting the vector input to 1, while reducing the flow rate in the iteration ( $Q_{previous}$  in Figure 4.2) to 5% of nominal flow. The disturbance is implemented to the variable in the flow matrix ( $\mathbf{q}$ ) that is indicated by the switch “response type”.

#### **4.1.2 Output**

The switch “response type” in the input switches on the position of the pressure head matrix ( $\mathbf{h}$ ) that is stored during the program iteration. The pressure, rotational speed and power responses can be plotted. The gain and angle of the response is determined and can be plotted in a Bode, Nichols, or frictional damping plot.

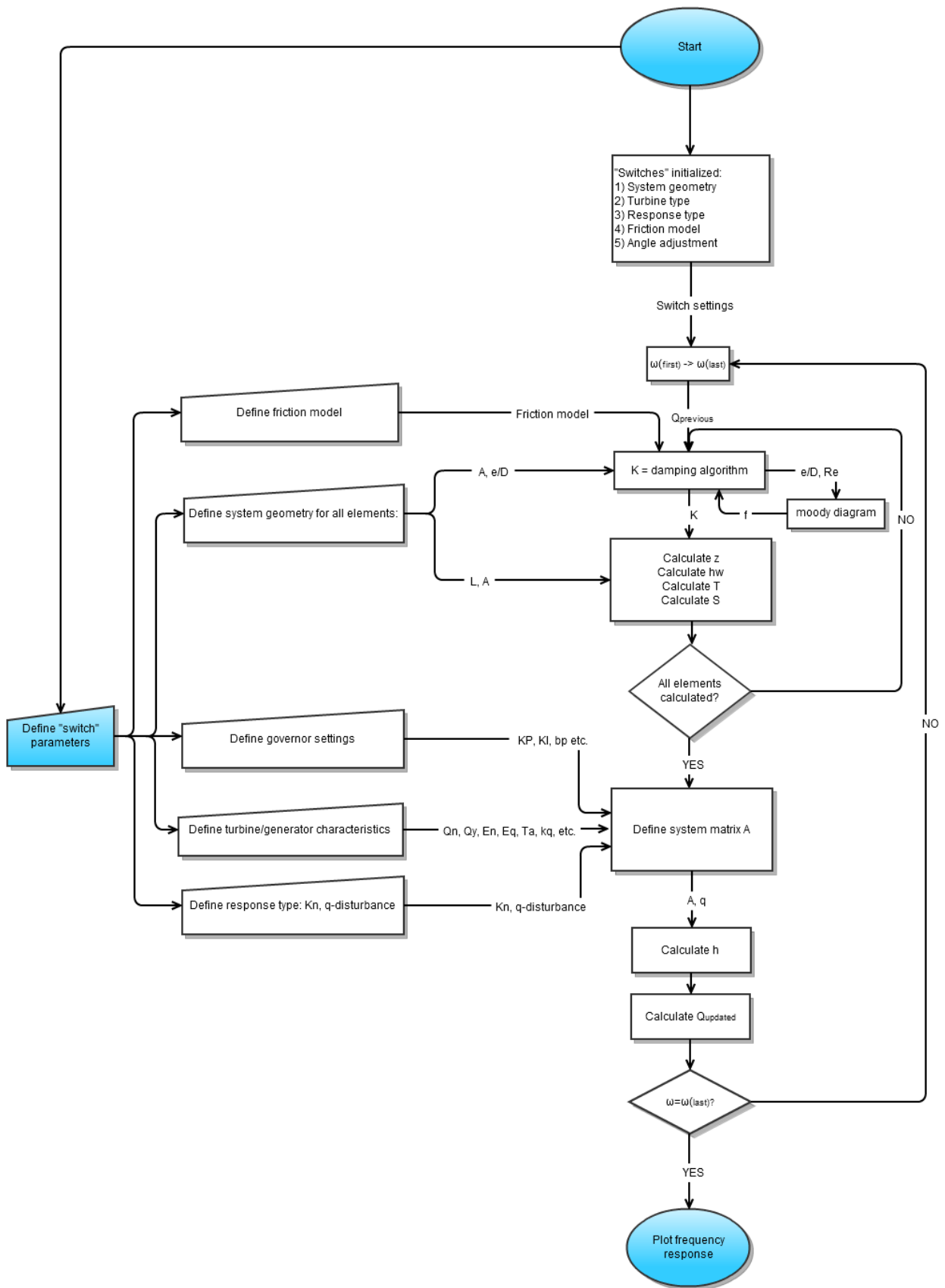


Figure 4.2 Matlab program flowchart

## 4.2 System stability

Some common definitions of the stability of a hydropower system must be established. The system block diagram and the related transfer functions are important tools for this purpose. A general block diagram representation of a hydropower system is supplied in Figure 4.3.

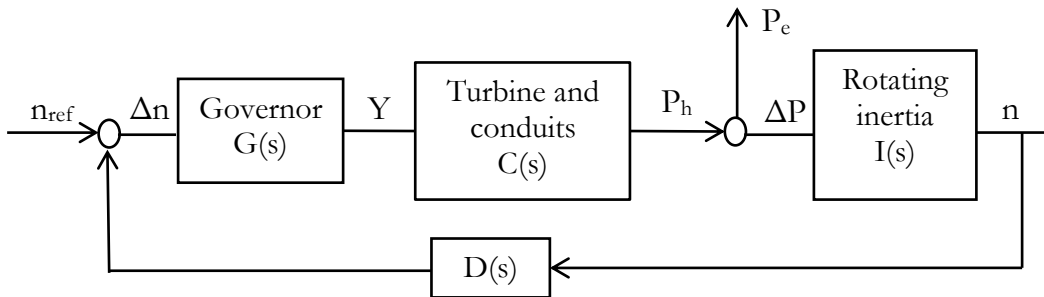


Figure 4.3 Block diagram of a hydropower system with feedback

An equation relating all blocks of the hydropower system is:

$$N(s) = \frac{\Delta n}{n_{ref}} = \frac{1}{1 + G(s)C(s)I(s)D(s)} \quad 4.1$$

For a simple hydropower system with an open loop (i.e.  $D$  is equal to zero), the transfer function becomes:

$$A(s) = G(s)C(s)I(s) = \frac{1 + T_d s}{b_t T_d s} \cdot \frac{1 - T_w s}{1 + 0.5 T_w s} \cdot \frac{1}{T_a s + b_s} \quad 4.2$$

In this instance  $A(s)$  represents the systems isolated response. If a disturbance is introduced into the system, it is of interest to investigate whether the system will stabilize or if a continuous oscillation will establish (instable system).

### 4.2.1 System stability criteria

The dynamic process can be modeled by analyzing the response to various system disturbances. When the system is linearized around the steady state operational point the transfer function of the system can be obtained. If a disturbance is applied over a range of frequencies  $\omega_1 < \omega < \omega_2$  the system response can be analyzed. A sine-wave disturbance on a system with a magnitude of  $y_0$  has the Laplace-transformed input:

$$y(s) = \frac{y_0 \omega}{s^2 + \omega^2} \quad 4.3$$

If the process transfer function is given by  $H(s)$ , the system frequency response is  $u(s) = A(s) \cdot y(s)$  and the inverse Laplace transform of  $u(s)$  returns:

$$u(t) = y_0 |h(j\omega)| \sin(\omega t + \angle h(j\omega)) \quad 4.4$$

The function  $h(j\omega)$  is the system frequency response and  $\angle h(j\omega)$  is the phase shift (or phase angle). The absolute values of  $h$ ,  $|h(j\omega)|$  is the amplitude ratio of response to disturbance, which is an important parameter in frequency analysis.

In Figure 4.3 the disturbance  $P_e$  from the electric grid will influence the stability of the hydropower system. The bottom line connecting  $n$  to  $n_{ref}$  and  $\Delta n$  is the feedback of the system, which signifies that  $\Delta n$  is adjusted to compensate for a change in  $n$ . The aim is to ensure that the response to a disturbance brings the system to equilibrium without over- or undershooting. This implies that the  $M$ -block in the reduced system in Figure 4.4 takes the value 1, so that  $n_{ref} = n$ .

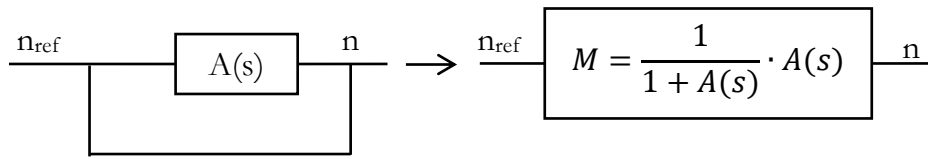


Figure 4.4 Simplified block diagram representation

The absolute stability criterion, known as the Nyquist criterion is given by:

$$\angle h(j\omega) > -180 \text{ and } |h(j\omega)| < 1 \quad 4.5$$

When the turbine's guide vane opening is reduced to reduce the power by reducing the flow rate, the pressure at the turbine is increased. Thus, if the turbine opening is reduced too rapidly, the pressure might increase significantly, causing an increase in power. Thus, rapid closing of the turbine might cause an increased hydraulic power, which is a result opposite to the intention of the control action. This is a practical effect of the  $-180^\circ$  phase lag requirement.

A common method of stability visualization is to illustrate the system frequency response in Bode-plots. A Bode plot graphs the transfer function of a linear time-invariant system versus frequency. It is plotted with a log-frequency axis to display the frequency response. In order to assure system stability phase and gain margins are notions that characterize the stability of the system. The phase margin,  $\Psi$ , signifies the separation from  $-180^\circ$  of the phase curve at the gain crossing frequency. The gain margin  $\Delta k$  is the separation in dB between 0 dB and the amplitude curve when the phase curve crosses  $-180^\circ$ . A common stability criterion is:

$$\psi > 45^\circ \text{ and } \Delta k > 2 (= 6dB) \quad 4.6$$

The closed loop system identity in Figure 4.4 can be simplified to  $M = |N| \cdot |A|$ . For frequencies below the crossing frequency  $M \approx 1$ , while at high frequencies  $M \approx |A|$ . Around the crossing frequency the value of  $|N|$  often peaks, which implies inefficiency in the control feedback. Thus, to ensure an efficient feedback response, the following criterion applies:

$$|N|_{max} < 4 - 6dB \quad 4.7$$

#### 4.2.2 Transfer function program

A simple program solving the transfer function response and plotting it in a Bode plot and root lotus was established. The basic program is based on transfer function solutions and is thus inelastic and frictionless. The program utilizes the inherent Matlab functions for plotting the mentioned graphs (Matlab, 2012). The program is used to study some general stability phenomena more efficiently than the iterative simulation program. The program is supplied in Appendix E.

## 5 The frictional damping factor

The frictional damping factor is of great importance to the agreement between the model and measurements. The aim of the model is to simulate an oscillatory behavior, which complicates the frictional factor compared to steady state factors. Frictional damping is generally a function of flow rate ( $q$ ), frequency ( $\omega$ ), cross-sectional area ( $A$ ) and friction factor ( $f$ ) (Brekke, 1984). Obtaining a function that satisfactorily models the steady-state and oscillatory damping factor is a challenging task. The theoretical friction equations applied in this section are based on literature by Brekke, Jonsson and Swart (Brekke, 1984) (Brekke & Xinxin, 1987)<sup>6</sup>.

The Darcy-Weisbach head loss equation is commonly applied to calculate the steady-state frictional influence in pipe flow:

$$h_f = \frac{fLv^2}{2gD} \quad 5.1$$

An alternative to this equation is the Manning's formula, which has traditionally been a preferred friction identity in open-channel flows:

$$h_f = \frac{Q_t^2}{M^2 R_h^{4/3} A} \quad 5.2$$

In order to determine the Darcy-Weisbach friction factor ( $f$ ) the Moody diagram can be applied. The wall roughness ( $\epsilon/D$ ) and Reynolds number are inputs and the friction factor returned. The explicit Haaland formula is used to give an initial guess for the friction factor:

$$\frac{1}{\sqrt{\lambda}} = -1.8 \log \left[ \left( \frac{\epsilon/D}{3.7} \right)^{1.11} + \frac{6.9(\pi\mu D)}{4\rho Q_t} \right] \quad 5.3$$

$\epsilon/D$  is the relative roughness (equivalent sand grain diameter) of the pipe or tunnel. Note that the denominator of the last term on the right hand side the Reynolds number is made explicit by an expression for  $Q_t$ .

---

<sup>6</sup> In Brekke's doctoral thesis (Brekke, 1984) some of Jonsson (Jonsson, 1980) and Swart's work is also summarized



## 5.1 Browns Model

Brown established one of the many theories for expressing friction forces in oscillatory turbulent flow (Brekke, 1984, p. 29). His theory is based upon the ratio of energy to velocity flow distribution across a circular pipe. The proposed expression for the damping constant  $K$ , is divided into a static and dynamic term, according to the following equation:

$$K = K_R + iK_I = \frac{4\lambda Q_t}{\pi D^3} + (C - 1)j\omega \quad 5.4$$

The ratio of energy to velocity distribution,  $C$ , is given by the equation in Figure 5.1 below.

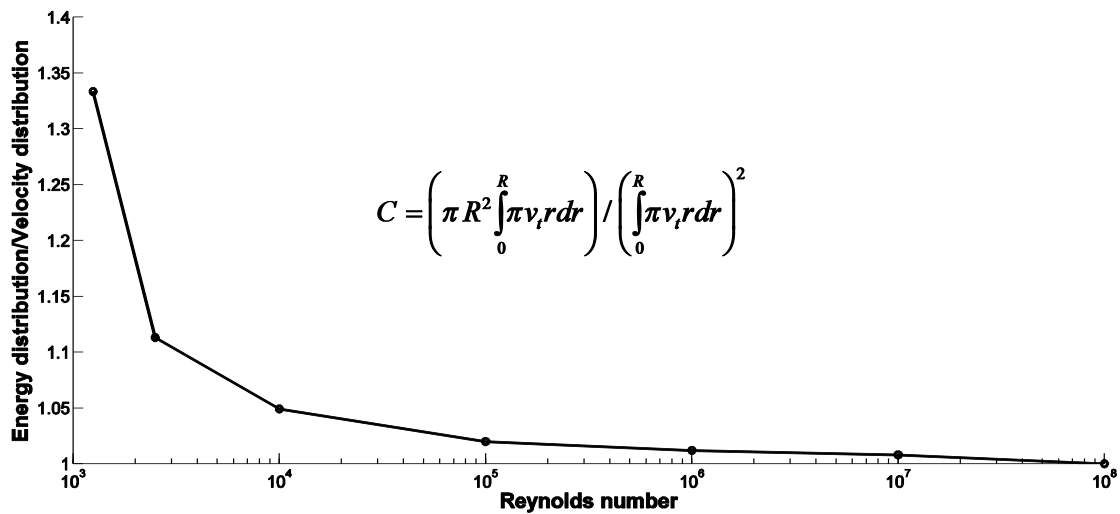


Figure 5.1 The ratio  $C$

The unsteady term  $K_I$  is not valid for low frequencies, thus it is set to zero for frequencies below 0.1 rad/s. The ratio  $C$  is interpolated between the marked points in the graph of Figure 5.1 in the Matlab code supplied in Appendix A. The frictional influence on large pipes is reported to be too small with Brown's theory (Brekke, 1984). In particular, the additional friction arising in oscillatory flows at high Reynolds numbers is underestimated. For the purpose of stability studies, Browns model will influence the system to be less stable than it in reality is. Thus Brekke (1984) developed the model that is presented in the next section.

## 5.2 Brekkes model

As in the previous friction model, the wall shear stress can be separated into two major parts, one arising from steady-state flow, the other from dynamic oscillations:

$$\tau = \tau_d + \tau_s$$

The dynamic shear stress is related to the shear force according to the following equation:

$$\tau_d = \frac{1}{2} f_d \rho \frac{Q_0 |\hat{q}|}{A}$$

According to both experiments and theory there exists a phase shift between flow oscillations and frictional shear force:

$$f_d = |f_d| \cos(\pi/8) + i |f_d| \sin(\pi/8)$$

Now the theoretical expressions for dynamic frictional force can be established. According to Swarts<sup>7</sup> theory it can be expressed as:

$$f_d = e^{-5.977} + 5.213 \cdot \left( AK_r \frac{\omega}{Q_0 |\hat{q}|} \right)^{0.194} \text{ if } AK_r \frac{\omega}{Q_0 |\hat{q}|} < 0.64 \quad 5.5$$

$$f_d = 0.4725 \left( AK_r \frac{\omega}{Q_0 |\hat{q}|} \right) \text{ if } AK_r \frac{\omega}{Q_0 |\hat{q}|} > 0.64 \quad 5.6$$

Inverting the first equation, and applying the classical Darcy-Weisbach friction factor for  $f_d$  (i.e.  $f_d = f_{D-W}$ ), one can obtain an explicit equation for the “fictitious roughness”,  $K_r$ :

$$K_r = \text{function}(A, \omega, f, Q_0 |\hat{q}|)$$

Now, one can return to the initial equation to establish a complete model of the frictional damping,  $K$ . Hermod Brekke proposed the two-term approach with a linearized steady-state and oscillatory term super-imposed respectively as presented below (Brekke & Xinxin, 1987):

$$K = K_R + iK_I = \frac{\pi D}{A^2} \left[ Q_t f + \frac{1}{2} Q_0 |q_{n-1}| f_d \cos(\pi/8) + i \frac{1}{2} Q_0 |q_{n-1}| f_d \sin(\pi/8) \right] \quad 5.7$$

Here  $Q_t$  is the steady state flow in the regarded pipe,  $A$  is the cross-sectional area and  $f$  is the Darcy-Weisbach friction factor. It should be noted that  $f_d$  is not equal to  $f$  in this

---

<sup>7</sup> Presented in (Jonsson, 1980).

equation (as it was assumed in the equation for  $K_r$  above). The significance of the real and imaginary parts can be explained as the phase shift between flow oscillations and frictional shear force. The phase  $\pi/8$  was applied as it proves to fit experiments well (Brekke, 1984).

Brekke applied a refined frequency stepsize to avoid large jumps in the absolute flow values. Another proposed approach is to use  $q_{n-1}$  as long as it does not deviate more than 10% from  $q_n$ . For larger deviations an averaging of the two values is then introduced. The first approach was applied in the program, as it mitigates iterations in this stage of the procedure.

### **5.3 The frictional subroutine**

The program routine was attempted with a direct explicit solution based on Haaland's formula alone, as well as the entire moody diagram routine. The moody program routine (see Appendix A) iterates to find the Darcy-Weisbach friction factor,  $f$ . The Haaland formula (equation 5.3) is a direct method for determining the friction factor. The Haaland formula was found to be more than two orders of magnitude faster than running the entire moody diagram routine (e.g. 5ms compared to 0.02ms). However, since the number of iterations applied in the program is fairly low, the complete Moody routine was applied for better accuracy.

The author did not implement Brekke's frictional model successfully in the computer model. Thus Brown's method was applied to the model and the effect of its implementation will be discussed in chapter 6. The complete frictional subroutine is organized according to the flowchart of Figure 5.2.

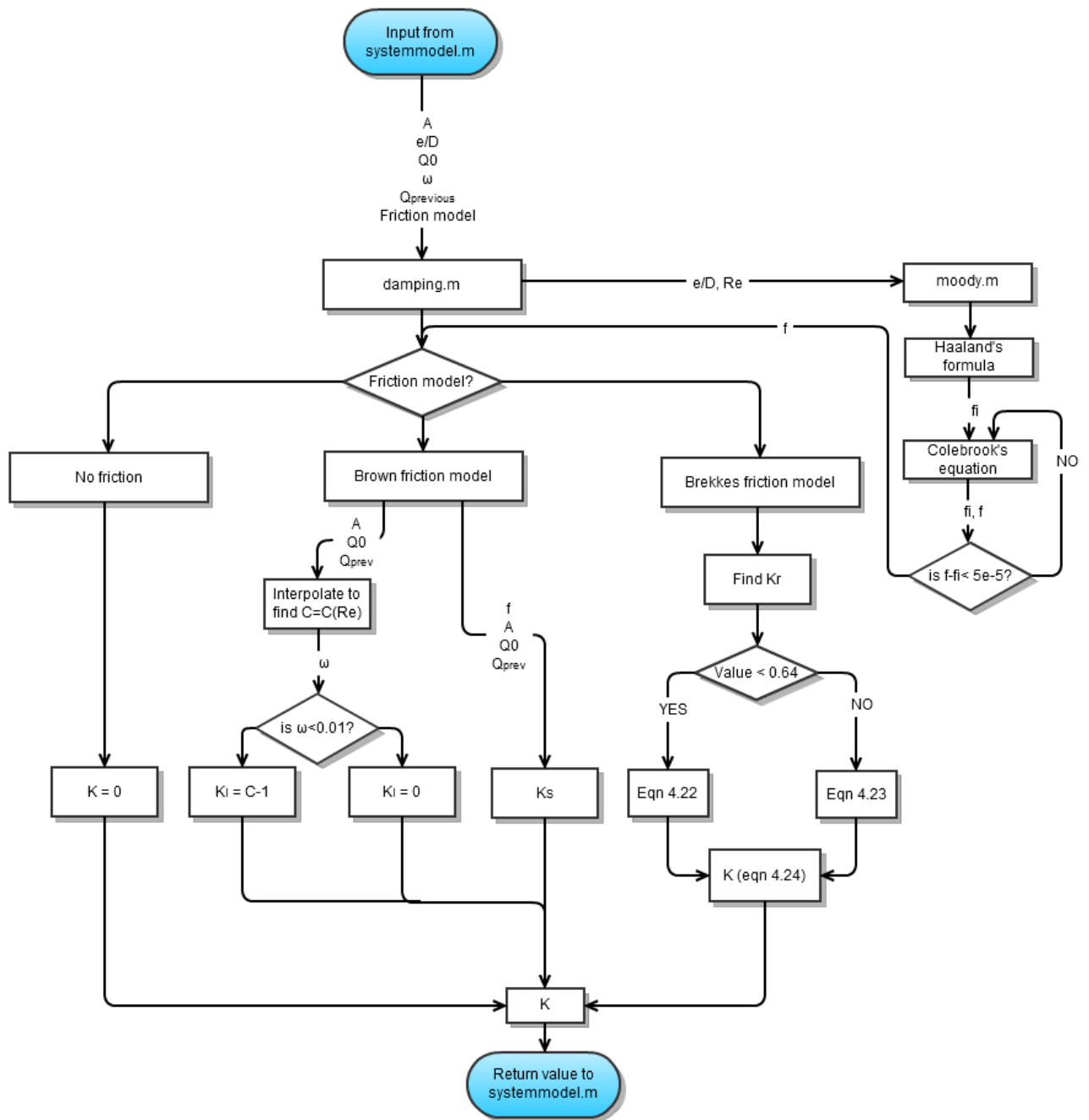


Figure 5.2 Simulation flowchart for determining system damping

## 6 Program Validation

This chapter aims to validate the hydro power simulation program. A validation of an earlier version of this program was performed by the author (Vogt-Svendsen, 2011). The current validation is performed by comparing the simulation results to measurements and externally produced simulations. Previously published results from hydropower systems at Kongsvinger and Tafjord are compared to the results produced by the simulation program. The two hydropower plants constitute significantly different systems. Kongsvinger has a short water conduit, large flow rate and a Kaplan Bulb turbine. Tafjord has a long water conduit, low flow rate and a Pelton runner unit. The measurements and information on the two hydropower plants are based on Brekkes investigations (Brekke, 1984).

### 6.1 Kongsvinger hydro power plant

The Kongsvinger power plant utilizes a 9.5m net head in the river Glomma. Production started in 1978, with one Kaplan Bulb turbine at a rated operating flow of  $108.5\text{m}^3/\text{s}$ , delivering 9.2MW power (NVE, 2012). The author chose this power plant since it is one of the few power plants with available frequency response measurement data for comparison. Hermod Brekke also studied this power plant, thus his stability analysis is also available for comparison (Brekke, 1984).

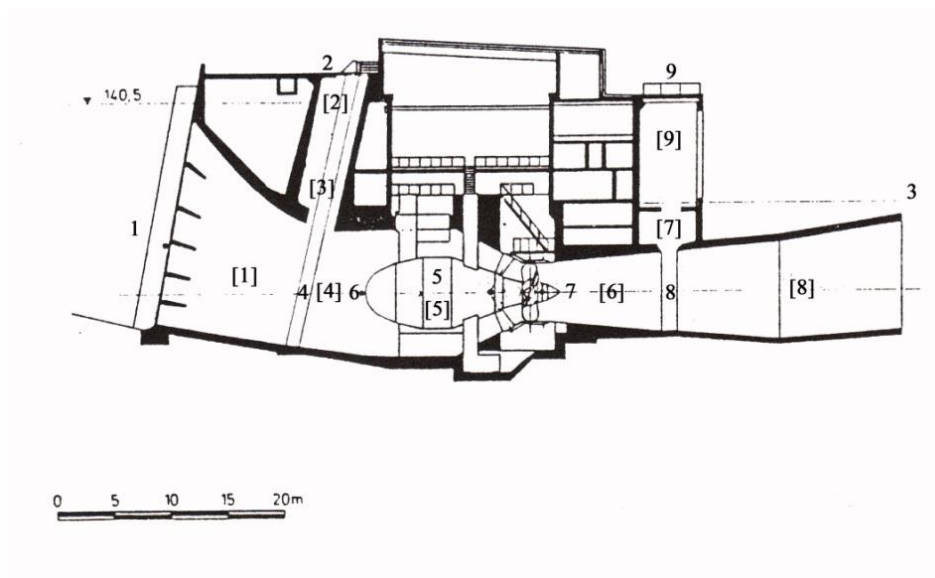


*Figure 6.1 Kongsvinger power plant layout<sup>8</sup>*

<sup>8</sup> (Brekke, 1984) The numbering of the original figure is modified.

The layout of Kongsvinger power plant is depicted in Figure 6.1. The related dimensions of the waterways are supplied in Table 6.1. The elements are incorporated in correspondence to the elements and node numbering shown previously. In Table 6.2 the turbine characteristics of the Kaplan Bulb turbine are given, along with characteristics related to the governor.

*Table 6.1 Main dimensions according to Figure 6.1*

<b>Element</b>	<b>Nodes</b>		<b>L (m)</b>	<b>A (m<sup>2</sup>)</b>
1	1	4	12	150
2+3	2	4	10	39
4	4	6	6	106
5	6	7	15	148
6	7	8	14	28.6
7	8	9	4	51
8	8	3	20.6	127
9	8	9	1	127

A frictionless simulation was run with the above inputs along with a plot of the reported measurements in Figure 6.2. This is a plot of the power response to guide vane excitations as the pressure response amplitudes are challenging to record. A large spike arises in the Bode diagram at above 0.8 rad/s. This corresponds well with the theoretical rule-of-thumb formula (eqn. 2.17) for the draft tube shaft, which returned a frequency of 0.896 rad/s. The oscillatory flow in the shaft was eliminated when the shaft surface area was increased to around 950m<sup>2</sup>.

*Table 6.2 Turbine and governor settings*

<b>Turbine characteristics</b>		<b>Governing characteristics</b>	
$Q_n$	0.55	$T_d$	15
$Q_y$	0.46	$T_a$	2.3
$E_q$	0.113	$b_t$	2.6
$E_n$	-0.18	$b_p$	0.041
$K_q$	1.0	$K_n$	0

Hermod Brekke (1984, p. 160) reported that the measurements showed somewhat larger (negative) angles. This was explained by the flexibility between the guide vane blades and the registered movement of one of the guide vane levers. This deviation was not apparent when comparing the measurements to the current simulations and they are likely not significant.

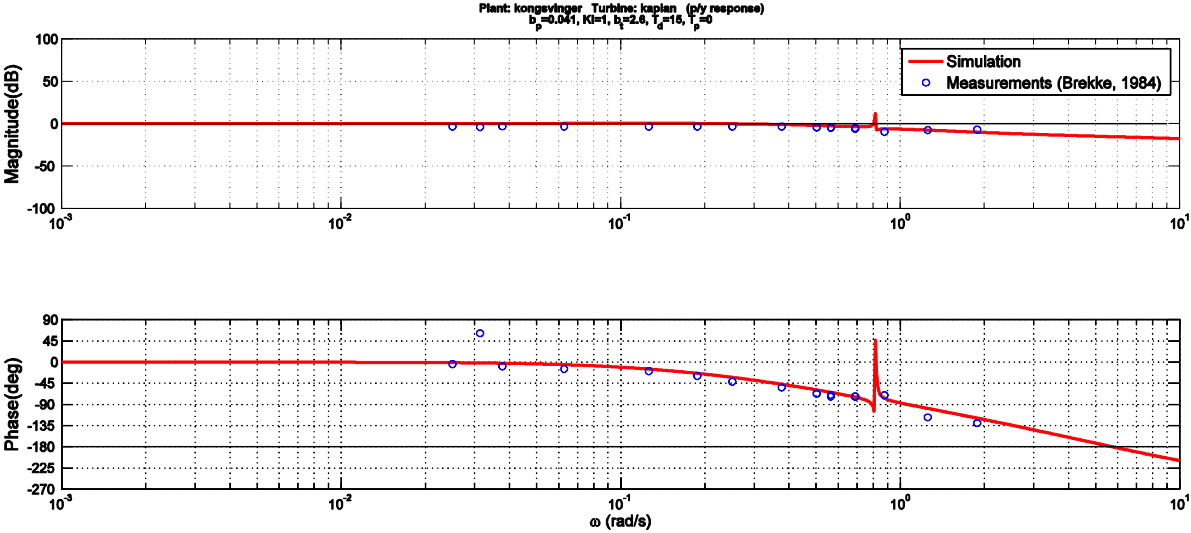


Figure 6.2 p/y plot and measurements for Kongsvinger

The Brown friction model was introduced in the second simulation. The damping constant  $K$  is plotted with respect to the frequency in Figure 6.3. The damping influence shows, as expected, increased frictional damping with increasing frequency. This is due to the growing absolute value of the oscillatory term of the damping representation. It is also apparent that the surge shaft damping holds a local peak at the surge shaft's resonance frequency. An increase of flow rate, and subsequently the Reynolds number, is expected in the surge shaft at the resonance frequency. According to Browns equation, such an increase will lead to a larger static friction. Thus, despite a small decrease of the ratio  $C$  in the unsteady frictional term, the damping factor will show an overall increased value at this frequency. It should be noted that the frictional damping does not influence the pipe flow significantly due to the large inertial forces of the mass flow.

The simulations include elastic effects. However no water hammer effect is apparent in the stability study. Due to the relatively short water conduits, an inelastic model would therefore also capture the mass oscillations. However, elastic effects should be included in

general stability analysis since the elasticity has a strong destabilizing effect on high frequency oscillations (Xinxin, 1989).<sup>9</sup>

When the frictionless and the friction plots are compared the influence of the friction model is most apparent at the resonance frequency. The response is dampened and the overall response is in close agreement with the experimental results. The phase of the response is pushed to slightly smaller angles (in absolute terms). In the gain response at the resonance frequency the resonance peak is a dampened trough, not an elevated gain as in the frictionless model. This is in line with the experimental values, which show a slight trough at the resonance frequency.

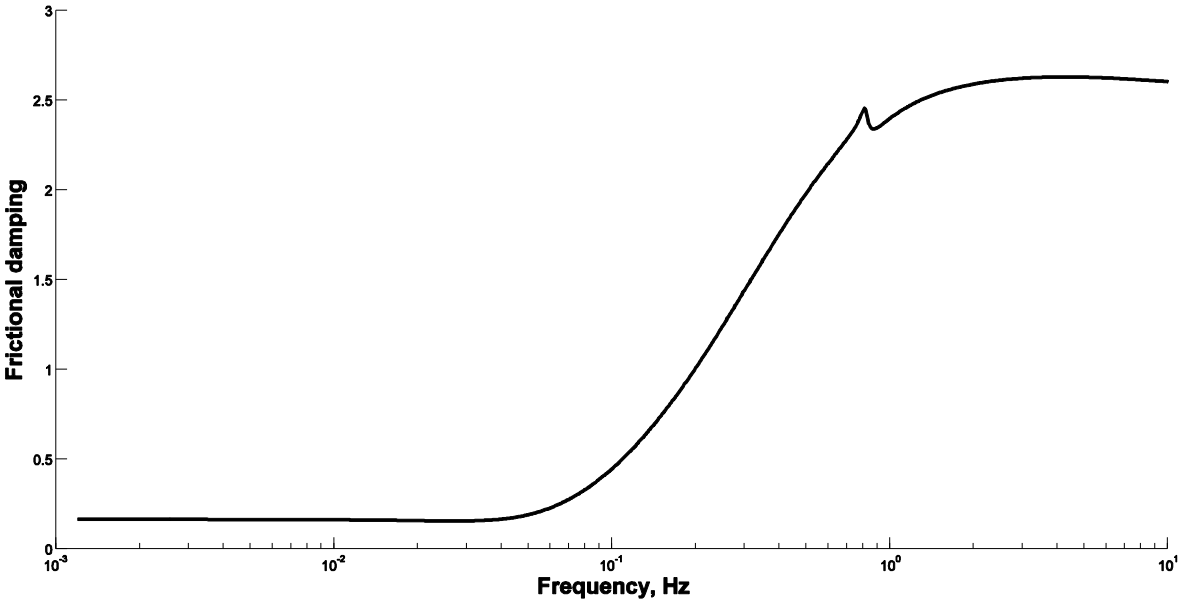


Figure 6.3 The frictional damping constants in the draft tube gate shaft

<sup>9</sup> The elastic effects are apparent in the study of Tafjord (chapter 6.2) due to the long high head penstock.



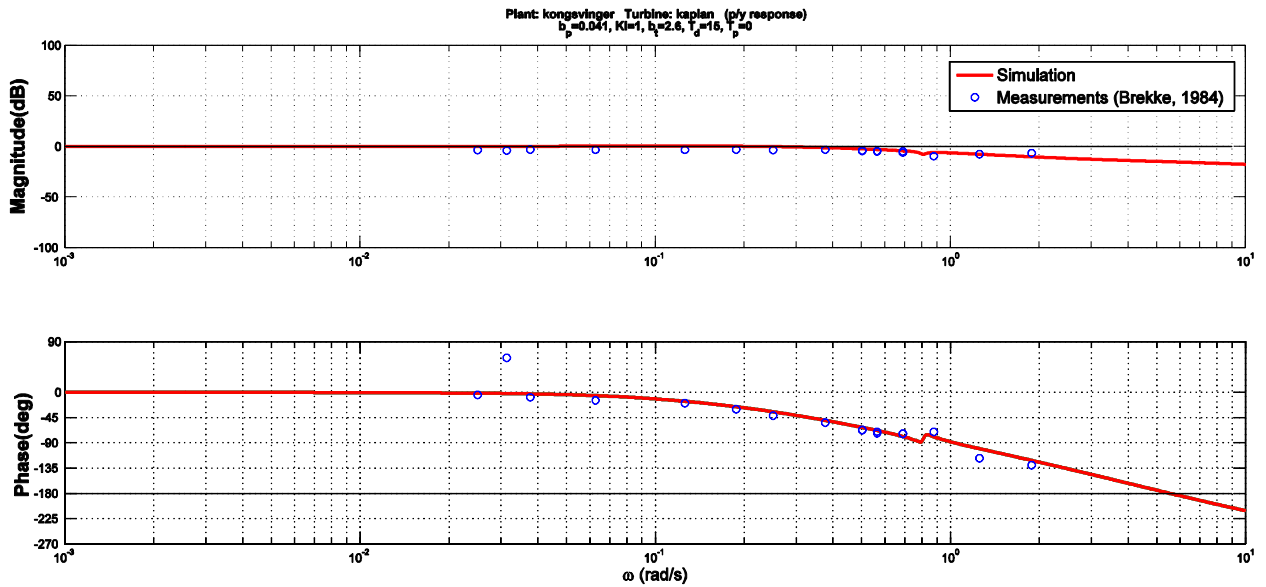


Figure 6.4 p/y plot including the Brown friction model

Finally the stability analysis of the Kongsvinger plant is presented in Figure 6.5. There were no experimental results for this analysis, thus it was compared to Hermod Brekkes simulations<sup>10</sup>. Note that to correct for the quadrant of the phase shift angles,  $\pi$  radians is subtracted for certain plots. Matlab's handling of angles beyond  $\pm \pi$  radians made both the unwrap function and an angle adjustment necessary in order to produce results according to convention. The unwrap function corrects for angular jumps of  $\pi$  radians for neighboring frequencies. The author has not identified a method that automatically produces these adjustments. The same adjustments are often required in the post-processing in SimuLink. Thus such adjustments are likely not manageable in Matlab.

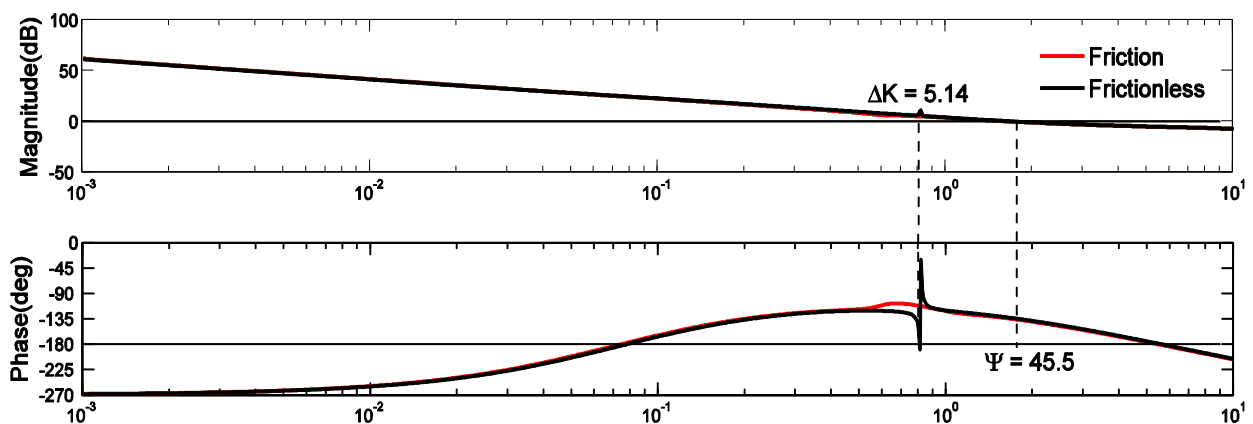


Figure 6.5 n/nref stability analysis

<sup>10</sup> The plot from Brekke's work is supplied in Appendix D for comparison.

The Kaplan Bulb runner causes the system to have a negative self-governing. The negative self-governing combined with zero permanent governing statics causes the phase response to originate from -270 degrees. In the case of permanent statics the phase response origin would be moved to -180 degrees. In Figure 6.6 a Nichols plot of the stability analysis is presented. The Nichols plot shows, in a compact manner how the governor is in effect up to fairly high frequencies. The stability margins are sufficient and the crossing frequency is close to 2 rad/s.

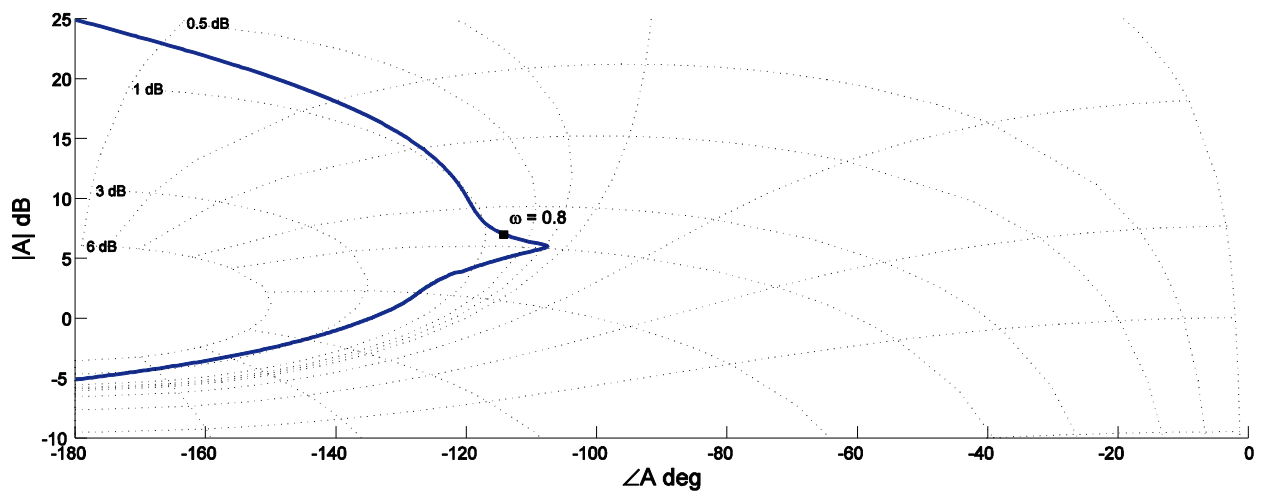


Figure 6.6  $n/n_{ref}$  stability analysis

## 6.2 Tafjord hydropower plant

Tafjord is a powerplant on the opposite end of the scale compared to the Kongsvinger plant. The plant has a high head of  $H_0 = 816.2$  and a small flow rate of  $Q_0 = 8.8\text{m}^3/\text{s}$  generating 64MW at a rotational speed of 500rpm (Brekke, 1984). In order to compare the system dynamics simulated in the Matlab program to the measured values, some simplifications must be made. The system layout is presented in Figure 6.7 below along with tables supplying an overview of the most important system parameters. The intake gate shaft was not included in the simulations. The frictional influence of expansions and contractions in head race tunnel were simplified.

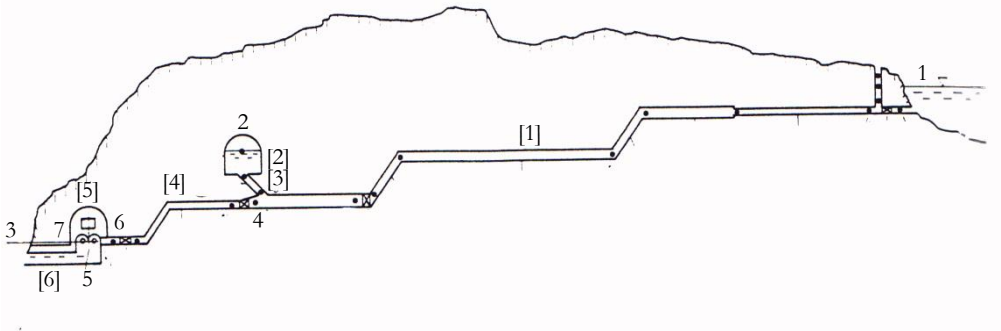


Figure 6.7 Tafjord power plant layout<sup>11</sup>

Table 6.3 Geometrical data related to Figure 6.7

Element	Nodes	L (m)	A (m <sup>2</sup> )
1	1 4	7567	11
2	2 4	7	130*
3	2 4	50	17.6
4	4 6	176	1.5
5	6 7	10	1.5
6	7 3	50	10
8	7 3	50	10

\*A<sub>eqv</sub> is given by eqn 3.16

<sup>11</sup> Based on layout in (Brekke, 1984), numbering modified

Table 6.4 Tafford turbine and governor characteristics

Turbine characteristics (Pelton)		Governing characteristics	
$Q_n$	0	$T_d=K_P/K_I$	10
$Q_y$	0.7	$T_a$	7.19
$E_q$	0	$b_t$	0.332
$E_n$	0	$b_p$	0
$K_q$	1.0	$K_n$	0

The equivalent area indicated in Table 6.3 is related to the air accumulator surge shaft in Figure 6.7. An air accumulator is an enclosed surge shaft filled with pressurized air. The equivalent area is estimated by equation 3.16:

$$A_{eqv} = \left[ \frac{1}{130} + \frac{1.25 \cdot 734}{50} \right] m^2 \approx 0.0544m^2$$

In order to reduce the complexity of the system to the algorithm of the computer simulation the tunnel area was estimated by a length-to-area weighted average of 10.94m<sup>2</sup>. The total tunnel length, from intake to the air accumulator is 7567m. The Pelton turbine was modeled by introducing simple characteristics according to Table 6.4. The rotating machinery has a time constant,  $T_a = 7.19$ , as indicated in the same table.  $b_t$  and  $T_d$  were set to 0.332 and 10 respectively to match the settings in the pressure response experiments.

The pressure response  $h/y$  is shown in Figure 6.8 and the experimental results are included for comparison. The gain plots correspond well with the experimental results, and are almost identical above 0.1rad/s. The overestimated amplitude of the simulations below 0.1rad/s indicate that the friction has larger influence on the pressure response at low frequencies. One noticeable characteristic in the plot is the corner that appears right above 0.2rad/s, which corresponds to a sharper peak in the phase plot at the same frequency. The surge shaft “rule-of-thumb” frequency (equation 2.17) was calculated to be at 0.51rad/s, which suggests that the rough calculation overestimates the frequency somewhat in this case. Frictional damping in the long headrace tunnel is likely the main reason for the poor coherence between the rough estimate and the simulation/measurements.

The phase plot has the same characteristics as the measurements. However, the simulated phase lag is overestimated throughout the entire frequency spectrum. Brekke reported

deviations in phase angle compared to his theoretical results<sup>12</sup>. This deviation was explained by the small amplitudes used in the input signal to the servomotor.

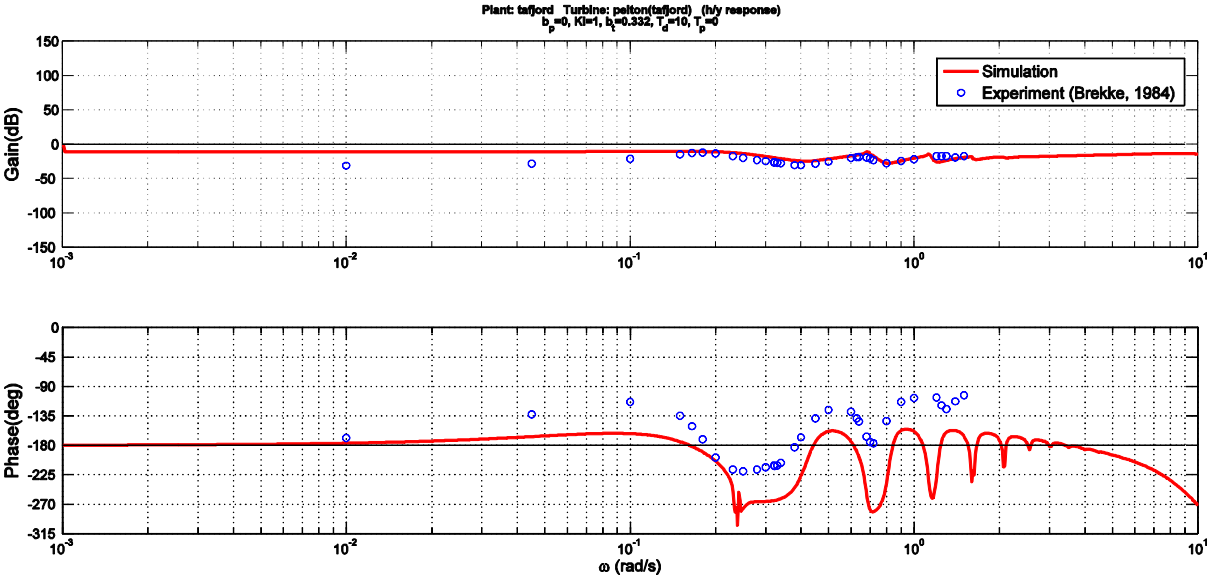


Figure 6.8 *h/y response with Brown friction model*<sup>13</sup>

The frictional damping factor,  $K$ , is plotted in Figure 6.9. The real part of the friction constant is highly influenced by the oscillations in the system and the magnitude oscillates around fairly consistent values throughout the frequency spectrum. This is expected as the real friction is primarily related to the flow rate in the surge shaft. The influence of the imaginary part of the friction contributes to a total increased frictional damping at higher frequencies as it is primarily frequency dependent. The frictional plot reflects the frictional dependence on primarily flow rate, tunnel geometry, as well as frequency.

In the previous case at Kongsvinger an inelastic model would have been sufficient to show the major system characteristics. However, for the high head and long conduits at Tafjord the full elastic model is required to incorporate the physical water hammer effects and high frequency dynamics of the system.

The  $n/n_{ref}$  stability is plotted in Figure 6.10. The surge shaft is exceptionally important to the hydropower system at Tafjord. Due to the surge shaft the crossing frequency is fairly low, which will affect the possible stable transient response of the system. The phase margin is well within the requirement; however it is defined by the air accumulator

<sup>12</sup> (Brekke, 1984, p. 146), the measurements show a systematic error of 0°-20° less negative phase shift compared with expected values due to experimental details.

<sup>13</sup> The phase plot is shifted by -180 degrees

frequency. The phase margin will therefore likely depend highly on the condition of the air accumulator. The  $n/n_{ref}$  plot generated by Brekke is almost identical, with slightly lower stability margins<sup>14</sup>. It should be remarked that air accumulators are rare in hydropower systems. The air accumulators often depend on quality rock and their dynamic behaviour is not necessarily easily predicted.

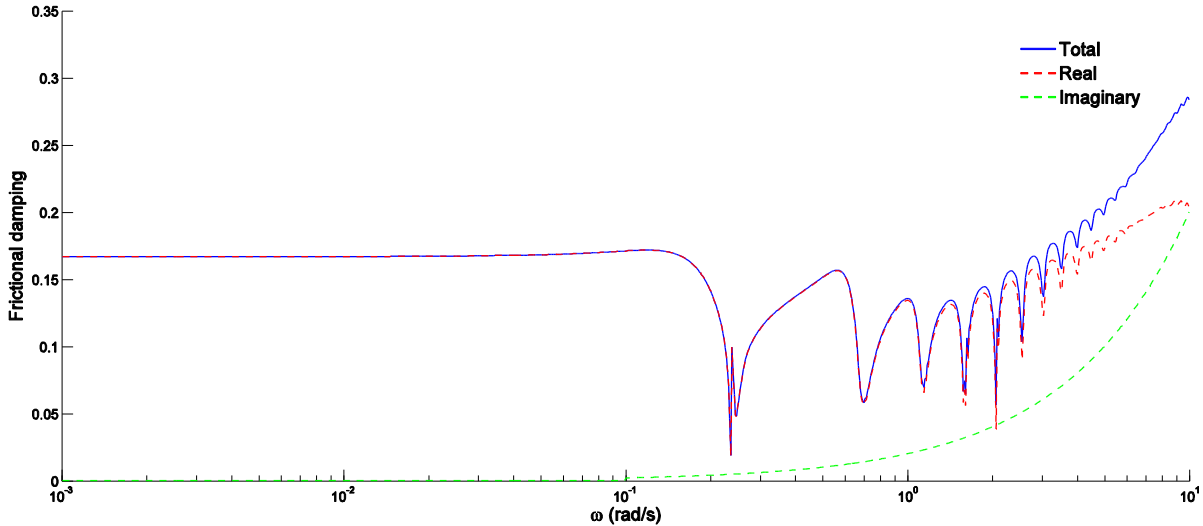


Figure 6.9 Friction damping,  $K$  (surge shaft)

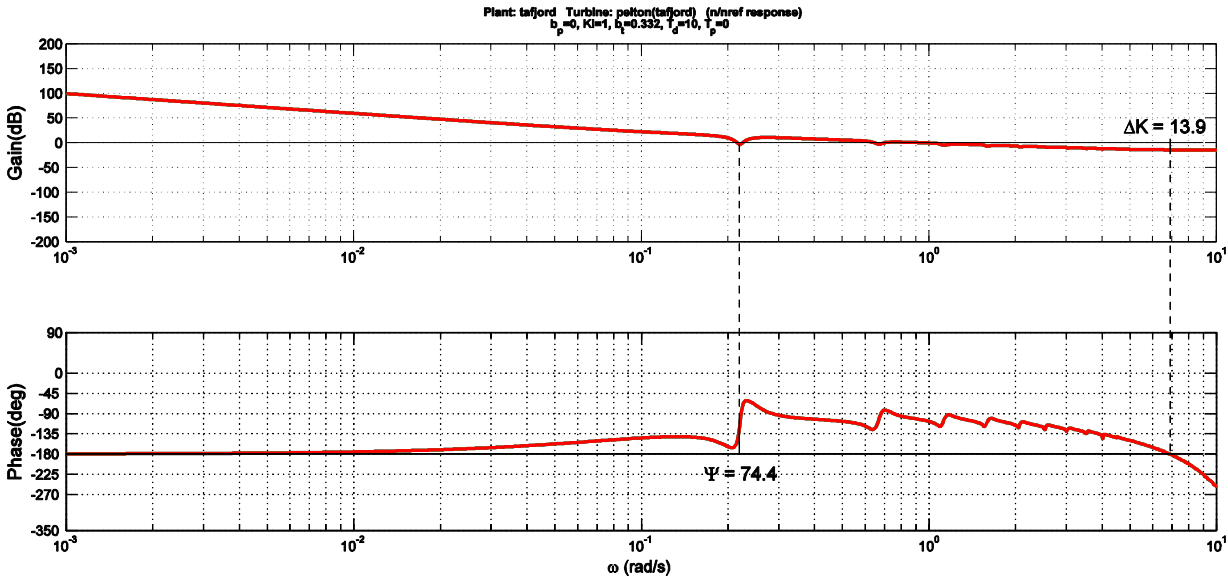


Figure 6.10  $n/n_{ref}$  stability analysis

<sup>14</sup> Brekke’s plot is supplied in Appendix D for comparison.

### 6.2.1 The damping factor

The long water conduits of the Tafjord waterways are ideal for evaluating the frictional model of the simulations. The frictional head loss was reported by Brekke at the Tafjord power plant along with the Manning numbers for the water conduit (Brekke, 1984).  $\epsilon/D= 0.007$  and  $0.0001$  for the head race and pressure tunnel respectively was used in the friction model, as a base for determining the friction factor ( $f$ ).<sup>15</sup> In order to tune the frictional influence of the pressure response at Tafjord, the tuning parameters  $a, \beta$  and  $\gamma$  were added to equation 5.4:

$$K = \frac{4\lambda Q_t}{\pi D^3} + \alpha(\beta C + \gamma - 1)j\omega \quad 6.1$$

The effects of the three variables are shown in Figure 6.11. When the three variables in equation 6.1 were increased, the gain of the response was flattened, while the phase response was shifted up and to lower (absolute) angles. The shifted phase of the response is mainly due to the earlier mentioned discrepancies in the physical measurements. The magnitude of the resulting damping mainly influences the gain response.

The gain below 0.1 rad/s is overestimated by the simulation. However, if the steady state frictional term in equation 6.1 is reduced by 30%, the gain follows the measurements smoothly. The gain of the original frictional damping matches the experiments fairly well and the adjustment would be purely empirically motivated. Such an adjustment would depart from principles of conservative simulations and could only be valid for similar systems. For these reasons the manipulation can hardly be justified if the program is to be used to evaluate the stability of new hydropower projects. Thus the author decided to persist using the Brown friction factor in its original form, despite the minor discrepancies. This friction model analysis concludes the validation of the simulation program.

---

<sup>15</sup> This roughness was calculated by equation 5.1 and 5.2 based on the reported Manning numbers throughout the tunnels.

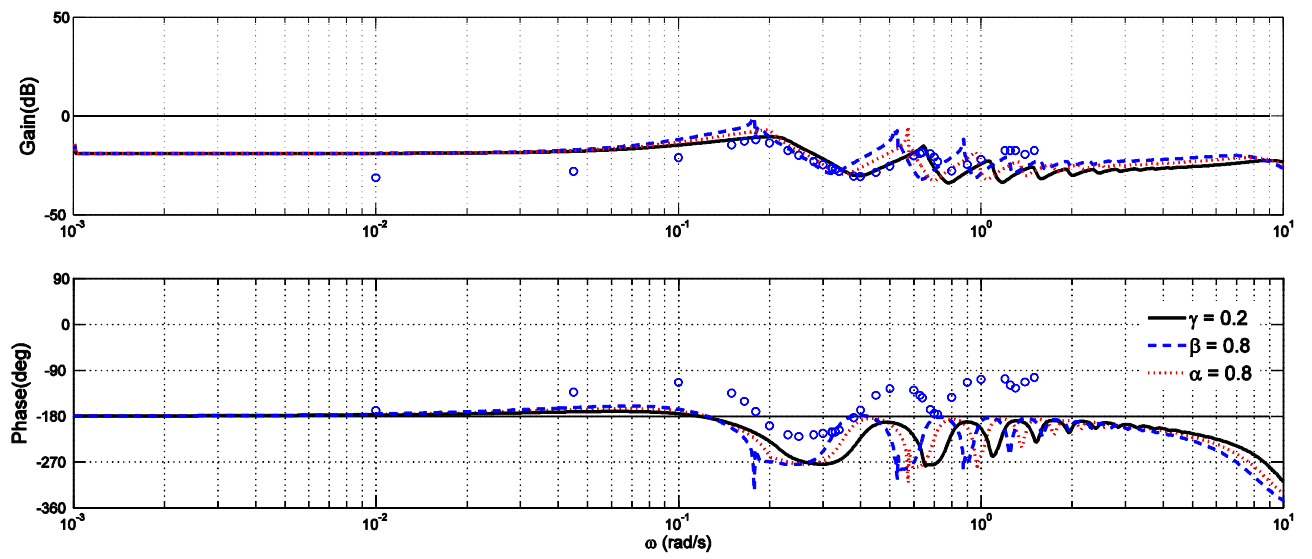


Figure 6.11 Influence of friction model scaling



## 7 Model Application

The model validation was presented in the previous chapter. This chapter will attempt to apply the simulations to the proposed new power plant at Aldal. Stud. Tech. Remi Stople has been studying the time responses at the proposed new hydropower system for BKK and has supplied the information about Aldal<sup>16</sup>.

### 7.1 Aldal powerplant

Aldal powerplant is a proposed new powerplant in Aldalen 50 km from Bergen. A complete new water conduit along with a powerhouse is proposed. A stability analysis of the system layout is desired.

The tunnel at Aldal powerplant originates at Grøndalsvatnet ( $H_0=198,1$ ) and is channeled through a  $30\text{m}^2$  tunnel, 5700m down to Samnangerfjorden. A Francis turbine unit at 61MW, with a rated flow rate of  $35\text{m}^3/\text{s}$  is proposed. A surge shaft is proposed 1191m upstream the Francis turbine unit. The system layout is shown in Figure 7.1.

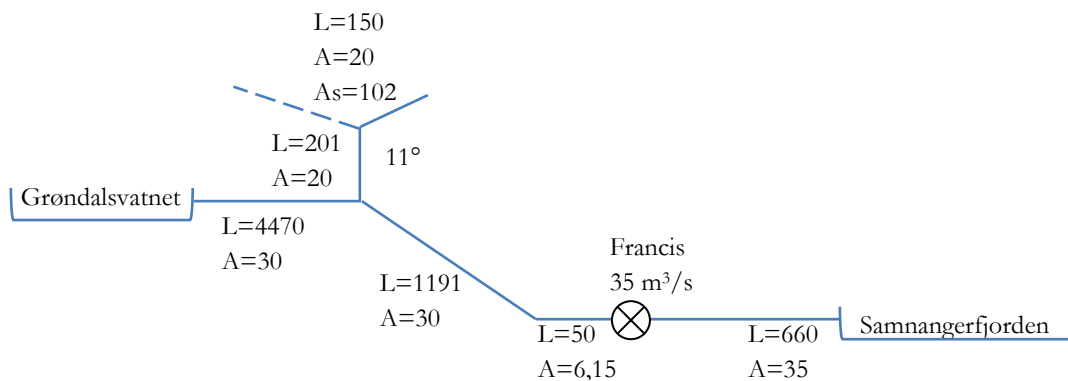


Figure 7.1 Simplified system layout of Aldal

Prior to modelling Aldal powerplant some simplifications and the key system parameters must be determined. The stream intake, shown by dotted lines in Figure 7.1 above was neglected. The intake will act as additional surface to the surge shaft and thus add system stability despite the additional oscillation between the two branches. The water conduit time constant,  $T_w=1,36\text{s}$ , and the Thoma criterion area is  $16,04\text{ m}^2$  (based on a 50% safety

<sup>16</sup> The projecting by BKK at Aldal is still under progress and the information is thus based on preliminary work.

factor and  $M=35$ ). First an estimate of the governing was executed by applying Stein's empirical governing formulas to generate the Bode diagram plot in Figure 7.2 (Nielsen, 1990):

$$T_d = 3 \cdot T_w \quad 7.1$$

$$b_t = 2.6 \cdot \frac{T_w}{T_a} \quad 7.2$$

The stability margins based on Stein's formulas do not fulfill the Nyquist criterion (eqn. 4.8). In particular the phase margin deviates significantly. However, from experience (Brekke, 1999) it is reported that the criterion can be reduced to  $30^\circ$  and 3dB if the system is connected to a separate ohmic network (which is the case for Aldal). The governor has to be adjusted in order to fulfill these limits. The  $b_t$  and  $T_d$  setting envelope is calculated based on the transfer function output<sup>17</sup> in equation 4.2 and Appendix E and presented in Figure 7.3. It is apparent that the phase margin is the limiting identity in this case.  $T_d=8$  and  $b_t=0.8$  were chosen and plotted together with the values from Stein's formula in Figure 7.2.

Notice that the self-regulating effect of the Francis turbine is included, as the phase lag originates from  $-90$  degrees. The self-regulation has a positive influence on the system stability as the flow rate will decrease with increased rotational speed. Permanent speed droop is however not included as it will only have a positive influence on the system stability. The dotted lines represent the closed-loop response  $|N|$ . With the adjustments, the blue line shows that the closed loop overshoot around the crossing frequency is within the requirement of  $|N|_{\max} < 4\text{dB}$ . It should be noted that by implementing the suggested governing parameters, the frequency of the open-to-closed loop crossing is fairly low. The closed loop system governing is efficient below this asymptotic crossing frequency. Above the crossing frequency  $N$  follows the 0 dB line and the open loop identity  $M = |A|$ .

---

<sup>17</sup> The stability margins based on the transfer functions at Aldal were calculated through a Matlab loop for the entire range  $0.1 < b_t < 2$  and  $1 < T_d < 14$ .

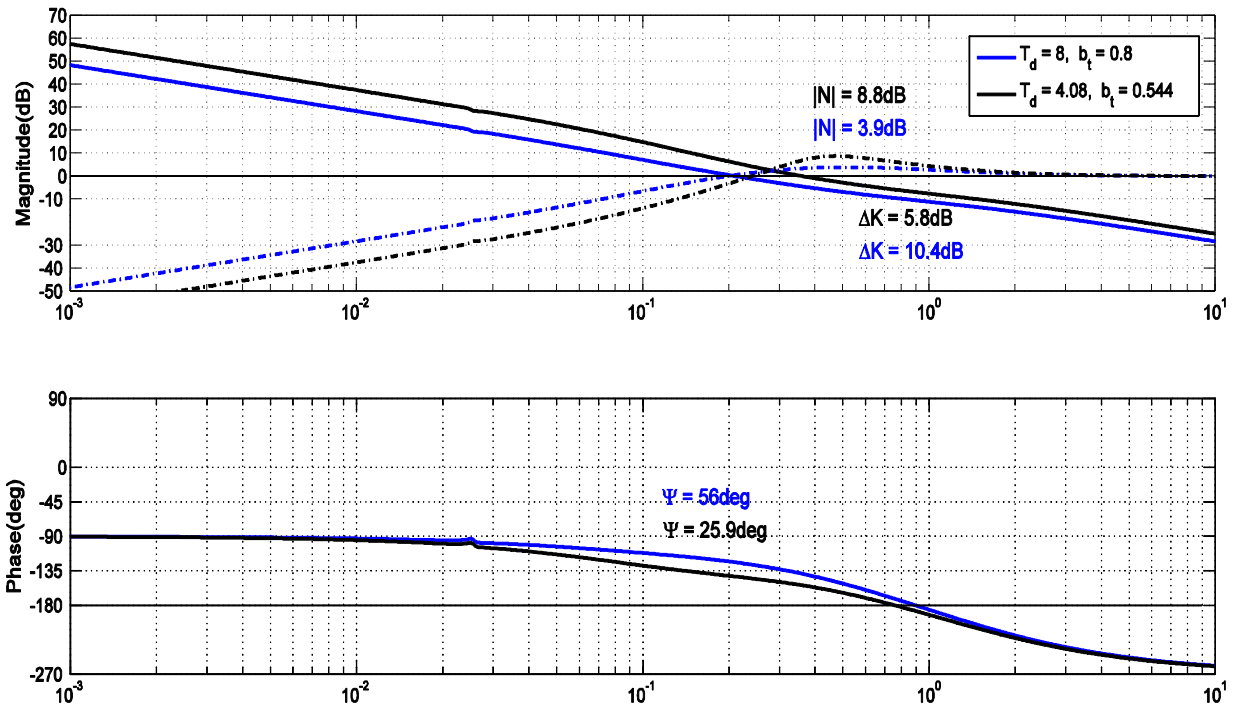


Figure 7.2 Bode diagram based on transfer function

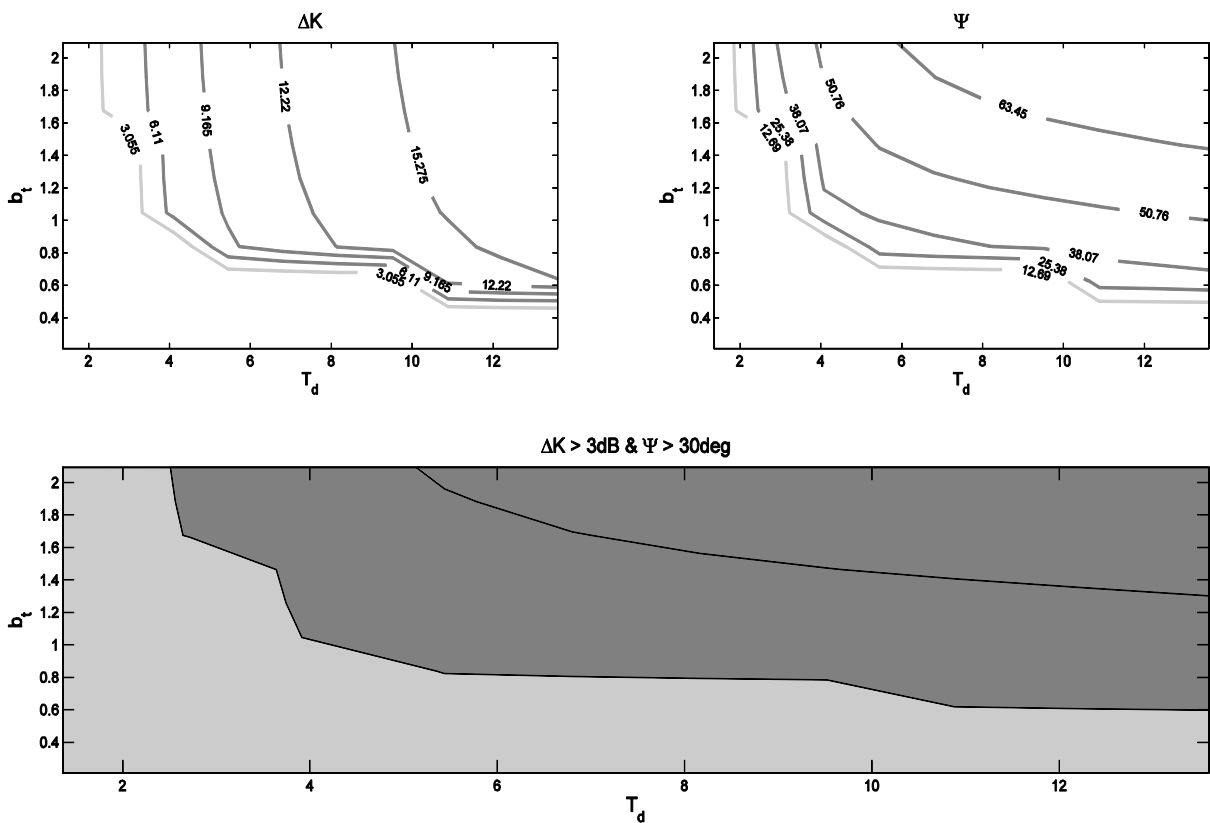


Figure 7.3  $b_t$  and  $T_d$  envelope (ref. Appendix E)

The turbine characteristics are not available, thus the values available for the similar powerplant at Jørundland are used to represent the turbine (Brekke, 1984). The choice of characteristics is justified by the similar speed numbers of 0.41 and 0.43, at Jørundland and Aldal respectively.

*Table 7.1 Turbine characteristics (Jørundland) and governing of Aldal*

<b>Turbine characteristics, Francis 55MW, 265m, 23m<sup>3</sup>/s</b>		<b>Governing characteristics</b>	
$Q_n$	-0.55	$T_d=K_P/K_I$	8
$Q_y$	0.9	$T_a$	6.5
$E_q$	0	$b_t$	0.8
$E_n$	0	$b_p$	0
$K_q$	1.19	$K_n$	0

A stability study of Aldal was performed and is presented in Figure 7.4. The smoothing “unwrap”-function was found necessary for presenting the phase angles at high frequencies, where the water hammer effects become significant<sup>18</sup>. This disables the presentation of waterhammer effects on the phase angle, which does not seem to influence the stability and thus only crowds the presentation in this case. The surge shaft appears at around 0.025rad/s, which matches the estimation by the rule-of-thumb equation (eqn. 2.17) perfectly.

The full-friction simulation is compared with a frictionless simulation in the same figure. The stability margins of the two simulations do not differ significantly and both are well within the stable region with the governing characteristics of Table 7.1. The gain and phase margin of the full frictional model is 17 dB and 67 degrees, respectively. The friction model show some oscillatory behaviour in the asymptotical region at the surge shaft resonant frequency. This effect arises from both the real and imaginary part of the frictional damping ( $K$ ) where the surge shaft level has the highest amplitude fluctuations.

<sup>18</sup> In simulations without the “unwrap” function, the phase response alternate between -180 and 180 degrees due to the rapid changes arising from the waterhammer effects. As this is only a matter of convention, the function was utilized. Information about the function is available in Matlab’s documentation (Matlab, 2012).

The effect of waterhammers are apparent on the gain plot and do not influence the stability of the system.

The surge shaft stability boundary with respect to surge shaft surface area with the proposed governing settings was found to be around 1 m<sup>2</sup>. This stability boundary is well below the Thoma criterion ( $A_T=16$  m<sup>2</sup>), which is expected as the criterion is conservative. Based on the simulations the location and surface area of the surge shaft is well within the stability bounds for the proposed power plant.

The lowest frequency where the waterhammer appears is just above 1 rad/s, which is close to the estimated frequency of 1.02 rad/s based on the reflection time ( $T_r=6.15$ s). The crossing frequency with the proposed governor is well below the waterhammer frequency. Thus the waterhammer will not destabilize the system control.

In Figure 7.5 the rotational speed response upon load variations is shown. The response is dampened, but the ratio is about -1.6 dB at the crossing frequency. The requirement for stable operation is often set to 0 dB. Nonlinear movements, friction and uncertainties in the control mechanisms are not accounted for, but can easily be included through experiments. As the information available and the geometries supplied are limited this concludes the application of the developed simulation program. In chapter 8 the control system of hydropower systems will be investigated closer.

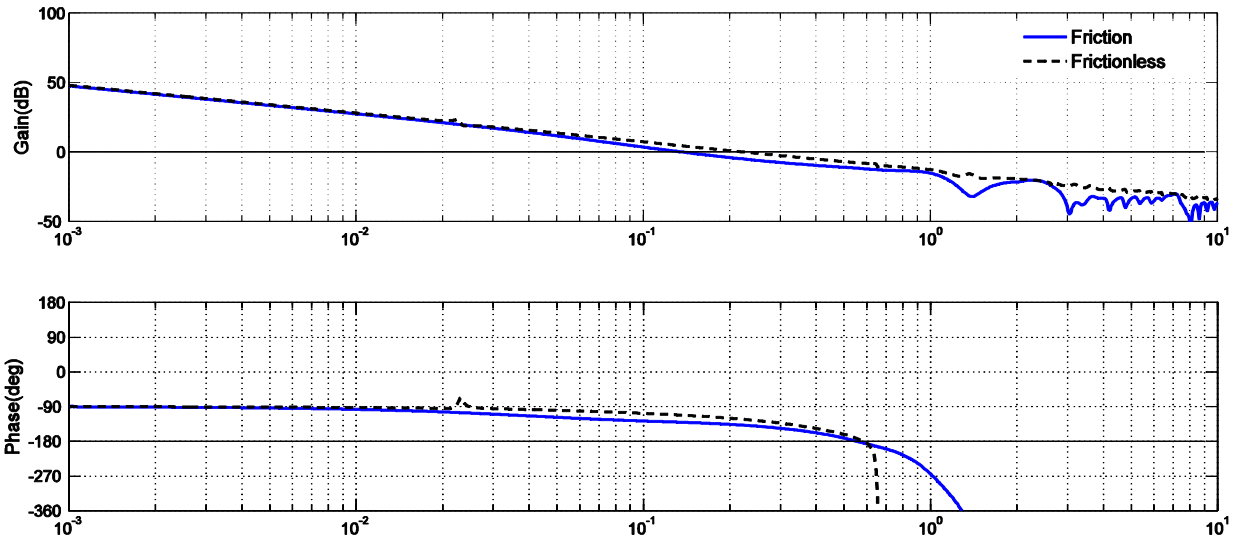


Figure 7.4 Aldal  $n/n_{ref}$  stability study

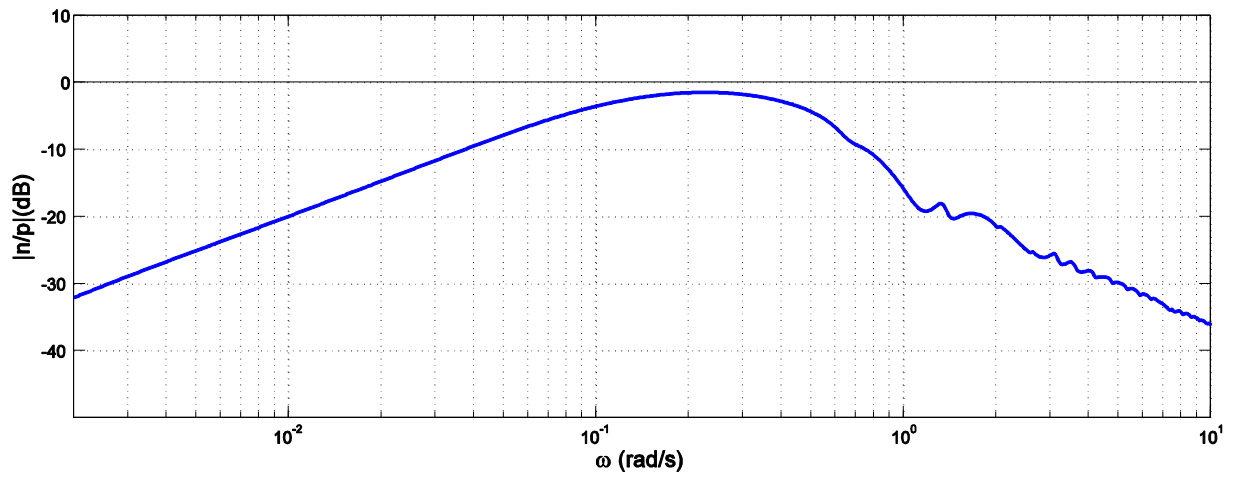


Figure 7.5  $n/P_{gen}$  response for Aldal

## 8 Hydropower governor control

Hydro-electric power plants are multivariable, non-linear and non-stationary systems often exposed to unpredictable load. The characteristics of the system vary significantly, requiring an efficient and reliable controller for stable operation. The task of adequately solving the challenges related to hydropower governing is still progressing. This section will present some of the proposed approaches and their application. The review is based on the research overview in (Kishor, et al., 2007) and transfer function analysis.

Methods for improving stability of hydropower systems have been discussed in several publications<sup>19</sup>. One possibility is to dampen or eliminate the governor. However, within the scope of practically possible values of  $T_d$  and  $b$ , this approach will actually worsen the situation. For power plants connected to large interconnected grids, the surge shafts will always be stable. Some systems have even applied surge shafts below the Thoma criterion for this reason (Xinxin, 1989, p. 101). In the following paragraphs some alternative approaches to hydropower system governing will be investigated.

### 8.1 Classical control approach

The classical approach in linear controller modeling is primarily based on single-input and single-output (SISO) control. The classical controls are mostly based on PID-governing and graphical or tuning guidelines to set the parameters. The more advanced classical methods are based on variable gain control through the root-locus method (Kishor, et al., 2007).

A range of modern approaches to hydro power control have been proposed. The modern approaches are often also suited for multiple inputs and outputs (MIMO). Some of these are optimal control, adaptive control, projective control, robust control and nonlinear control.

---

<sup>19</sup> The publications discussed in this thesis are exerts from reference (Kishor, et al., 2007), (Xinxin, 1989), (Xinxin, 1989), (Herron & Wozniak., 1991), (Imsland, 2010).

### 8.1.1 Water column compensator

In a few prior articles additional compensators have been investigated to extend the governing stability. Such a compensator can be integrated as shown in Figure 8.1. The compensator transfer function can take various representations in the block diagram. Shen suggested this simple transfer function for a water column compensator (Xinxin, 1989):

$$K(s) = \frac{-T_w s}{(1 + 0.5T_w s + 0.1T_r^2 s^2)} \quad 8.1$$

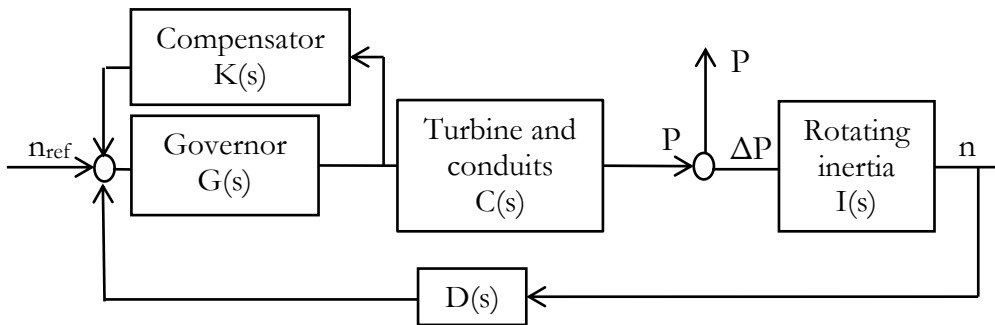


Figure 8.1 Water column compensator

An open-loop transfer function is established in equation 8.2. The transfer function is based on general reduction of block diagrams and is derived in Appendix E.

$$A(s) = \frac{(1 + T_d s)(1 + 0.5T_w s + 0.1T_r^2 s^2) - b_t T_w T_d s^2}{(b_t T_d s + b_p)(1 + 0.5T_w s + 0.1T_r^2 s^2)} \cdot \frac{p}{y} \cdot \frac{1}{T_a s + b_s} \quad 8.2$$

If the  $p/y$ -fraction is replaced by the conduit equation in Appendix E, the Aldal hydropower plant can be represented by the root locus shown in Figure 8.2.<sup>20</sup>

<sup>20</sup> The plot is generated by the code supplied in Appendix E



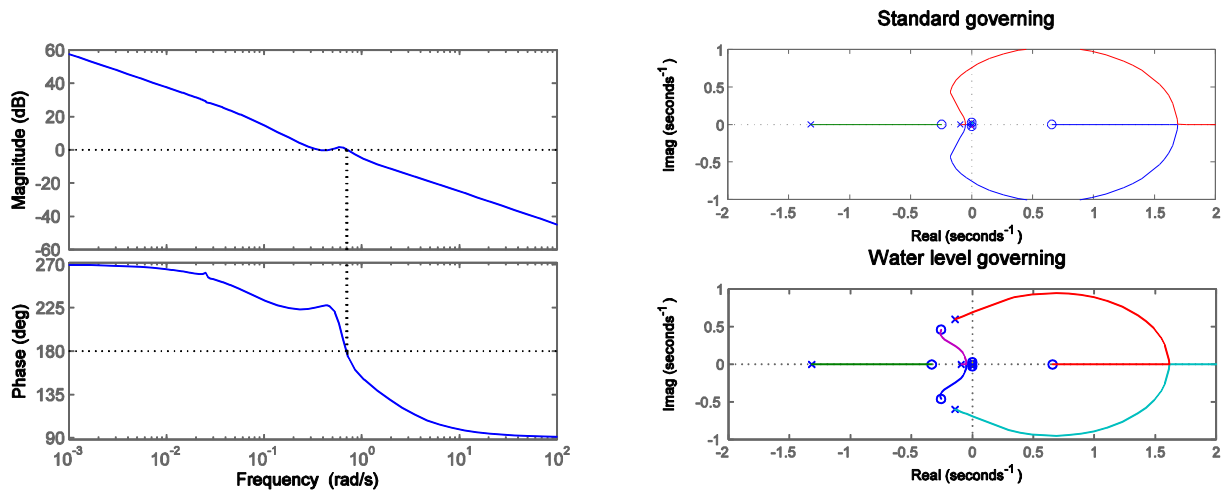


Figure 8.2 Effect of water level governor on Aldal

Xinxin (Xinxin, 1989) mentions that the water column compensator should not be used for hydropower systems with  $h_w < 0.6$ . At Aldal  $h_w \approx 0.3$  and the system has a pair of complex conjugates poles close to the imaginary axis. This clearly affects the stability of the system and adding a water column governor is in this case not advisable. In order to implement this extra control feature to the simulation program equation 8.3 could be applied.

$$y = K_p + \frac{K_I}{s} + K_w y = \frac{1 + T_d s(1 + b_t K_w y)}{b_t T_d s} \quad 8.3$$

### 8.1.2 Pressure compensator

Some authors have suggested that adding a pressure compensator to the control system will improve the governing (Kishor, et al., 2007) (Xinxin, 1989) (Herron & Wozniak., 1991). Herron and Wozniak proposed the layout in Figure 8.3, with an observer block in the compensator feedback loop. This approach will be simplified somewhat to study the effect of a pressure compensator at Aldal.

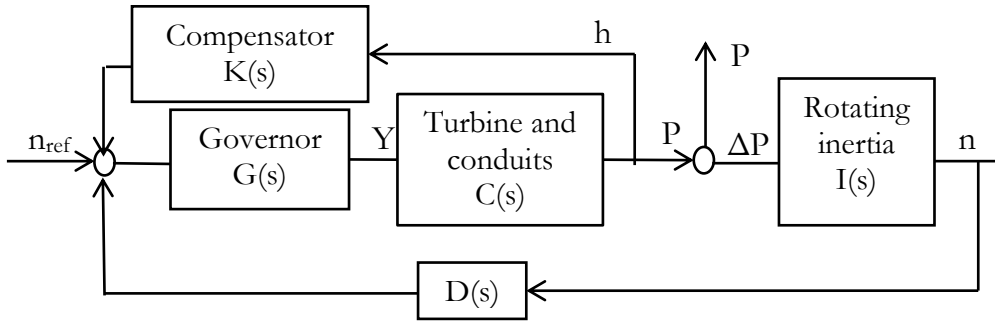


Figure 8.3 Governor with integrated compensator

Xinxin (Xinxin, 1989) suggests that the general compensator filter transfer function should take the form of:

$$K(s) = \frac{-T_1 s}{(T_2 s + 1)(T_3 s + 1)} \quad 8.4$$

This transfer function of  $K(s)$  will act as a band pass filter, filtering out high frequency and dc components. An important consideration is the interaction between the  $n$ - $n_{ref}$  feedback and the compensator feedback. The compensator must have a response that is significantly quicker than the  $n$ - $n_{ref}$  feedback in order to avoid “competing” control signals. The pressure feedback will add a term in the governor equation:

$$y = K_p + \frac{K_I}{s} + K_h h = \frac{1 + T_d s(1 + b_t K_h h)}{b_t T_d s} \quad 8.5$$

The Bode plot and root locus of Aldal with standard governing and with a pressure compensator is shown in Figure 8.4.<sup>21</sup>

<sup>21</sup> The figures are generated by implementing the inelastic transfer functions presented in Appendix E Transfer functions.

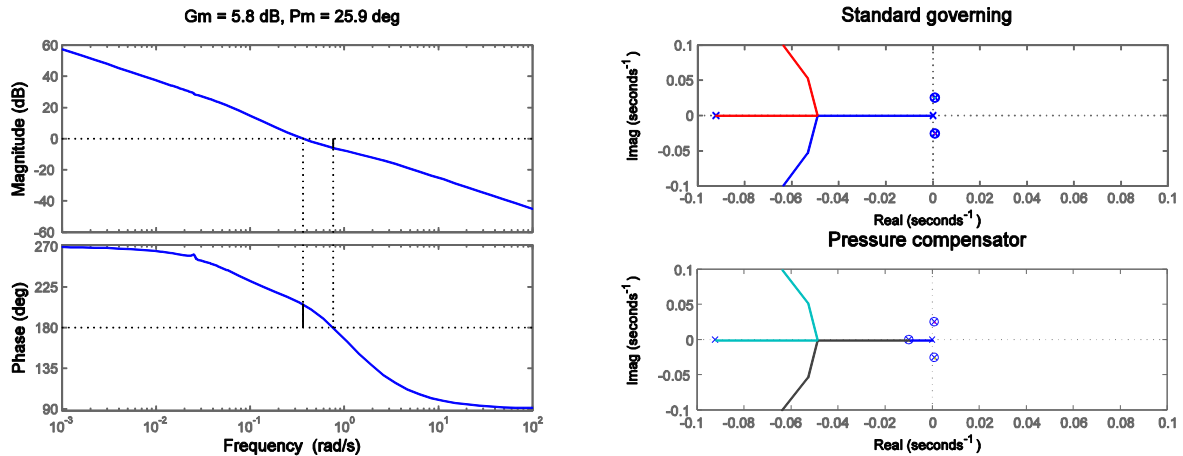


Figure 8.4 Effect of pressure compensator on Aldal

The pressure compensator has little influence on the stability at Aldal. However, the root locus in Figure 8.2 shows that the pressure compensator add an additional pole and zero on the left half plane on the real axis. This will improve the transient response of the system. The improvement shown by the root loci follows the observed improvements reported by (Herron & Wozniak., 1991). Equation 8.5 can be included in the simulation program by storing the value of the pressure head vector ( $h$ ) at the turbine from the previous frequency and applying it directly to the governor.

## 8.2 Optimal control (LQR og MPC)

A large compromise with classical approaches is often the general parameter settings. Optimal control seeks to find a “performance cost equation” and minimize its index based on the internal set of performance objectives. The technique allows for flexible creation of a performance equation which is well suited for MIMO systems. Two optimal control strategies are Linear Quadratic Control (LQR) and Model Predictive Control (MPC).

Linear Quadratic Control (LQR) is a simple approach for optimal control. No model is required and a cost function with an infinite horizon is established. LQR is incorporated with the same block diagram as presented earlier. It is a proportional control, but the system is modeled based on the established function. The proportional matrix ensures stable operation at all operating points.

MPC is able to ensure that the control parameters stay optimal through an extended range of operating conditions. MPC is also referred to as the constrained LQR and is organized as shown in the block diagram of Figure 8.5. MPC is an optimal control design that takes into account constraints on the system signals. MPC is a widely used technique in process control, but has not been studied extensively for hydropower applications (Kishor, et al., 2007).

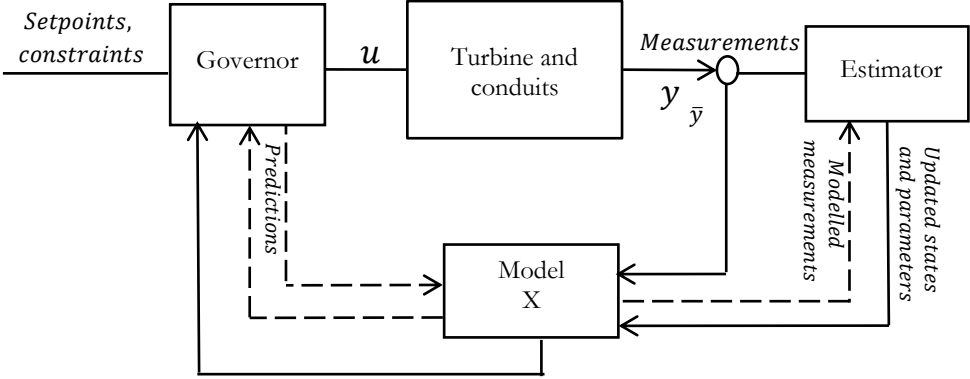


Figure 8.5 Model Predictive Control (Imsland, 2010)

The model is typically obtained by linearization or by establishing system identification based on measured data (Imsland, 2010). The method offers a prediction of a finite system response and optimizes the future behavior at each time step.

One main source of inaccuracy in the controller is the linearization of nonlinear systems (Herron & Wozniak., 1991). The sometimes significant uncertainties arising are related to parameter changes, unmodeled dynamics, unmodeled time delays, sensor noise and unpredicted disturbance inputs. The estimator seeks to filter noise from the measurement by application of for example Kalman filters. System states that are not measured can also be estimated by a feedback sequence between the estimator and model. The system model processes the measurements and estimates the optimal settings. The final control action is performed upon predictions after feedback between the governor and system model.

While requiring a customly made model, MPC is an intuitive control method. The proportional control actions are based on interaction between the model and governor optimization. Referring to Figure 8.5,  $u_t = K \cdot x_t$  if  $K$  is a proportionality input and  $t$  refers to the time step. The constraint settings are straightforward compared to most other control methods. Boundary or “box” constraints are applied directly to  $u$  and  $x$ . Thus MPC allows optimal system settings close to the operational boundaries. MPC can thereby obtain satisfactory stability and optimal turbine performance is maintained over a wide set of operating conditions.

MPC requires a thorough understanding of the process in order to model the system and define the cost function. Further investigations is beyond the scope of this thesis. MPC control has not yet been studied extensively in hydropower plants (Kishor, et al., 2007). However, with increasing issues related to hydropower governing, the method might constitute a part of the future solution.

## 9 Discussion

The simulation program validation and application has been discussed throughout the previous chapters. The supereminent objective of the validation is to describe the abilities and limitations of the simulations. Some last remarks on the simulations are therefore in its place.

The Simulations of the Kongsvinger power plant showed excellent correspondence with the experimental results. The  $n/n_{ref}$  response was close to equivalent to the results produced by Brekke's simulations. Thus it can be argued that the current simulation program models the dynamics of short conduits well.

The Tafjord powerplant has a long and somewhat complicated water conduit. Some simplifications where made to simulate the pressure response. The simplifications might have influenced the resulting Bode plot to a certain degree. The major simplifications are however conservative as the friction in bends and contractions are not included. The deviations in phase response are to a large degree explained by the previously mentioned systematic error in the measurements. A range of uncertainties related to the experimental mechanics, the air accumulator interactions and nonlinearities are not captured by the simulations. The frictional damping of the model underestimates the real frictional influence as it has been purposely held conservative. Overall, the simulations do however capture the trend of the physical measurements. Viewed against this background the open-loop stability analysis also reflects the dynamic situation at Tafjord well.

The proposed powerplant at Aldal is not compared to other sources and the mentioned limitations should be regarded. The simulations suggest that the power plant is sufficiently stable with the proposed governor settings and turbine characteristics. Since the turbine characteristics at Aldal are not available the dynamical analysis is limited to operation at the steady-state point.

The suggested alternative governing methods are limited to previously established control strategies. The investigation suggest that the water column compensator is not advisable at Aldal, while the pressure compensator might give improved transient responses. Since the modeling of these control strategies were limited to transfer function analysis these results should only be considered as preliminary suggestions. The risk of relying on the governor alone to obtain system stability has not been discussed in this thesis. Considering the possible concequences of severe instabilities this risk might on its own motivate the design of inherently stable hydropower systems.

## 10 Conclusion

A system model based on the structure matrix method has been implemented in a Matlab simulation program. The program allows for simulation of hydropower systems with up to two upstream and one downstream surge shafts. A method to incorporate the turbine characteristics more efficiently compared to manual inputs was developed. Further a frictional damping model based on Brown's theory was included and the effect investigated.

The simulation program was validated through comparison of measurements and prior simulations at Kongsvinger and Tafjord power plants. The program generally showed good coherence to the physical dynamics of the two systems. The frictional influence is slightly underestimated, rendering the program a conservative measure of system stability and dynamics.

The simulation program was applied to investigate frequency stability at a proposed new power plant at Aldal. Based on the geometry and an estimated turbine model the governor setting for a PI governor was proposed. System stability is achieved with the proposed geometry at operation around the steady state point.

Three alternative control strategies have finally been suggested. In the case of Aldal, a water column compensator is not advisable, while a pressure compensator will likely yield improved transient responses. Optimal control is an interesting alternative that, while requiring more investigation, likely will give improved hydropower governing.

## 11 Further work

In future development of the simulation program, the following should be considered:

- Include a flexible matrix algorithm for complete geometrical freedom in the implementation of hydropower systems.
- Improve the user interface of the simulation program
- Incorporate a more complete and complex electrical-hydraulic interface of the system simulation.
- Simulate dynamics of multiple hydropower systems on an interconnected grid.
- Implement some of the investigated alternative control system designs and investigate their effect on hydropower system stability.



## 12 Bibliography

- Brekke, H., 1984. *A Stability Study on Hydro Power Plant Governing Including the Influence from a Qasi Nonlinear Damping of Oscillatory Flow and from the Turbine Characteristics*. Trondheim: NTNU, Phd Thesis.
- Brekke, H., 1999. *Regulering Av Hydrauliske Strømningsmaskiner*. Trondheim: Vannkraftlaboratoriet.
- Brekke, H. & Xinxin, L., 1987. *Mathematical Modelling of Oscillatory Flow in Hydro Power Plant Conduits*. Lille, France, s.n.
- Eek, J., Gjengedal, T. & Uhlen., K., 2006. *Influence of High Wind Power Penetration on the Nordic Power Grid Primary Control Response*. Paris. Print.: CIGRÉ.
- Herron, J. R. & Wozniak., J., 1991. A State-space Pressure and Speed Sensing Governor for Hydrogenerators. *IEEE Transactions on Energy Conversion*, Vol. 6(3rd. Print), pp. 414-418.
- Imslund, L., 2010. *Introduction to Model Predictive Control*. Notes ed. Trondheim: NTNU.
- Jonsson, I., 1980. A New Approach to Oscillatory Rough Turbulent Boundary Layers. *Ocean Engineering*, Volume 7.1, pp. 52-109 .
- Kishor, N., Saini, . R. & Singh., S., 2007. A Review on Hydropower Plant Models and Control.. *Renewable and Sustainable Energy Reviews*, 11.5(Print), pp. 776-96.
- Lindeberg, 2010. *Frekvensavvik*. Ålesund, Servomøtet 2010, 20.10 - 21.10, Høgskolen i Ålesund .
- Matlab, 2012. *Matlab Documentation*. [Online]  
Available at: <http://www.mathworks.se/help/techdoc/ref/inv.html>  
[Accessed 09 may 2012].
- Nielsen, T., 1990. *Dynamisk Dimensjonering Av Vannkraftverk..* Trondheim: SINTEF, Strømningsmaskiner.
- NVE, 2012. *NVE documentation*. [Online]  
Available at: <http://www.nve.no/no/Sok/?search=kongsvinger>  
[Accessed 1 may 2012].
- Rydning, A., 2007. *Systemdynamisk Analyse Av Vannkraftsystem*. Trondheim: NTNU.
- Sand, T. W., 1999. *Regulering av Vannturbiner*. Master thesis ed. Trondheim: NTNU.

Vogt-Svendsen, S., 2011. *Stability of Hydro Power Systems (Project Thesis)*, Trondheim: Vannkraftlaboratoriet, NTNU.

Wylie, E. B. & Streeter, V. L., 1993. *Fluid Transients in Systems*. Print ed. Englewood Cliffs: NJ: Prentice Hall.

Xinxin, L., 1988. *Hydropower System Modelling by Structure Matrix Method*. Trondheim: NTNU.

Xinxin, L., 1989. *Stability Analysis and Mathematical Modeling of Hydropower Systems*. Phd. Thesis. Print ed. Trondheim: Norges Tekniske Høgskole.

Xinxin, L., 1989. *Stability Analysis and Mathematical Modeling of Hydropower Systems*. Trondheim: Norges Tekniske Høgskole. Trondheim: NTNU. Phd. Thesis.

Xinxin, L. & Brekke, H., 1988. A new Approach to the Mathematic Modeling of Hydropower Governing Systems. *The Norwegian Institute of Technology*, pp. 371-376.





# Appendix A (hydropower model)

## systemmodel.m

```
% System definitions
clear all;
clc;

%%%%%%%%%%%%%%%%%%%%%%%%%%%%%%%%%%%%%%%%%%%%%%%%%%%%%%%%%%%%%%%%%%%%%%%% choose system geometry and configurations %%%%%%%%%

system_geometry='aldal';           % "case2", "case3", "froland", "aldal" or
"tyinoset", "kongsvinger","tafjord"
turbine='francis(joerundland)';    % "pelton", "francis1" or
"francis(joerundland)"
response_type='n/nref';           % "n/nref", "p/pref", "h/y", "p/y" or
"original"
angle_handling='plain';           % "plain", "unwrap" or "unwrap_upper"
angleadjustment=0;                % angle asjstment for plotting
friction_model=1;                 % 1 for no friction, 2 Brown, 3 for Brekke84
and 4 for Brekke88
friction_scaling=1;               % scaling of the friction models

%governor settings
KP = 1.25;%10;
KI = 0.15625;%1;
KD = 0;
bt = 0.332;
Td = KP/KI;
bp = 0.00;
Tp = 0.00;

value=[1 1 1];
%%%%%%%%%%%%%%%%%%%%%%%%%%%%%%%%%%%%%%%%%%%%%%%%%%%%%%%%%%%%%%%%%%%%%%%%

countvalue=1000;
R9=zeros(countvalue,length(value));
theta9=zeros(countvalue,length(value));
omega=logspace(-3,1,countvalue);

    %System constants
    g=9.81;
    a=1200;

switch system_geometry
case 'case2'
    Q0=20;
    H0=100;
    Qinit=[Q0 Q0];
    area=[20 20 20 20 20 20 20];
    L=[2586 500 10 10 10 10 10 ];
    ed=0.0001;

    getq=zeros(countvalue,2);
    getQ=ones(countvalue,2);
    double(getq);

case 'case3'
    Q0=124;
    H0=580;
    Aeqv2=680;
    Aeqv9=0.001;
    Qinit=[Q0 0 Q0 Q0 Q0 Q0 Q0 Q0 0];
    area=[56.7 Aeqv2 50 60 20 80 20 20 Aeqv9];
    L=[6120 200 904 520 50 400 5 5 5];
    pipe_el=[ 1 90 45 45 0 0 90 0 90 ];
```

```

getq=ones(countvalue,2,length(L));
getQ=getq;

case 'tafjord'
% Sectional geometrical constants for Tafjord
Q0=8.8;
H0=816.2;
Aeqv2=0.0544;
Aeqv9=0.0000001;
A_drafftube=100;
Qinit=[Q0 0 Q0 Q0 Q0 Q0 Q0 Q0 0];
area=[ 11 Aeqv2 17.6 1.5 1.5 A_drafftube 0.0001 A_drafftube Aeqv9 ];
L=[ 7567 7 50 176 5 50 1 50 1 ];
pipe_el=[ 0 90 90 0 0 0 90 0 90 ];

getq=zeros(countvalue,2,length(L));
getQ=getq;

case 'kongsvinger'
% Sectional geometrical constants for Kongsvinger
Q0=108.5;
H0=9.5;
Aeqv2=39;
Aeqv9=127;
Qinit=[Q0 0 Q0 Q0 Q0 Q0 Q0 Q0 0];
area=[ 150 Aeqv2 39 106 148 286 51 127 Aeqv9 ];
L=[ 12 10 10 6 15 14 4 20.6 1 ];
pipe_el=[ 0 90 90 0 0 0 90 0 90 ];

% M=[ 32 32 32 32 32 32 32 32 32 ];
getq=zeros(countvalue,2,length(L));
getQ=getq;

case 'tyinaset'
% Sectional geometrical constants for Tyinaset
Q0=30;
H0=30;
Aeqv2=20;
Aeqv9=0.0001;
Qinit=[Q0 0 Q0 Q0 Q0 Q0 Q0 Q0 0];
area=[ 19.8 Aeqv2 19.8 7 19.8 19.8 19.8 19.8 Aeqv9 ];
L=[ 2586 10 20 75 5 30 90 10 5 ];
pipe_el=[ 0 90 90 30 0 0 90 0 90 ];

% M=[ 32 32 32 32 32 32 32 32 32 ];
getq=zeros(countvalue,2,length(L));
getQ=getq;

case 'froland'
% Sectional geometrical constants for Frøland
Q0=30;
H0=158; %Lowest waterlevel minus lower reservoir head
Aeqv2=20;
Aeqv9=0.001;
Qinit=[Q0 0 Q0 Q0 Q0 Q0 Q0 Q0 0];
area=[ 30 Aeqv2 30 30 30 30 30 20 Aeqv9 ];
L=[ 5600 100 50 1500 50 5 100 200 50 ];
pipe_el=[ 0 11 11 30 0 0 90 0 90 ];

% M=[ 32 32 32 32 32 32 32 32 32 ];
getq=zeros(countvalue,2,length(L));
getQ=getq;

case 'aldal'
% Sectional geometrical constants for Aldal
Q0=35;
H0=198;

```

```

Aeqv2=102;
Aeqv9=156;
Qinit=[Q0 0 Q0 Q0 Q0 Q0 Q0 0];
area=[ 30 Aeqv2 20 30 6.15 6.15 20 35 Aeqv9 ];
L=[ 4000 150 200 1000 10 50 70 450 10 ];
pipe_el=[ 0 11 90 30 0 0 90 0 90 ];

%           M=[ 32 32 32 32 32 32 32 32 32 ];
getq=zeros(countvalue,2,length(L));
getQ=getq;

case 'complex'
% Sectional geometrical constants for Tyinoset
Q0=35;
H0=198;
Aeqv2=1;
Aeqv9=1;
Qinit=[Q0 0 0 0 Q0 0 0 0 Q0 Q0 Q0 Q0];
area=[ 30 Aeqv2 30 30 30 Aeqv9 30 30 30 30 30 30 30 30 ];
L=[ 1500 100 100 15 6000 5 100 460 50 ];
pipe_el=[ 0 45 45 30 0 0 90 0 90 ];

%           M=[ 32 32 32 32 32 32 32 32 32 ];
getq=zeros(countvalue,2,length(L));
getQ=getq;

end

%%%%%%%%%%%%%%%%%%%%%%%%%%%%%%%%%%%%%%%%%%%%%%%%%%%%%%%%%%%%%%%%%%%%%%%%%%%%%%Wait bar%%%%%%%%%%%%%%%%%%%%%%%%%%%%%%%%%%%%%%%%%%%%%%%%%%%%%%%%%%%%%%%%%%%%%%%%%%%%%%
waiter=0;
hwbar = waitbar(0, 'Please
wait...', 'CreateCancelBtn', 'setappdata(gcf, 'cancelling', true)');
setappdata(hwbar, 'cancelling', false)
%%%%%%%%%%%%%%%%%%%%%%%%%%%%%%%%%%%%%%%%%%%%%%%%%%%%%%%%%%%%%%%%%%%%%%%%%%%%%%

for count=1:1:length(value)
%governor settings
KP = KP;
KI = KI;
KD = KD;
bt = bt;
Td = Td;
bp = bp;
Tp = Tp; %time constant in electric hydraulic amplifier
%friction_scaling=value(count);

%FREQUENCY ANALYSIS ROUTINE
for counter=2:countvalue

%%%%%%%%%%%%%%%%%%%%%%%%%%%%%%%%%%%%%%%%%%%%%%%%%%%%%%%%%%%%%%%%%%%%%%%%%%%%%%Wait bar%%%%%%%%%%%%%%%%%%%%%%%%%%%%%%%%%%%%%%%%%%%%%%%%%%%%%%%%%%%%%%%%%%%%%%%%%%%%%%
waiter=waiter+1;
if getappdata(hwbar, 'cancelling');
    delete(hwbar)
    break
end
waitbar(waiter / (length(value)*countvalue),hwbar)
%%%%%%%%%%%%%%%%%%%%%%%%%%%%%%%%%%%%%%%%%%%%%%%%%%%%%%%%%%%%%%%%%%%%%%%%%%%%%%

s=li*omega(counter);

switch system_geometry

case 'case2'

    if counter==2
        getQ(counter-1,:)=Qinit(1);
        getQ(counter,:)=Qinit(1);
    end
end

```

```

for num=1:length(L)
    K(num)=damping(area(1),ed,Q0,omega(counter-1),getQ(counter-1,1));
%!
    z(num)=(s^2+(K(num)*s))^0.5;
    hw(num)=(Q0*a)/(2*area(num)*g*H0);
    T(num)=s/(2*hw(num)*z(num)*tanh((L(num)*z(num))/a));
    S(num)=s/(2*hw(num)*z(num)*sinh((L(num)*z(num))/a));
end

case {'case3','tyinoset','aldal','froland','kongsvinger','tafjord'}

    %Surge shaft values
    H02=H0;
    H09=0;
    Aeqv2=area(2)/sin(pipe_el(2));
    Aeqv9=area(9)/sin(pipe_el(9));
    Q02=Q0;
    Q09=Q0;
    ed_hr=0.01;
    ed_pt=0.0001;
    ed=[ed_hr ed_hr ed_hr ed_pt ed_hr ed_hr ed_hr ed_hr ed_hr];
    friction_scaling=value(count);

    if counter==2
        getQ(counter-1, :, :) = Qinit(1);
        getQ(counter, :, :) = Qinit(1);
    end

    for num=1:length(L)
        K(num)=damping(area(num),ed(num),Q0,omega(counter),getQ(counter-
1,1,num),friction_model,friction_scaling); %!
        z(num)=(s^2+(K(num)*s))^0.5;
        hw(num)=(Q0*a)/(2*area(num)*g*H0);
        T(num)=s/(2*hw(num)*z(num)*tanh((L(num)*z(num))/a));
        S(num)=s/(2*hw(num)*z(num)*sinh((L(num)*z(num))/a));
    end

case 'complex'
    %Surge shaft values
    H02=H0;
    H09=H0;
    Aeqv2=area(2)/sin(pipe_el(2));
    Aeqv6=area(6)/sin(pipe_el(6));
    Q02=Q0;
    Q06=Q0;
    ed=0.00001;

    if counter==2
        getQ(counter-1, :, :) = Qinit(1);
        getQ(counter, :, :) = Qinit(1);
    end

    for num=1:length(L)
        K(num)=damping(area(num),ed,Q0,omega(counter),getQ(counter-
1,1,num),friction_model); %!
        z(num)=(s^2+(K(num)*s))^0.5;
        hw(num)=(Q0*a)/(2*area(num)*g*H0);
        T(num)=s/(2*hw(num)*z(num)*tanh((L(num)*z(num))/a));
        S(num)=s/(2*hw(num)*z(num)*sinh((L(num)*z(num))/a));
        Kres(num)=0.0002; %
    end

end

% a PI-governor has the characteristics:
% G=(1+Td*s)/(bt*Td*s);
G=KP+KI/s+KD*s;
C=1/(1+Tp*s);

```



```

E=-bp-(1/G);
F=(G*bp+1)/(G*C);
Kn=0; % open(0)/closed(1) loop

% Turbine equations
switch turbine
    case 'pelton1'
        Qn=0;
        Eq=0;
        En=0;
        Qy=1;
        Kq=1;
        Ta=6;

    case 'pelton(tafjord)'
        Qn=0;
        Eq=0;
        En=0;
        Qy=0.7;
        Kq=1;
        Ta=7.19;

    case 'kaplan' %Kongsvinger kaplan turbine used
        eta = 0.913; %efficiency
        n0 = 500; %rev per min
        Qn = 0.55;
        Qy = 0.46;
        Eq = 0.113;
        En = -0.18;
        kq = 1.0;
        Ta= 4.8;

    case 'francis' %Driva Francis turbine used
        eta = 0.928; %efficiency
        Qn = -0.62;
        Qy = 1.0;
        Eq = -0.045;
        En = 0;
        kq = 1.16;
        Ta = 6.0;

    case 'francis(joerundland)' %Driva Francis turbine used
        eta = 0.94; %efficiency
        Qn = -0.55;
        Qy = 0.9;
        Eq = 0;
        En = 0;
        kq = 1.19;
        Ta = 6.5;
end

B5=0.5*(1-Qn);
C5=Qy;
J5=(3-En-(1+Eq)*Qn)/(2*(1+Eq));
K5=Qn+En/(1+Eq);
L5=Qy;
M5=-1/(1+Eq);
Q5=Qn;

switch system_geometry
    % Matrix definitions
    case 'casel'
        %inititalize the matrices
        q=zeros(2,1);
        q(1)=1;
        A=[Kn E F; 0 1 0];

```

```

case 'case2'
    q=zeros(7,1);
    q(3)=1;
    A=[-T(1) S(1) 0 0 0 0 0;
        S(1) -T(1)-B5 -Q5 0 -C5 0 B5;
        0 0 Kn E F 0 0;
        0 0 0 1 0 0 0;
        0 J5 K5 0 L5 M5 -J5;
        0 0 -Ta*s 0 0 1 0;
        0 B5 Q5 0 -C5 0 B5];

case {'case3','tyinoset','aldal','froland','kongsvinger','tafjord'}
    q=zeros(9,1);

    switch response_type
        case {'n/nref','original'}
            q(9)=1;
            Kn=0;
        case 'p/pref'
            q(8)=1;
            Kn=1;           %closed(1) loop
        case 'p/y'
            q(3)=1;
            Kn=1;           %closed(1) loop
        case 'h/y'
            q(3)=1;
            Kn=1;           %closed(1) loop
    end

    A=[-T(3)-(s*H02*Aeqv2)/Q02 S(3) 0 0 0 0 0 0 0;
        S(3) -T(3)-T(4)-T(1) 0 S(4) 0 0 0 0 0;
        0 0 L5 -J5 J5 0 0 M5 K5;
        0 S(4) C5 -B5-T(4) B5 0 0 0 Q5;
        0 0 -C5 B5 -B5-T(6) S(6) 0 0 -Q5;
        0 0 0 0 S(6) -T(6)-T(7)-T(8) S(7) 0 0;
        0 0 0 0 0 S(7) -T(7)-((s*H09*Aeqv9)/Q09) 0 0;
        0 0 0 0 0 0 0 1 -Ta*s;
        0 0 F 0 0 0 0 0 Kn];

case 'complex'
    q=zeros(15,1);

    switch response_type
        case {'n/nref','original'}
            q(11)=1;
            Kn=0;
        case 'p/pref'
            q(12)=1;
            Kn=1;           %closed(1) loop
        case 'p/y'
            q(13)=1;
            Kn=1;           %closed(1) loop
        case 'h/y'
            q(10)=1;
            Kn=1;           %closed(1) loop
    end

    A=[ 1 0 0 0 0 0 0 0 0 0 0 0 0 0 0;
        0 1 0 0 0 0 0 0 0 0 0 0 0 0 0;
        0 0 -T(3)-(s*H02*Aeqv2)/Q02 S(3) 0 0 0 0 0 0 0 0 0 0 0;
        0 0 S(3) -T(3)-Kres(4) Kres(4) 0 0 0 0 0 0 0 0 0 0;
        0 0 0 Kres(4) -T(1)-Kres(4)-T(5) 0 0 S(5) 0 0 0 0 0 0 0;
        0 0 0 0 0 -T(7)-(s*H06*Aeqv6)/Q06 S(7) 0 0 0 0 0 0 0 0;
        0 0 0 0 0 S(7) -T(7)-Kres(8) Kres(8) 0 0 0 0 0 0 0;
        0 0 0 0 S(5) 0 Kres(8) -T(5)-Kres(8)-T(9) S(9) 0 0 0 0 0 0;
        0 0 0 0 0 0 0 S(9) -T(9)-Kres(10) Kres(10) 0 0 0 0 0;
        0 0 0 0 0 0 0 0 Kres(10) -Kres(10)-B5 Q5 0 -C5 0 B5;
        0 0 0 0 0 0 0 0 0 0 0 Kn E F 0 0;

```

```

0 0 0 0 0 0 0 0 0 0 0 0 1 0 0 0;
0 0 0 0 0 0 0 0 0 0 J5 K5 0 L5 M5 -J5;
0 0 0 0 0 0 0 0 0 0 -Ta*s 0 0 1 0;
0 0 0 0 0 0 0 0 0 B5 Q5 0 -C5 0 -B5-T(12)];

end

switch system_geometry
case 'case1'
% Get n/nref system response
h=A\q;
nspeed(counter)=h(1);
frequency(counter)=omega(counter);

case 'case2'
% Get n/nref system response
h=A\q;
nspeed(counter)=h(3);
frequency(counter)=omega(counter);

% get the updated flow rates
h_upd=[h(1) h(2)];
A_upd= [-T(1) S(1);
        S(1) -T(1)];
getq(counter,:)=A_upd*h_upd';
getQ(counter,:)=[Qinit(1) Qinit(2)].*getq(counter,:)+[Qinit(1)
Qinit(2)];

case {'case3','tyinoset','aldal','froland','kongsvinger','tafjord'}
% Get system response
h=A\q;
dampingfactor(counter)=abs(K(1));
dampingfactorimag(counter)=imag(K(1));
dampingfactorreal(counter)=real(K(1));
dampingfactor2(counter)=K(3);
dampingfactor2imag(counter)=imag(K(3));
dampingfactor2real(counter)=real(K(3));
switch response_type
case {'n/nref','original'}
nspeed(counter)=h(9); % measuring point n
case {'p/pref','p/y'}
nspeed(counter)=h(8); % measuring point p
case 'h/y'
nspeed(counter)=h(4); % measurement point at 6
end

frequency(counter)=omega(counter);

% get the updated flow rates

h_upd=ones(length(L),2);
A_upd=ones(2,2,length(L));

h_upd(1,:)=h(1) h(2)];
A_upd(:, :, 1)= [-T(3) S(3);
                S(3) -T(3)];
h_upd(4,:)=h(2) h(4)];
A_upd(:, :, 4)= [-T(3) S(3);
                S(3) -T(3)];
h_upd(6,:)=h(3) h(7)];
A_upd(:, :, 6)= [-T(6) S(6);
                S(6) -T(6)];
h_upd(7,:)=h(3) h(7)];
A_upd(:, :, 7)= [-T(6) S(6);
                S(6) -T(6)];

getq(counter,:,1)=A_upd(:, :, 1)*h_upd(1,:)' ;
getq(counter,:,4)=A_upd(:, :, 4)*h_upd(4,:)' ;

```

```

        getq(counter, :, 6)=A_upd(:, :, 6)*h_upd(6, :)' ;
        getq(counter, :, 7)=A_upd(:, :, 7)*h_upd(7, :)' ;

    Qinit(2)];
        getQ(counter, :, 1)=[Qinit(1)      Qinit(2)].*getq(counter, :, 1)+[Qinit(1)
    Qinit(4)];
        getQ(counter, :, 4)=[Qinit(2)      Qinit(4)].*getq(counter, :, 2)+[Qinit(2)
    Qinit(6)];
        getQ(counter, :, 6)=[Qinit(5)      Qinit(6)].*getq(counter, :, 3)+[Qinit(5)
    Qinit(7)];
        getQ(counter, :, 7)=[Qinit(6)      Qinit(7)].*getq(counter, :, 4)+[Qinit(6)

    case 'complex'

        h=A\q;
        dampingfactor(counter)=K(1);
        dampingfactor2(counter)=K(9);
        switch response_type
            case {'n/nref', 'original'}
                nspeed(counter)=h(11); % measuring point n
            case {'p/pref', 'p/y'}
                nspeed(counter)=h(12); % measuring point p
            case 'h/y'
                nspeed(counter)=h(10); % measurement point at 6
        end

        frequency(counter)=omega(counter);

        % get the updated flow rates

        h_upd=ones(length(L), 2);
        A_upd=ones(2, 2, length(L));

        h_upd(1, :)= [h(1) h(7)];
        A_upd(:, :, 1)= [-T(1) S(1);
            S(1) -T(1)];
        h_upd(5, :)= [h(5) h(8)];
        A_upd(:, :, 5)= [-T(5) S(5);
            S(5) -T(5)];
        h_upd(9, :)= [h(8) h(9)];
        A_upd(:, :, 9)= [-T(9) S(9);
            S(9) -T(9)];
        h_upd(7, :)= [h(6) h(7)];
        A_upd(:, :, 12)= [-T(7) S(7);
            S(7) -T(7)];

        getq(counter, :, 1)=A_upd(:, :, 1)*h_upd(1, :)' ;
        getq(counter, :, 2)=A_upd(:, :, 5)*h_upd(5, :)' ;
        getq(counter, :, 3)=A_upd(:, :, 9)*h_upd(9, :)' ;
        getq(counter, :, 4)=A_upd(:, :, 12)*h_upd(12, :)' ;

    Qinit(7)];
        getQ(counter, :, 1)=[Qinit(1)      Qinit(7)].*getq(counter, :, 1)+[Qinit(1)
    Qinit(8)];
        getQ(counter, :, 5)=[Qinit(5)      Qinit(8)].*getq(counter, :, 2)+[Qinit(5)
    Qinit(11)];
        getQ(counter, :, 9)=[Qinit(10)     Qinit(11)].*getq(counter, :, 3)+[Qinit(10)
    Qinit(9)];
        getQ(counter, :, 7)=[Qinit(8)      Qinit(9)].*getq(counter, :, 4)+[Qinit(8)

    end

    x=10^-3:1:10^1;
    y1=zeros(1, length(x));
    y2=-ones(1, length(x)).*180;
    end

    %%%%%%%%%%%%%%%%%%%%%%%%%%%%%%%%%%%%%%%%%%%%%%%%%%%%%%%%%%%%%%%%%%%%%%%%%%% gain and phase values %%%%%%%%%%%%%%%%%%%%%%%%%%%%%%%%%%%%%%%%%%%%%%%%%%%%%%%%%%%%%%%%%%%%%%%%%%%

```

```

R9(:,count) = db(abs(nspeed)); %Gain
in dB (20*log(abs(nspeed))
switch angle_handling
%adjustment for Matlabs handling of angles

    case 'unwrap'
        theta9(:,count) = (180/pi)*unwrap(angle(nspeed)); %get phase
angle in degrees

    case 'unwrap_upper'
        for index=1:countvalue/2
            theta9(index,count) = (180/pi)*(angle(nspeed(index)));
%get phase angle in degrees
        end
        for index=countvalue/2:countvalue
            theta9(index,count) = (180/pi)*unwrap(angle(nspeed(index)));
%get phase angle in degrees
        end

    case 'plain'
        theta9(:,count) = (180/pi)*(angle(nspeed));

end
theta9(:,count) = theta9(:,count)+angleadjustment;
%%%%%%%%%%%%%%%%%%%%%%%%%%%%%%%%%%%%%%%%%%%%%%%%%%%%%%%%%%%%%%%%%%%%%%%%

%%%%%%%%%%%%%%%%%%%%%%%%%%%%%%%%%%%%%%%%%%%%%%%%%%%%%%%%%%%%%%%%%%%%%%%% Find gain and phase margins%%%%%%%%%%%%%%%%%%%%%%%%%%%%%%%%%%%%%%%%%%%%%%%%%%%%%%%%%%%%%%%%%%%%%%%%
[valueR9, index_phasemarg] = min(abs(R9(2:end,count)));
[valuetheta9, index_gainmarg] = min(abs(theta9(2:end,count)+180));

if min(theta9(2:end,count)+180)<0 && max(theta9(2:end,count)+180)>0
    gainmargin(count)=-R9(index_gainmarg,count);
else
    gainmargin(count)=NaN;
end

if min(R9(2:end,count))<0 && max(R9(2:end,count))>0
    phasemargin(count)=180+theta9(index_phasemarg,count);
else
    phasemargin(count)=NaN;
end
%%%%%%%%%%%%%%%%%%%%%%%%%%%%%%%%%%%%%%%%%%%%%%%%%%%%%%%%%%%%%%%%%%%%%%%%

end

close(hwbar)

%PLOTS
switch response_type
case 'original'
    %BODE PLOT
    figure(1)
    subplot(2,1,1)

semilogx(frequency,R9(:,1),'b',frequency,R9(:,2),'g',frequency,R9(:,3),'r','LineWidth',2)

    hold on;
    plot(x,y1,'black'),grid;
    set(get(1,'CurrentAxes'),'YTick',[-200 -150 -100 -50 0 50 100 150 200])
    set(get(1,'CurrentAxes'),'YLim',[-200 200])
    title([' Kn=', num2str(Kn), ', b_p=', num2str(bp), ', KI=', num2str(KI), ',
b_t=', num2str(bt), ', T_d=', num2str(Td), ', T_p=', num2str(Tp)], 'FontSize',16)
    legend1=legend([' K_P=', num2str(value(1))], [' K_P=', num2str(value(2))], ['
K_P=', num2str(value(3))]);
    set(legend1,'Location','NorthEast')
    ylabel('Gain(dB)', 'FontSize',16)
    subplot(2,1,2)

```

```

semilogx(frequency, theta9(:,1), 'b', frequency, theta9(:,2), 'g', frequency, theta9(:,3),
'r', 'LineWidth',2), grid;
    set(get(1, 'CurrentAxes'), 'YTick', [-270 -225 -180 -135 -90 -45 0 90])
    set(get(1, 'CurrentAxes'), 'YLim', [-270 90])
    legend1=legend([' K_P=', num2str(value(1))], [' K_P=', num2str(value(2))], ['
K_P=', num2str(value(3))]);
    set(legend1, 'Location', 'NorthEast')
    hold on;
    plot(x, y2, 'black')
    ylabel('Phase(deg)', 'FontSize', 16)

%NICHOLS PLOT
figure(2)
% hold on;

plot(theta9(:,1), R9(:,1), 'b', theta9(:,2), R9(:,2), 'g', theta9(:,3), R9(:,3), 'r')
ngrid
hold on;
title([' Kn=', num2str(Kn), ', b_p=', num2str(bp), ', KI=', num2str(KI), ',
b_t=', num2str(bt), ', T_d=', num2str(Td), ', T_p=', num2str(Tp)])
    legend2=legend([' K_P=', num2str(value(1))], [' K_P=', num2str(value(2))], ['
K_P=', num2str(value(3))]);
    set(legend2, 'Location', 'SouthEast')
    xlabel('Phase(deg)', 'FontSize', 16)
    ylabel('Gain(dB)', 'FontSize', 16)

case 'n/nref'
%BODE PLOT
figure(1)
subplot(2,1,1)

semilogx(frequency, R9(:,1), 'b', frequency, R9(:,2), 'g', frequency, R9(:,3), 'r', 'LineWid
th', 2)
    hold on;
    plot(x, y1, 'black'), grid;
    set(get(1, 'CurrentAxes'), 'YTick', [-200 -150 -100 -50 0 50 100 150 200])
    set(get(1, 'CurrentAxes'), 'YLim', [-200 200])
    title(['Plant: ', num2str(system_geometry), ' Turbine:
', num2str(turbine), ' (n/nref response)']; [' Kn=', num2str(Kn), ',
b_p=', num2str(bp), ', KI=', num2str(KI), ', b_t=', num2str(bt), ', T_d=', num2str(Td), ',
T_p=', num2str(Tp)]), 'FontWeight', 'bold', 'FontSize', 10)
    legend1=legend([' ed=', num2str(value(1)), ',
\DeltaK=', num2str(gainmargin(1))], [' ed=', num2str(value(2))
\DeltaK=', num2str(gainmargin(2))], [' ed=', num2str(value(3))
\DeltaK=', num2str(gainmargin(3))]);
    set(legend1, 'Location', 'Northeast')
    ylabel('Gain(dB)', 'FontSize', 16)
    subplot(2,1,2)

semilogx(frequency, theta9(:,1), 'b', frequency, theta9(:,2), 'g', frequency, theta9(:,3),
'r', 'LineWidth',2), grid;
    set(get(1, 'CurrentAxes'), 'YTick', [-360 -270 -225 -180 -135 -90 -45 0])
    set(get(1, 'CurrentAxes'), 'YLim', [-360 0])
    legend1=legend([' ed=', num2str(value(1)), ',
\Psi=', num2str(phasemargin(1))], [' ed=', num2str(value(2))
\Psi=', num2str(phasemargin(2))], [' ed=', num2str(value(3))
\Psi=', num2str(phasemargin(3))]);
    set(legend1, 'Location', 'NorthEast')
    pmargin=legend([' \Psi=', num2str(phasemargin(1))], ['
\Psi=', num2str(phasemargin(2))], [' \Psi=', num2str(phasemargin(3))]);
    set(pmargin, 'Location', 'SouthEast')
    hold on;
    plot(x, y2, 'black')
    ylabel('Phase(deg)', 'FontSize', 16)

%NICHOLS PLOT
figure(2)

```

```

plot(theta9(:,1),R9(:,1),'b',theta9(:,2),R9(:,2),'g',theta9(:,3),R9(:,3),'r')
    ngrid
    hold on;
    title([' Kn=', num2str(Kn), ', b_p=', num2str(bp), ', KI=', num2str(KI), ',
b_t=', num2str(bt), ', T_d=', num2str(Td), ', T_p=', num2str(Tp)])
    legend2=legend([' K_P=', num2str(value(1))], [' K_P=', num2str(value(2))], ['
K_P=', num2str(value(3))]);
    set(legend2, 'Location', 'SouthEast')
    xlabel('Phase(deg)', 'FontSize', 16)
    ylabel('Gain(dB)', 'FontSize', 16)
    hold off;

%FRICTIONAL DAMPING PLOT

figure(3)
semilogx(frequency, dampingfactor, 'b')
hold on;
semilogx(frequency, dampingfactorreal, '--r')
hold on;
semilogx(frequency, dampingfactorimag, '--g')
title('Frictional damping, K', 'FontWeight', 'bold', 'FontSize', 16)
xlabel('Frequency, Hz', 'FontSize', 16)
ylabel('Frictional damping', 'FontSize', 16)
legend1=legend(' Total', 'Real', 'Imaginary', 'FontSize', 8);
set(legend1, 'Location', 'NorthEast')
hold off;

case 'p/pref'
%BODE PLOT
figure(1)
subplot(2,1,1)

semilogx(frequency, R9(:,1), 'b', frequency, R9(:,2), 'g', frequency, R9(:,3), 'r', 'LineWidth', 2)
    hold on;
    plot(x, y1, 'black'), grid;
    set(get(1, 'CurrentAxes'), 'YTick', [-200 -150 -100 -50 0 50 100 150 200])
    set(get(1, 'CurrentAxes'), 'YLim', [-200 200])
    title(['Plant: ', num2str(system_geometry), ' Turbine: ', num2str(turbine), '
(p/pref response)']); [' K_n=', num2str(Kn), '
b_p=', num2str(bp), ', KI=', num2str(KI), ', b_t=', num2str(bt), ', T_d=', num2str(Td), ',
T_p=', num2str(Tp)], 'FontWeight', 'bold', 'FontSize', 10)
    %legend1=legend([' ed=', num2str(value(1))], ['
\DeltaK=', num2str(gainmargin(1))], [' ed=', num2str(value(2))
\DeltaK=', num2str(gainmargin(2))], [' ed=', num2str(value(3))
\DeltaK=', num2str(gainmargin(3))], 'FontSize', 8);
    %set(legend1, 'Location', 'Northeast')
    ylabel('Gain(dB)', 'FontSize', 16)
    subplot(2,1,2)

semilogx(frequency, theta9(:,1), 'b', frequency, theta9(:,2), 'g', frequency, theta9(:,3),
'r', 'LineWidth', 2), grid;
    set(get(1, 'CurrentAxes'), 'YTick', [-270 -225 -180 -135 -90 -45 0 90])
    set(get(1, 'CurrentAxes'), 'YLim', [-270 90])
    %legend1=legend([' ed=', num2str(value(1))], ['
\Psi=', num2str(phasemargin(1))], [' ed=', num2str(value(2))
\Psi=', num2str(phasemargin(2))], [' ed=', num2str(value(3))
\Psi=', num2str(phasemargin(3))], 'FontSize', 8);
    %set(legend1, 'Location', 'NorthEast')
    hold on;
    plot(x, y2, 'black')
    ylabel('Phase(deg)', 'FontSize', 16)

figure(2)
semilogx(frequency, abs(dampingfactor), 'b')
title('Frictional damping, K', 'FontWeight', 'bold', 'FontSize', 16)

```

```

xlabel('Frequency, Hz','FontSize',16)
ylabel('Frictional damping','FontSize',16)
hold off;

figure(3)
semilogx(frequency(20:1000),abs(dampingfactor2(20:1000)),'b')
title('Frictional damping at downstream surge shaft,
K','FontWeight','bold','FontSize',16)
xlabel('Frequency, Hz','FontSize',16)
ylabel('Frictional damping','FontSize',16)
hold off;

case 'p/y'
%BODE PLOT
figure(1)
subplot(2,1,1)

semilogx(frequency,R9(:,1),'b',frequency,R9(:,2),'g',frequency,R9(:,3),'r','LineWidth',2)

hold on;
plot(x,y1,'black'),grid;
set(get(1,'CurrentAxes'),'YTick',[-200 -150 -100 -50 0 50 100 150 200])
set(get(1,'CurrentAxes'),'YLim',[-200 200])
title({'Plant: ',num2str(system_geometry),' Turbine: ',num2str(turbine),'
(p/y response)'}; [' Kn=', num2str(Kn),'
b_p=',num2str(bp),' KI=',num2str(KI),' b_t=',num2str(bt),' T_d=',num2str(Td),'
T_p=',num2str(Tp)]},'FontWeight','bold','FontSize',10)
legend1=legend([' ed=',num2str(value(1))','
\DeltaK=',num2str(gainmargin(1))],[ ' ed=',num2str(value(2))
\DeltaK=',num2str(gainmargin(2))],[ ' ed=',num2str(value(3))
\DeltaK=',num2str(gainmargin(3))]');
set(legend1,'Location','Northeast','FontSize',8)
ylabel('Gain(dB)','FontSize',16)
subplot(2,1,2)

semilogx(frequency,theta9(:,1),'b',frequency,theta9(:,2),'g',frequency,theta9(:,3),
'r','LineWidth',2), grid;
set(get(1,'CurrentAxes'),'YTick',[-270 -225 -180 -135 -90 -45 0 90])
set(get(1,'CurrentAxes'),'YLim',[-270 90])
legend1=legend([' ed=',num2str(value(1))','
\DeltaPsi=',num2str(phasemargin(1))],[ ' ed=',num2str(value(2))
\DeltaPsi=',num2str(phasemargin(2))],[ ' ed=',num2str(value(3))
\DeltaPsi=',num2str(phasemargin(3))]');
set(legend1,'Location','NorthEast','FontSize',8)
hold on;
plot(x,y2,'black')
ylabel('Phase(deg)','FontSize',16)

figure(2)
semilogx(frequency,dampingfactor,'b')
title('Frictional damping, K','FontWeight','bold','FontSize',16)
xlabel('Frequency, Hz','FontSize',16)
ylabel('Frictional damping','FontSize',16)
hold off;

case 'h/y'
%BODE PLOT
figure(1)
subplot(2,1,1)

semilogx(frequency,R9(:,1),'b',frequency,R9(:,2),'g',frequency,R9(:,3),'r','LineWidth',2)

hold on;
plot(x,y1,'black'),grid;
hold on;
set(get(1,'CurrentAxes'),'YTick',[-200 -150 -100 -50 0 50 100 150 200])
set(get(1,'CurrentAxes'),'YLim',[-200 200])

```



```

        title(['Plant:          ', num2str(system_geometry), '          Turbine:
', num2str(turbine), '          (h/y response)']; ['   Kn=', num2str(Kn), ',
b_p=', num2str(bp), ',   KI=', num2str(KI), ',   b_t=', num2str(bt), ',   T_d=', num2str(Td), ',
T_p=', num2str(Tp)]), 'FontSize', 'bold', 'FontSize', 10)
        legend1=legend(['          ed=', num2str(value(1)), ',
\DeltaK=', num2str(gainmargin(1))], ['          ed=', num2str(value(2))
\DeltaK=', num2str(gainmargin(2))], ['          ed=', num2str(value(3))
\DeltaK=', num2str(gainmargin(3))], 'FontSize', 8);
        set(legend1, 'Location', 'Northeast')
        ylabel('Gain (dB)', 'FontSize', 16)
        subplot(2,1,2)

semilogx(frequency, theta9(:,1), 'b', frequency, theta9(:,2), 'g', frequency, theta9(:,3),
'r', 'LineWidth', 2), grid;
        set(get(1, 'CurrentAxes'), 'YTick', [-360 -270 -225 -180 -135 -90 -45 0])
        set(get(1, 'CurrentAxes'), 'YLim', [-360 90])
        legend1=legend(['          ed=', num2str(value(1)), ',
\Psi=', num2str(phasemargin(1))], ['          ed=', num2str(value(2))
\Psi=', num2str(phasemargin(2))], ['          ed=', num2str(value(3))
\Psi=', num2str(phasemargin(3))], 'FontSize', 8);
        set(legend1, 'Location', 'NorthEast')
        hold on;
        plot(x, y2, 'black')
        ylabel('Phase (deg)', 'FontSize', 16)

figure(2)
subplot(2,2,[1 3])
semilogx(frequency, dampingfactor, 'b')
hold on;
semilogx(frequency, dampingfactorreal, '--r')
hold on;
semilogx(frequency, dampingfactorimag, '--g')
set(get(1, 'CurrentAxes'), 'XLim', [10^-3 10^1])
title('Head race channel', 'FontWeight', 'bold', 'FontSize', 16)
xlabel('Frequency, Hz', 'FontSize', 16)
ylabel('Frictional damping', 'FontSize', 16)
legend1=legend(' Total', 'Real', 'Imaginary', 'FontSize', 16);
set(legend1, 'Location', 'NorthWest')

subplot(2,2,[2 4])
semilogx(frequency, dampingfactor2, 'b')
hold on;
semilogx(frequency, dampingfactor2real, '--r')
hold on;
semilogx(frequency, dampingfactor2imag, '--g')
set(get(1, 'CurrentAxes'), 'XLim', [10^-3 10^1])
title('Surge shaft channel', 'FontWeight', 'bold', 'FontSize', 16)
xlabel('Frequency, Hz', 'FontSize', 16)
ylabel('Frictional damping', 'FontSize', 16)
legend1=legend(' Total', 'Real', 'Imaginary', 'FontSize', 16);
set(legend1, 'Location', 'NorthWest')
hold off;

end

% legend1=legend(['   b_p=', num2str(value(1))], ['   b_p=', num2str(value(2))], ['
b_p=', num2str(value(3))]);
% set(legend1, 'Location', 'NorthEast')
% hold on;
% plot(x, y2, 'black--')
% ylabel('Phase (deg)')

% Waitbar closing
switch system_geometry
case 'kongsvinger'
switch response_type
case {'p/pref', 'p/y'}
run kongsvinger_freqresponse
end
end

```

```

        case 'tafjord'
            switch response_type
                case {'p/pref', 'p/y', 'h/y'}
                    run tafjord_freqresponse
            end
        end
end

F = findall(0,'type','figure','tag','TMWWaitbar');
delete(F);

```

## damping.m

```

% Find the damping factor
function K = damping(area, ed, Q0,omega,q_previous,friction_model,friction_scaling)
% Input:
% - Ai, Area of each section
% - epsilon/D, Roughness factor for each section
% - Q0, mean reference flow rate
% -

% Output:
% - K, Damping factor

% constants:
g = 9.81;
rho = 1000;
mu = 1.519*10^-3; % at 5 deg
q_previous=abs(q_previous); % |q|

%Variables
D = sqrt(4*area/pi());
Qt = Q0*q_previous;

% Get the friction factor from the Moody diagram:
Reynolds = (rho * Qt * D)/(area * mu);

for Reynolds=NaN
    Reynolds=10^6;
end

% f = 1/(1.8*log10(6.9/Reynolds + (ed/3.7)^1.11))^2;
f=moody(ed,Reynolds);

%%%%%%%%%%%%%%%%%%%%%%%%%%%%%%%%%%%%%%%%%%%%%%%%%%%%%%%%%%%%%%%%%%%%%%%%NO FRICTION MODEL%%%%%%%%%%%%%%%%%%%%%%%%%%%%%%%%%%%%%%%%%%%%%%%%%%%%%%%%%%%%%%%%%%%%%%%%

if friction_model==1

K_I=0;
K_S=0;

End

%%%%%%%%%%%%%%%%%%%%%%%%%%%%%%%%%%%%%%%%%%%%%%%%%%%%%%%%%%%%%%%%%%%%%%%%BROWNS MODEL%%%%%%%%%%%%%%%%%%%%%%%%%%%%%%%%%%%%%%%%%%%%%%%%%%%%%%%%%%%%%%%%%%%%%%%%
% Calculate the damping factors (according to ref. 11)
%friction variable

if friction_model==2

%Define table and interpolate to find frictional value:
Re=[1250 2500 10^4 10^5 10^6 10^7 10^8];
fric_h=[4/3 1.113 1.049 1.020 1.012 1.008 1.000];
fric_var1=interp1(Re,fric_h,Reynolds);

lambda=4*f;

```

```

K_S=friction_scaling*(4*lambda*Qt)/(pi()*D^3);

cut_off=0.01;
if omega<=cut_off
    K_I=0;
else if omega>cut_off
    K_I=friction_scaling*(fric_var1-1);
end
end
K_I=1i*omega*K_I;
End

%%%%%%%%%%%%%%%%%%%%%%%%%%%%%%%%%%%%%%%%%%%%%%%%%%%%%%%%%%%%%%%%%%%%%%%%%%%%%%BREKKES MODEL 1984%%%%%%%%%%%%%%%%%%%%%%%%%%%%%%%%%%%%%%%%%%%%%%%%%%%%%%%%%%%%%%%%%%%%%%%%%%%%%%
% Calculate damping factors (according to ref. 11, eqn 67b):
if friction_model==3
lambda=4*f;

fric_var2=(Q0*q_previous)/(area*D*omega);

if fric_var2<0.1446535
    tau=(2.665-7.3*fric_var2)*rho*sqrt(omega*(mu/rho))*(Q0*q_previous)/area;
else
    tau=0.85*rho*((D*omega)^(1/3))*(sqrt(omega*mu/rho))*(Q0*q_previous/area)^(2/3);
end

K=(4*lambda*Qt)/(pi*D^3) + ((pi*D*tau)/(rho*Q0*q_previous));return

end

%%%%%%%%%%%%%%%%%%%%%%%%%%%%%%%%%%%%%%%%%%%%%%%%%%%%%%%%%%%%%%%%%%%%%%%%%%%%%%BREKKES MODEL 1988%%%%%%%%%%%%%%%%%%%%%%%%%%%%%%%%%%%%%%%%%%%%%%%%%%%%%%%%%%%%%%%%%%%%%%%%%%%%%%
% Calculate damping factors (according to ref. 18):
if friction_model==4
lambda=4*f;

% Nikuradze's roughness:
K_r=sqrt(area/pi)*10^-(((0.5*(lambda^-0.5))-0.86));
fric_var3=(Q0*q_previous)/(area*K_r*omega);

if fric_var3>1.57
    f_d=exp(-5.977)+(5.213*(1/fric_var3)^0.194);
else
    f_d=0.4725/fric_var3;
end
f_d=abs(f_d)*cos(pi/8) + 1i*abs(f_d)*sin(pi/8);

tau_s=(2*lambda*rho*q_previous*Q0^2)/(8*area^2);
K_S=(tau_s*pi*D)/(rho*Q0*q_previous);

tau_d=0.5*f_d*((Q0*q_previous)/area)^2;
K_I=1i*(tau_d*pi*D)/(rho*Q0*q_previous);

end

%%%%%%%%%%%%%%%%%%%%%%%%%%%%%%%%%%%%%%%%%%%%%%%%%%%%%%%%%%%%%%%%%%%%%%%%%%%%%%
K = K_S + K_I;return
end

```

## moody.m

```

function f = moody(ed,Re)
% Input: ed = relative roughness = epsilon/diameter
% Re = Reynolds number
%
% Output: f = friction factor
%
% Note: Laminar and turbulent flow are correctly accounted for

```

```

if Re<0
error(sprintf('Reynolds number = %f cannot be negative',Re));
elseif Re<2000
f = 64/Re; return % laminar flow
end
if ed>0.05
warning(sprintf('epsilon/diameter ratio = %f is not on Moody chart',ed));
end
if Re<4000, warning('Re = %f in transition range',Re); end
% --- Use fzero to find f from Colebrook equation.
% coleFun is an inline function object to evaluate F(f,e/d,Re)
% fzero returns the value of f such that F(f,e/d/Re) = 0 (approximately)
% fi = initial guess from Haaland equation, see White, equation 6.64a
% Iterations of fzero are terminated when f is known to within +/- dfTol
coleFun = inline('1.0/sqrt(f) + 2.0*log10( ed/3.7 + 2.51/( Re*sqrt(f)) )',...
'f','ed','Re');
fi = 1/(1.8*log10(6.9/Re + (ed/3.7)^1.11))^2; % initial guess at f
dfTol = 5e-6;
f = fzero(coleFun,fi,optimset('TolX',dfTol,'Display','off'),ed,Re);
% --- sanity check:
if f<0, error(sprintf('Friction factor = %f, but cannot be negative',f)); end

```

## Appendix B (General Matrix Representation)

### One upstream and one downstream surge shaft

$$\begin{bmatrix}
 -\frac{sH_{02}A_{eqv2}}{Q_{02}} - T_3 & S_3 & 0 & 0 & 0 & 0 & 0 & 0 & 0 \\
 S_3 & -T_1 - T_3 - T_4 & 0 & S_4 & 0 & 0 & 0 & 0 & 0 \\
 0 & 0 & L & -J & J & 0 & 0 & M & K \\
 0 & S_4 & C & -B - T_4 & B & 0 & 0 & 0 & Q \\
 0 & 0 & -C & B & -B - T_6 & S_6 & 0 & 0 & -Q \\
 0 & 0 & 0 & 0 & S_6 & -T_6 - T_7 - T_8 & S_7 & 0 & 0 \\
 0 & 0 & 0 & 0 & 0 & S_7 & -\frac{sH_{09}A_{eqv9}}{Q_{09}} - T_7 & 0 & 0 \\
 0 & 0 & 0 & 0 & 0 & 0 & 0 & 1 & -T_{as} \\
 0 & 0 & F & 0 & 0 & 0 & 0 & 0 & K_n
 \end{bmatrix}
 \cdot
 \begin{bmatrix}
 h_2 \\
 h_4 \\
 y_5 \\
 h_6 \\
 h_7 \\
 h_8 \\
 h_9 \\
 p \\
 n
 \end{bmatrix}
 =
 \begin{bmatrix}
 0 \\
 0 \\
 y_{ref} \\
 0 \\
 0 \\
 0 \\
 0 \\
 p \\
 n_{ref}
 \end{bmatrix}$$



## Appendix C (Turbine Characteristics)

### Turbine\_char\_routine.m

```
%% Turbine characteristics routine:

% Run Rawdataimport.m and import the desired text-file.
% Remember to add the nurbs_toolbox folder to the file path.
%

Ned_value=0.20;
Qed_value=0.15;

%%
% First run "rawdata_import.m" and open "Tokketurbindata.txt"
for ii=3:9
tokke{ii-2,1}=ans{ii};
end
tokke{8,1}=ans{11};

figure(1)
[c,knots]=spline_interpolation(3,tokke{1}(1:end-1,:));
crv{1}=nrbbmak(c',knots);
crv{1}=nrbbreverse(crv{1});
[c,knots]=spline_interpolation(3,tokke{2}(1:end-1,:));
crv{2}=nrbbmak(c',knots);
srf1=nrbbuled(crv{1},crv{2});
nrbbplot(srf1,[50 50])

% % nrbbplot(crv{1},100)
% % nrbbplot(crv{2},100)
% % plot3(tokke{2}(:,1),tokke{2}(:,2),tokke{2}(:,3),'o')

hold on;
[c,knots]=spline_interpolation(3,tokke{3}(1:end-1,:));
crv{3}=nrbbmak(c',knots);
[c,knots]=spline_interpolation(3,tokke{4}(1:end-1,:));
crv{4}=nrbbmak(c',knots);
srf3=nrbbuled(crv{3},crv{4});
nrbbplot(srf3,[50 50])
%
hold on;
srf2=nrbbuled(crv{2},crv{3});
nrbbplot(srf2,[50 50])

hold on;
[c,knots]=spline_interpolation(3,tokke{5}(1:end-1,:));
crv{5}=nrbbmak(c',knots);
crv{5}=nrbbreverse(crv{5});
[c,knots]=spline_interpolation(3,tokke{6}(1:end-1,:));
crv{6}=nrbbmak(c',knots);
crv{6}=nrbbreverse(crv{6});
srf5=nrbbuled(crv{5},crv{6});
nrbbplot(srf5,[50 50])

hold on;
srf4=nrbbuled(crv{4},crv{5});
nrbbplot(srf4,[50 50])

hold on;
[c,knots]=spline_interpolation(3,tokke{7}(1:end-1,:));
crv{7}=nrbbmak(c',knots);
crv{7}=nrbbreverse(crv{7});
[c,knots]=spline_interpolation(3,tokke{8}(1:end-1,:));
crv{8}=nrbbmak(c',knots);
srf7=nrbbuled(crv{7},crv{8});
```

```

nrbplot(srf7,[50 50])

hold on;
srf6=nrb ruled(crv{6},crv{7});
nrbplot(srf6,[50 50])
%%
dline1=nrbderiv(crv{1})
tt = linspace(0.0, 1.0, 100);
[pnt1, jac1] = nrbdeval(crv{1}, dline1, tt);
ind1=searchclosest(fliplr(pnt1(1,:)),Ned_value);
derivative1=jac1(1,ind1)

% for linenumber=1:8
% dline=nrbderiv(crv{1});
% tt = linspace(0.0, 1.0, 100);
% [pnt1, jac1] = nrbdeval(crv{linenumber}, dline, tt);
% ind=searchclosest(fliplr(pnt1(1,:)),Ned_value);
% derivative(linenumber)=jac1(1,ind);
% end
% derivative
%%
%%%%%%%%dsurface1=nrbderiv(crv{1})

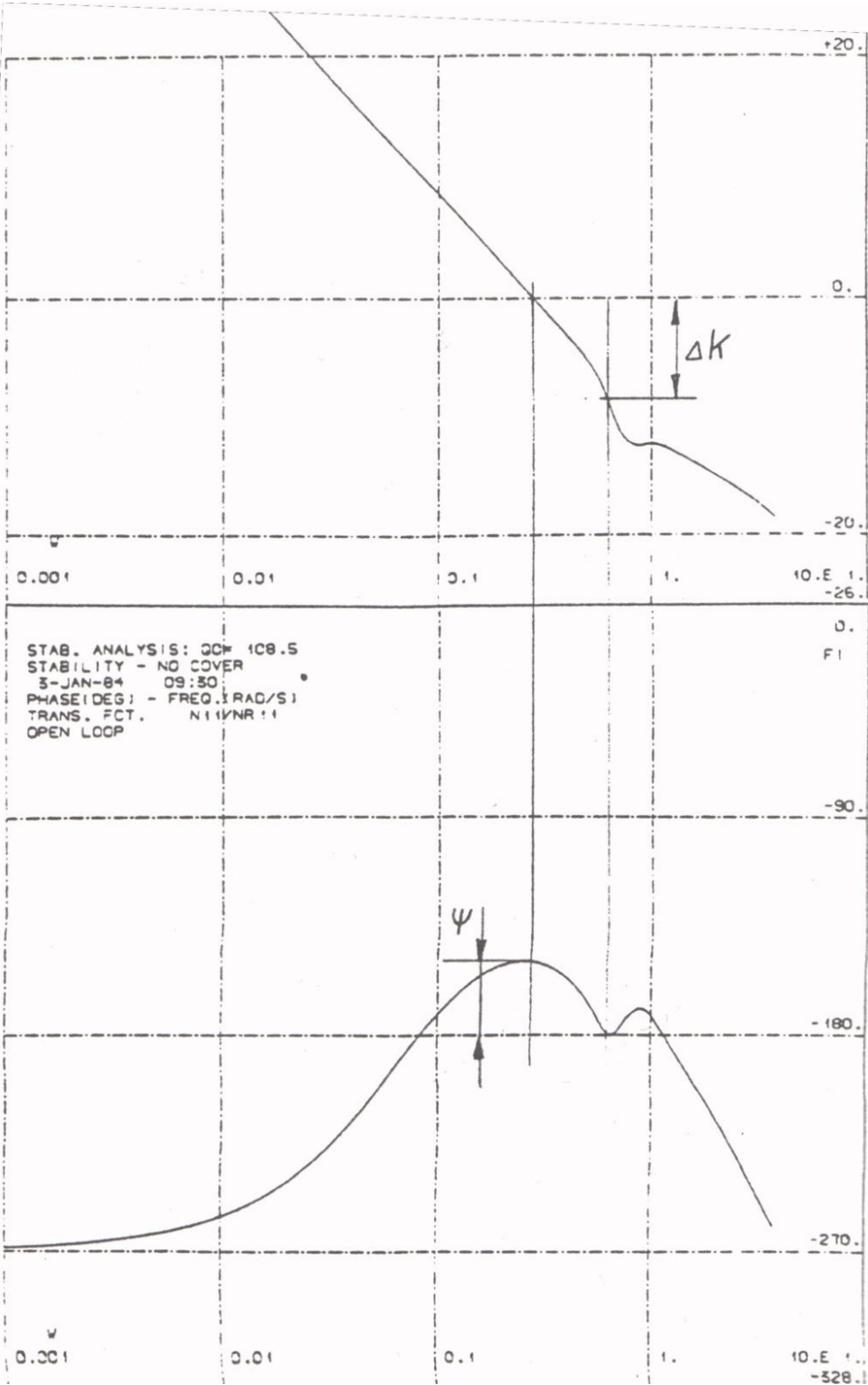
% tt = linspace(0.0, 1.0, 100);
% [pnt1, jac1] = nrbdeval(crv{1}, dline1, tt)
% ind1=searchclosest(fliplr(pnt1(1:)),0.16);
% derivative1=jac1(1,ind1)
%
% Find the first derivative of the relevant operating point:
% tt = linspace(0.0, 1.0, 9);
% dcrv = nrbderiv(crv);
% [pnts,jac] = nrbdeval(crv, dcrv, tt);

```

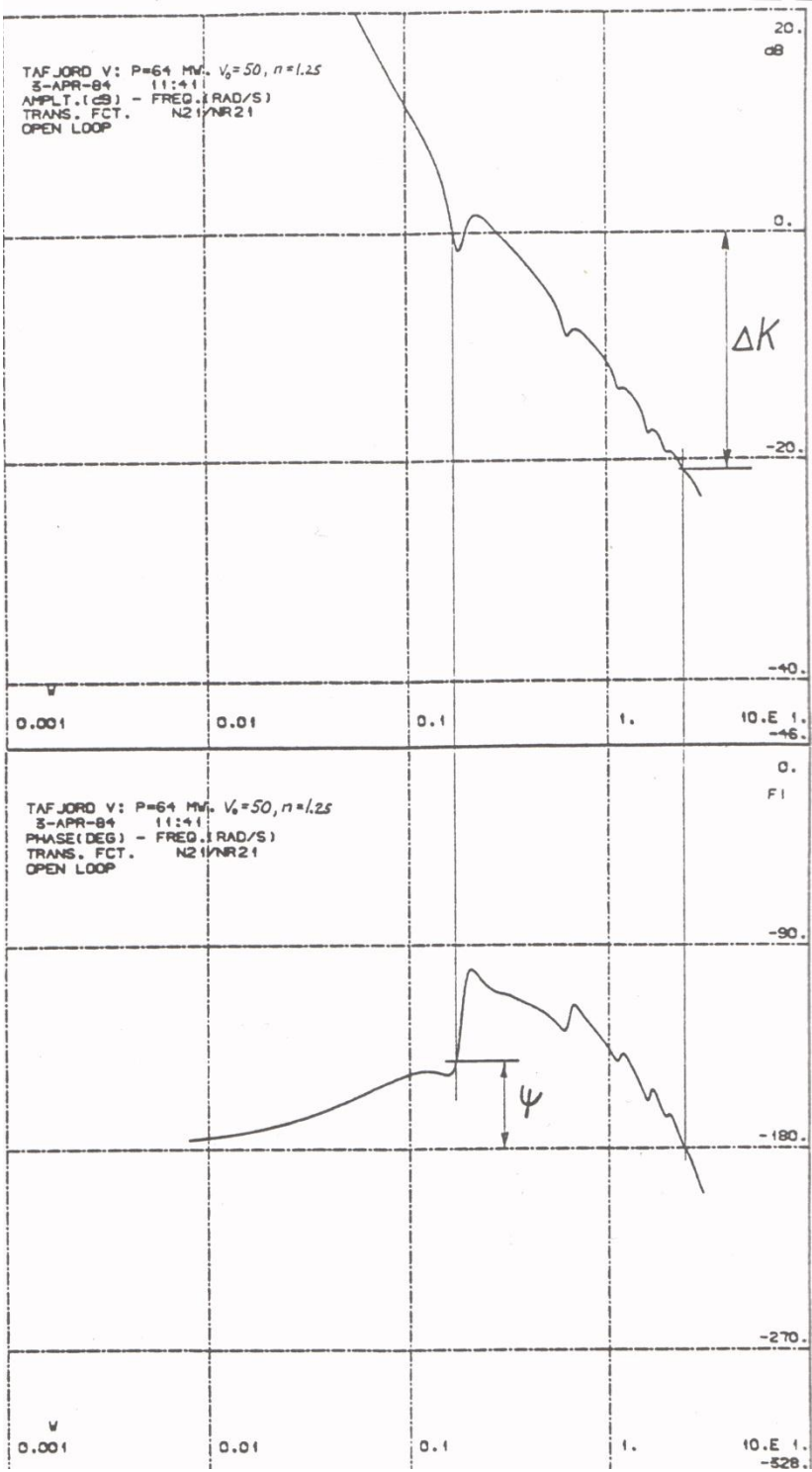


# Appendix D Stability plots

n/nref plot of Kongsvinger power plant as it is presented in (Brekke, 1984, Figure 159f).



n/nref plot of Tafjord power plant as it is presented in (Brekke, 1984, Figure 143f) .



## Appendix E Transfer functions

For a simple hydropower system with an open loop (i.e. D is equal to zero), the transfer function becomes:

$$A(s) = G(s)C(s)I(s) = \frac{1 + T_d s}{b_t T_d s} \cdot \frac{1 - T_w s}{1 + 0.5 T_w s} \cdot \frac{1}{T_a s + b_s}$$

Where:

$$\frac{p}{y} = \frac{1 - T_w s}{1 + 0.5 T_w s}$$

Represents the system, with only a penstock directly from the reservoir to the turbine. If a tunnel and surge tank is included, the water conduits can be represented by (Xinxin, 1989):

$$\frac{p}{y} = \frac{-T_{ws} T_{wt} T_w s^3 + (T_{ws} T_{wt} - K T_{ws} T_w) s^2 + (K T_{ws} - T_{wt} - T_w) s + 1 - K}{0.5 T_{ws} T_{wt} T_w s^3 + (T_{ws} T_{wt} + 0.5 K T_{ws} T_w) s^2 + (K T_{ws} + 0.5 T_{wt} + 0.5 T_w) s + 1 + K/2}$$

Where:

$$T_{ws} = \frac{A_s H_0}{Q_0}$$

$$T_{wt} = \frac{L_t V_0}{g H_0}$$

$$T_w = \frac{1}{g} \sum \frac{L}{A}$$

With Shen's transfer function for water level governor (Xinxin, 1989):

$$A(s) = \frac{(1 + T_d s)(1 + 0.5 T_w s + 0.1 T_r^2 s^2) - b_t T_w T_d s^2}{(b_t T_d s + b_p)(1 + 0.5 T_w s + 0.1 T_r^2 s^2)} \cdot \frac{p}{y} \cdot \frac{1}{T_a s + b_s}$$

The proposed pressure compensator will have the transfer function:

$$A(s) = \frac{(1 + T_d s)(1 + T_2 s)(1 + T_3 s) \cdot p - b_t T_1 T_d s^2 \cdot y}{(b_t T_d s + b_p) \cdot y \cdot (1 + T_2 s)(1 + T_3 s)} \cdot \frac{1}{T_a s + b_s}$$

A Matlab program that calculates the Bode plot, Root locus and Nichols plot of transfer functions was developed by the author and the code is supplied below.

### Hydropowersystem.m

```
governor='self-regulation';
compensator='waterlevel'; %none, araki, waterlevel or pressure
water_conduits='complete'; %penstock or complete
bode=1; %1 for ON, 0 for OFF
rootlocus=0; %1 for ON, 0 for OFF
nichols=0; %1 for ON, 0 for OFF
altbode=0; %1 for ON, 0 for OFF

%CONSTANTS
Q0=35;
H0=198;
A=30;
M=32;
g=9.81;
a=1200;
As=102;
Lt=4470;
V0=Q0/A;
At=0.0083*( (M^2)*A^(5/3) )/H0;

%CALCULATIONS
Tw=Q0/(g*H0)*((660/35)+(50/6.15)+(1191/30)+(201/20)+(150/20));
Tws=(As*H0)/Q0;
Twt=(Lt*V0)/(g*H0);
K=0.00001; %?
Tr=(4/a)*(1191+201+150);
Fn=1;
Td=4.08;
bt=0.544;
Ta=6.5;
bs=0.6; % self-regulation
bp=0.0; % statics
as=As/At;

hw=(Q0*a)/(2*A*g*H0);
hw=Tw/Tr

%%Compensator control parameters:
T1=1;
T2=100;
T3=10;
%% PID regulation tuning (Hagihara et al (1979):
% KP = (4*Ta)/(5*Tw);
% KP/KI=Tw/3;
% KP/KD=3/Tw;

%%Stein empirical regulation formulas:
%PI
% Gain=zeros(10,10);
% Phase=zeros(10,10);
% variable1=1:1:10;
% variable2=0:0.2:2;
```

```

% for counter1=1:length(variable1)
%   for counter2=1:length(variable2)
%     Td=variable1(counter1);%*Tw;
%     bt=variable2(counter2);%*(Tw/Ta);

%PID
% Td=3*Tw;
% TN=0.5*Tw;
% KP=1.5*(Tw/Ta);

switch water_conduits
  case 'penstock'
    p=[-Tw 1];
    y=[0.5*Tw 1];
  case 'complete'
    p=[-Tw*Tws*Twt (Tws*Twt-K*Tws*Tw) (K*Tws-Twt-Tw) 1-K];
    y=[0.5*Tws*Twt*Tw (Tws*Twt-0.5*K*Tws*Tw) (K*Tws-0.5*Twt-0.5*Tw) 1-0.5*K];
end

switch governor
  case 'pi'
    KP=Ta*bt*Td;
    TF_num=(1/KP)*conv([Td 1],[-Tw 1]);
    TF_denom=conv([0.5*Tw 1],[1 0 0]);
  case 'pid'
    TF_num=conv([Td 1],[-Tw 1]);
    TF_denom=conv([0.5*Tw*Ta Ta 0],[bt*Td bp]);
  case 'self-regulation'

    switch compensator
      case 'araki'
        TF_denom=conv([0.5*Tw 1],[Ta Fn]);
      case 'pressure'
        compensator=conv([Td 1],conv(p,conv([T2 1],[T3 1]))) - conv([0
bt*T1*Td 0 0],y);
        TF_num=compensator;
        TF_denom=conv(conv([T2 1],[T3 1]),conv([Ta bs],conv(y,[bt*Td
bp]))));
      case 'waterlevel'
        compensator=conv([Td 1],[0.1*Tr^2 0.5*Tw 1])+[0 bt*Tw*Td 0 0];
        TF_num=conv(compensator,p);
        TF_denom=conv([0.1*Tr^2 0.5*Tw 1],conv([Ta bs],conv(y,[bt*Td
bp]))));
      case 'none'
        TF_num=conv([Td 1],p);
        TF_denom=conv([Ta bs],conv(y,[bt*Td bp]));
    end
end

hd = tf(TF_num,TF_denom);
w=logspace(-3,1,1000);

%%plot
if bode==1
figure(2)
subplot(2,2,[1 3])
[Gm,Pm,Wg,Wp] = margin(hd);
% Gain(counter1,counter2)=db(Gm);
% Phase(counter1,counter2)=Pm;
margin(hd)
hold on;
%N=feedback(hd,1)
% ltiview('step',T)
end

% N=1/(1+hd);

```

```

% % [Closedloop_Gm,Closedloop_Pm,CLWg,CLWp] = margin(N);
% margin(N)
% hold off;
if rootlocus==1
figure (2)
subplot(2,2,4)
rlocus(hd);
hold on;
zero(hd);
% hold off;
end

if nichols==1
figure(4)
nichols(hd)
end
w=logspace(-3,1,1000);
% %%%Alternative plotting algorithm%%
if altbode==1
figure(5)
x=10^-3:1:10^1;
y1=zeros(1,length(x));
y2=-ones(1,length(x)).*180;

subplot(2,1,1)
[amp0 phase0]=bode(TF_num, TF_denom, w);
semilogx(w,20*log10(amp0),'LineWidth',2),grid;
hold on;
plot(x,y1,'black')
set(get(1,'CurrentAxes'),'YTick',[-50 -40 -30 -10 0 10 20 30 40 50 60 70])
set(get(1,'CurrentAxes'),'YLim',[-50 70])
hold on;
ylabel('Magnitude (dB)')
title(['  b_{p}= ',num2str(bp),'  b_{s}= ',num2str(bs)];['T_{w}= ',num2str(Tw),'
T_{a}= ',num2str(Ta),'  T_{d}= ',num2str(Td),'  b_{p}= ',num2str(bp),'  b_{s}=
',num2str(bs),'  b_{t}= ',num2str(bt),'  T_{d}=
',num2str(Td)]),'FontWeight','bold')

N=1/(1+hd);
% [Closedloop_Gm,Closedloop_Pm,CLWg,CLWp] = margin(N);
[amp1 phase1]=bode(N,w);
amp2=zeros(size(w));
semilogx(w,20*log10(amp1(1,:)),'-.r','LineWidth',2)
hold off;

subplot(2,1,2)
semilogx(w,phase0-360,'LineWidth',2),grid
hold on;
plot(x,y2,'black')
set(get(1,'CurrentAxes'),'YTick',[-270 -180 -135 -90 -45 0 90])
set(get(1,'CurrentAxes'),'YLim',[-270 90])
ylabel('Phase (deg)')
end

```

## Appendix F Plots

Some of the plots in the thesis are supplied in full size.

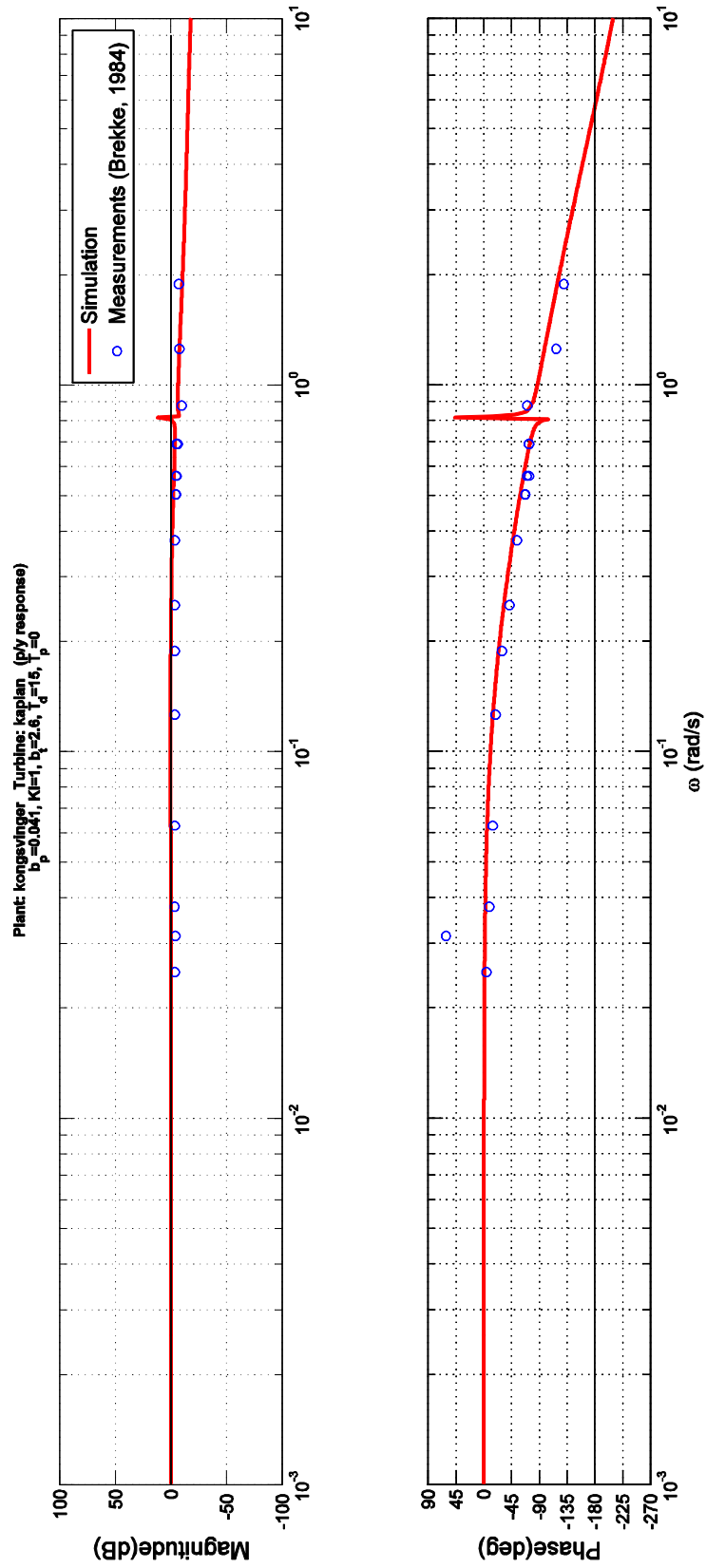


Figure 6.2



Figure 6.4



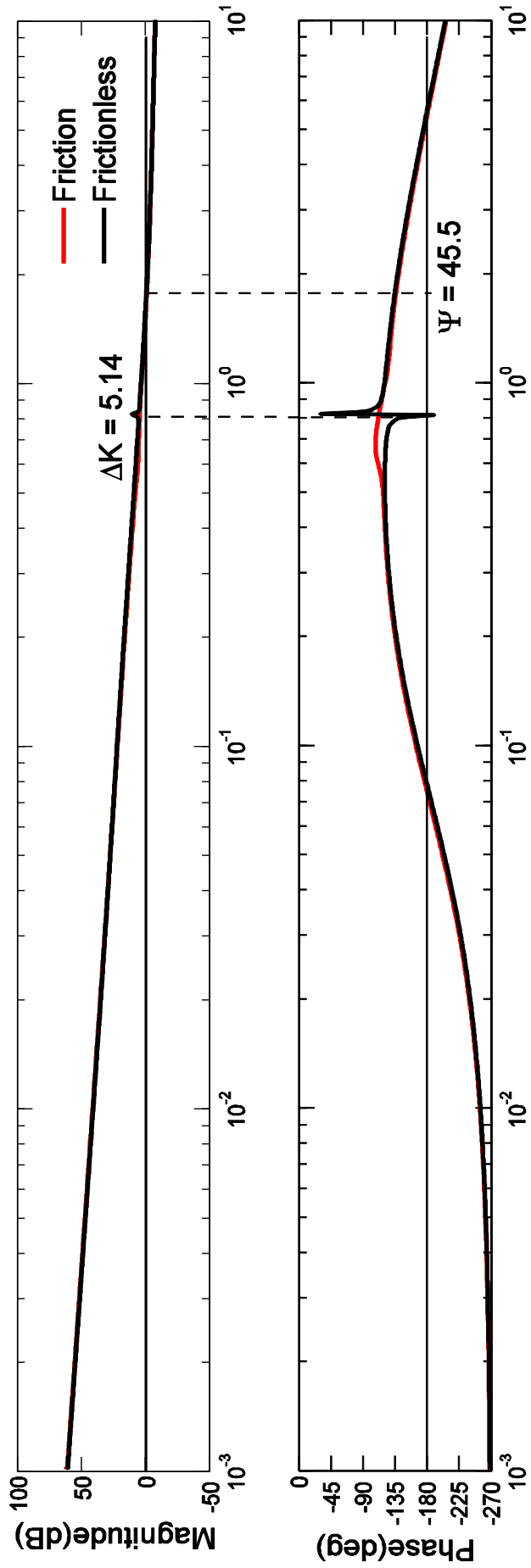


Figure 6.5

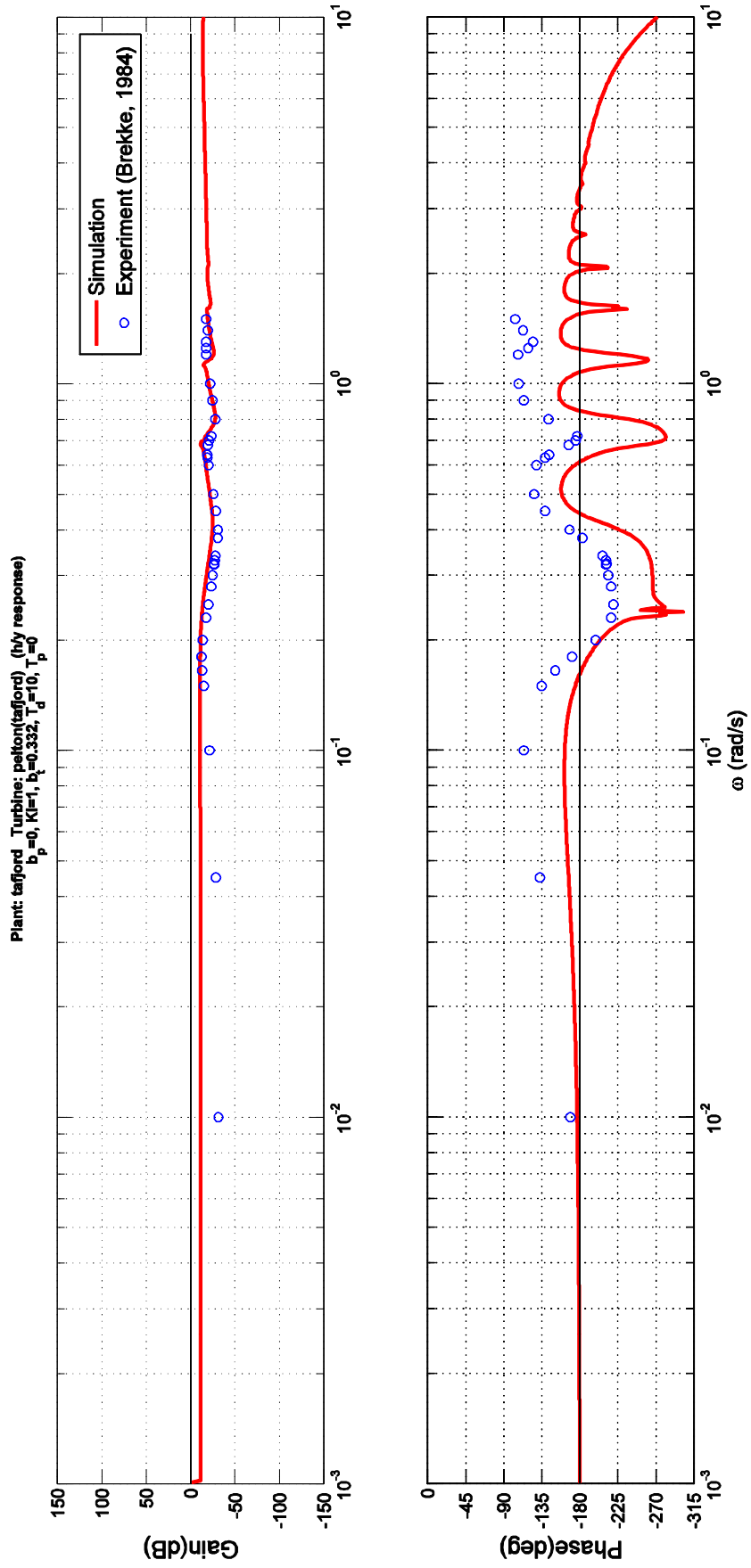


Figure 6.8

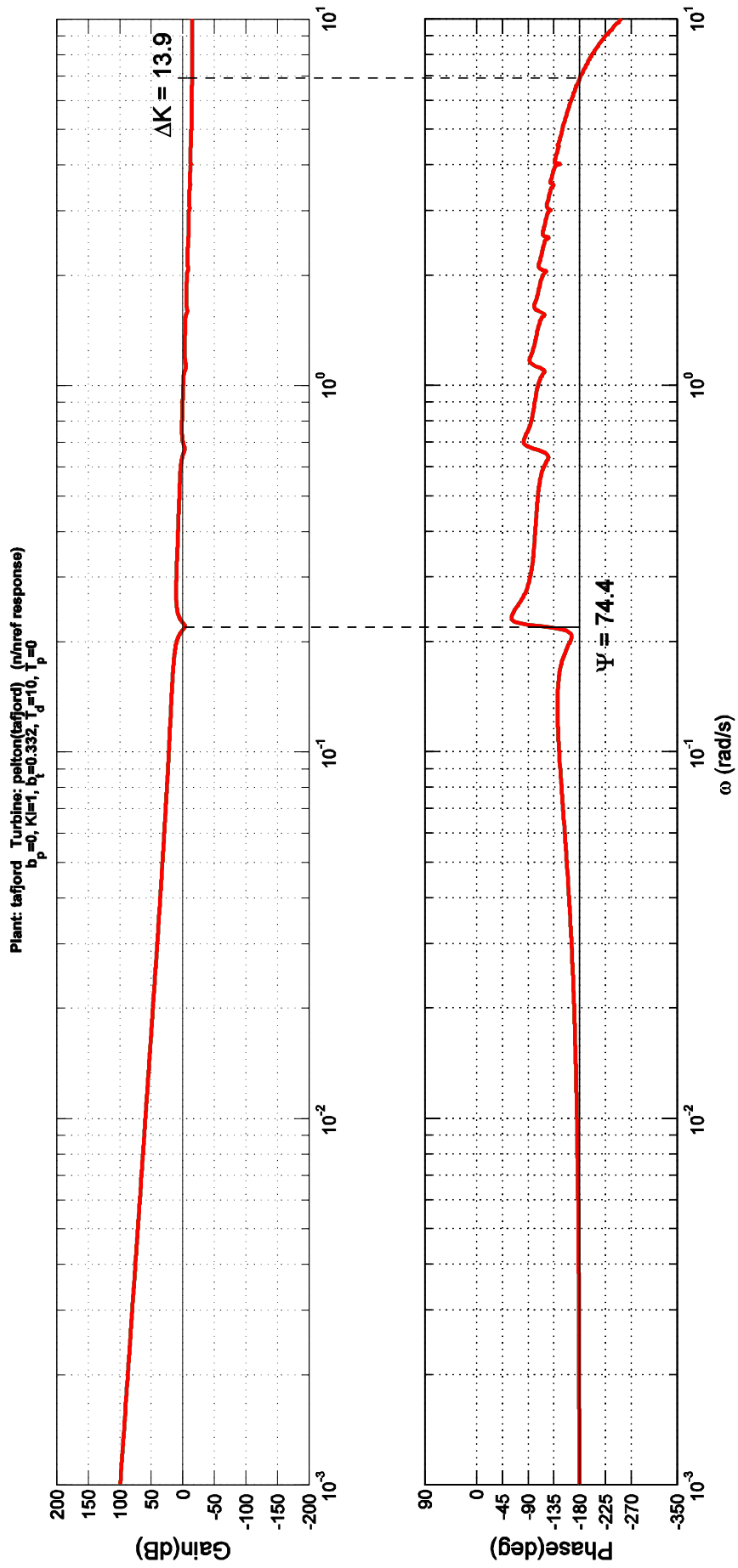


Figure 6.10

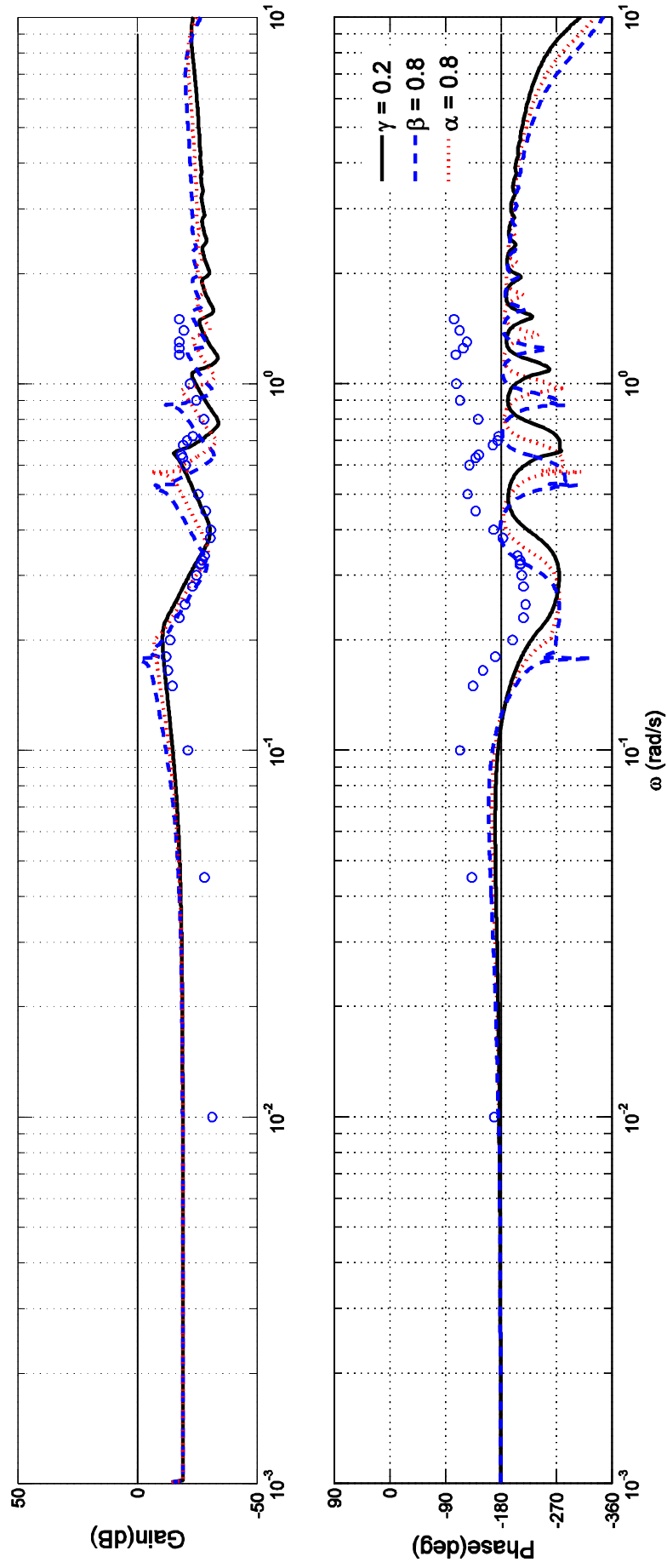


Figure 6.11

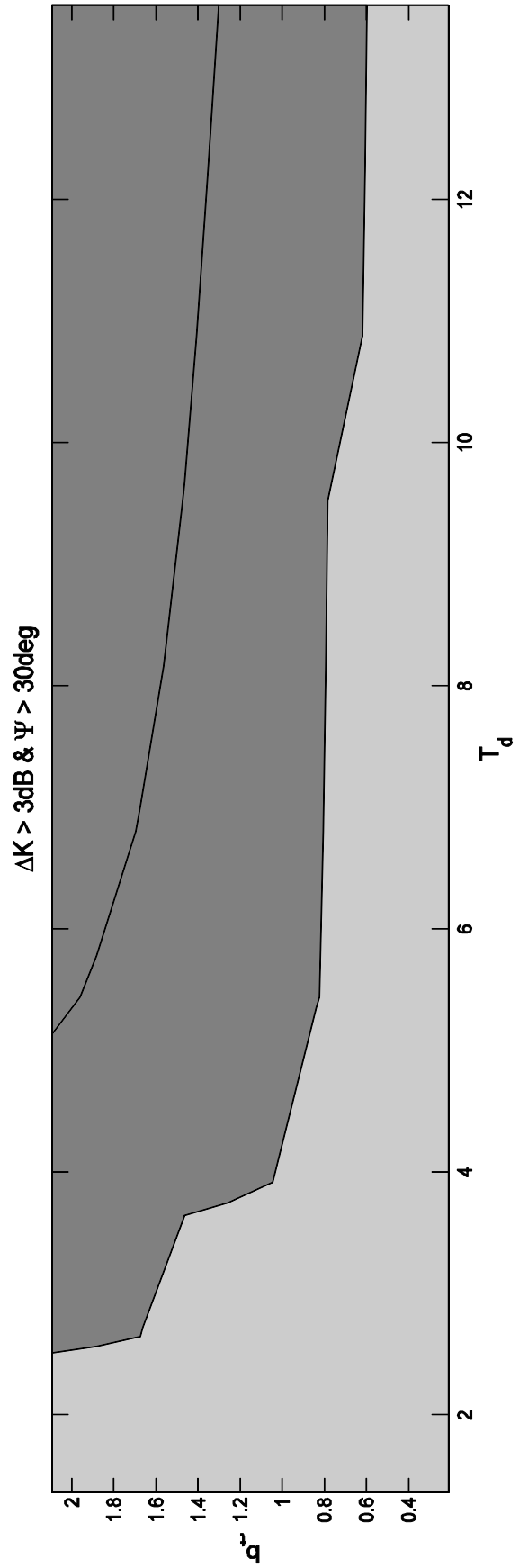
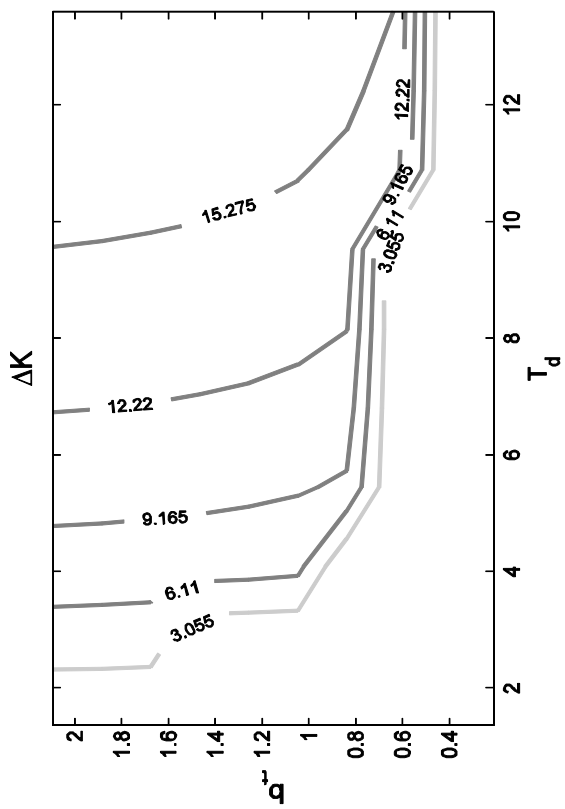
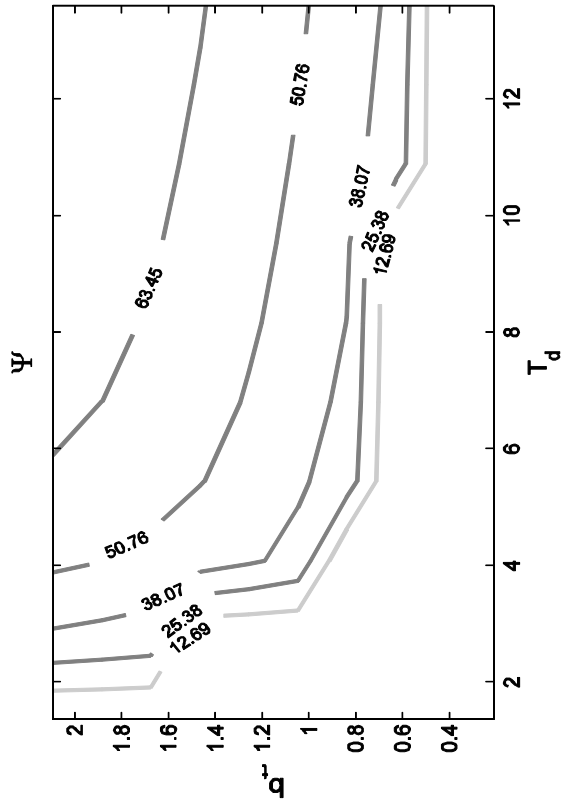


Figure 7.3

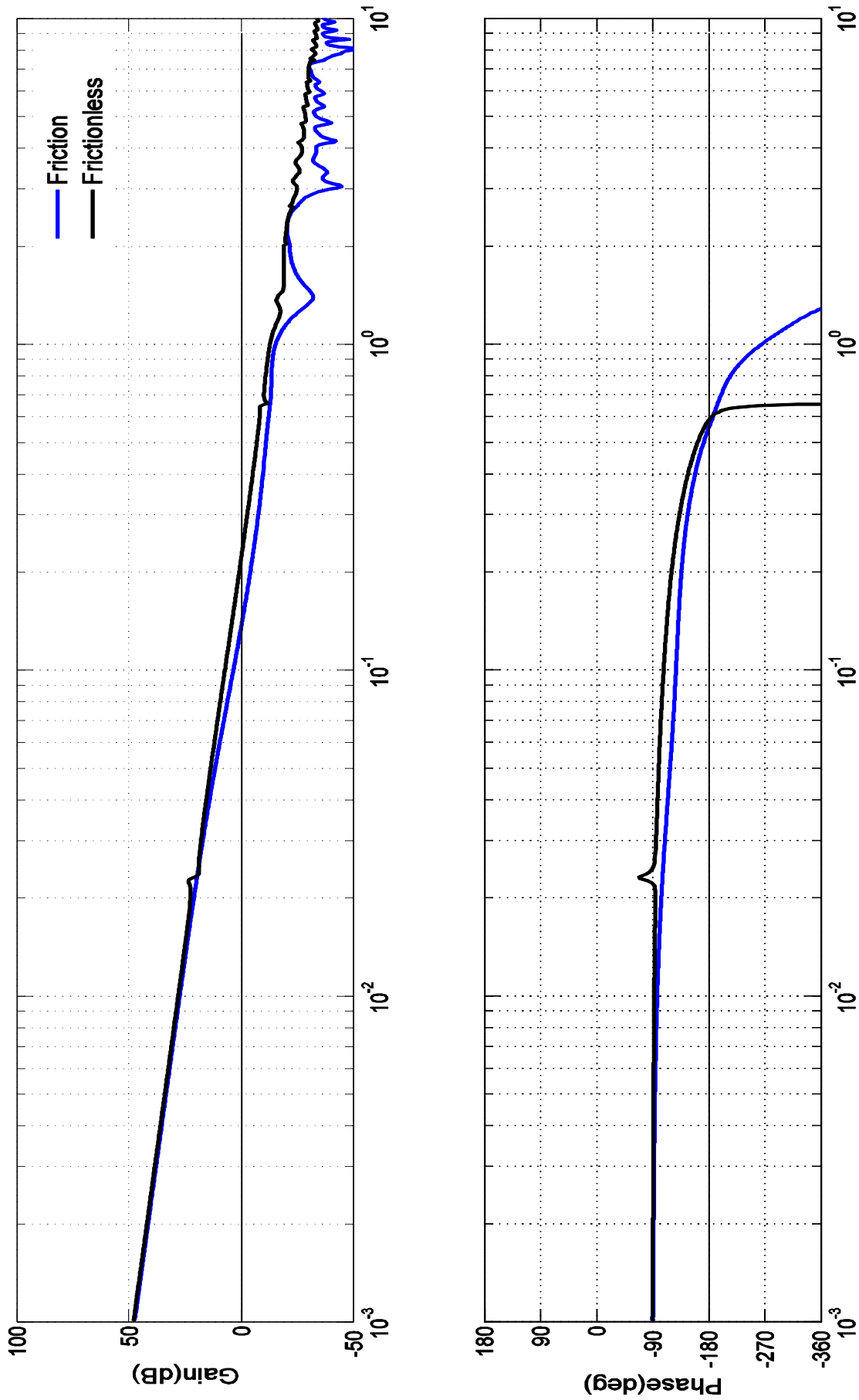


Figure 7.4

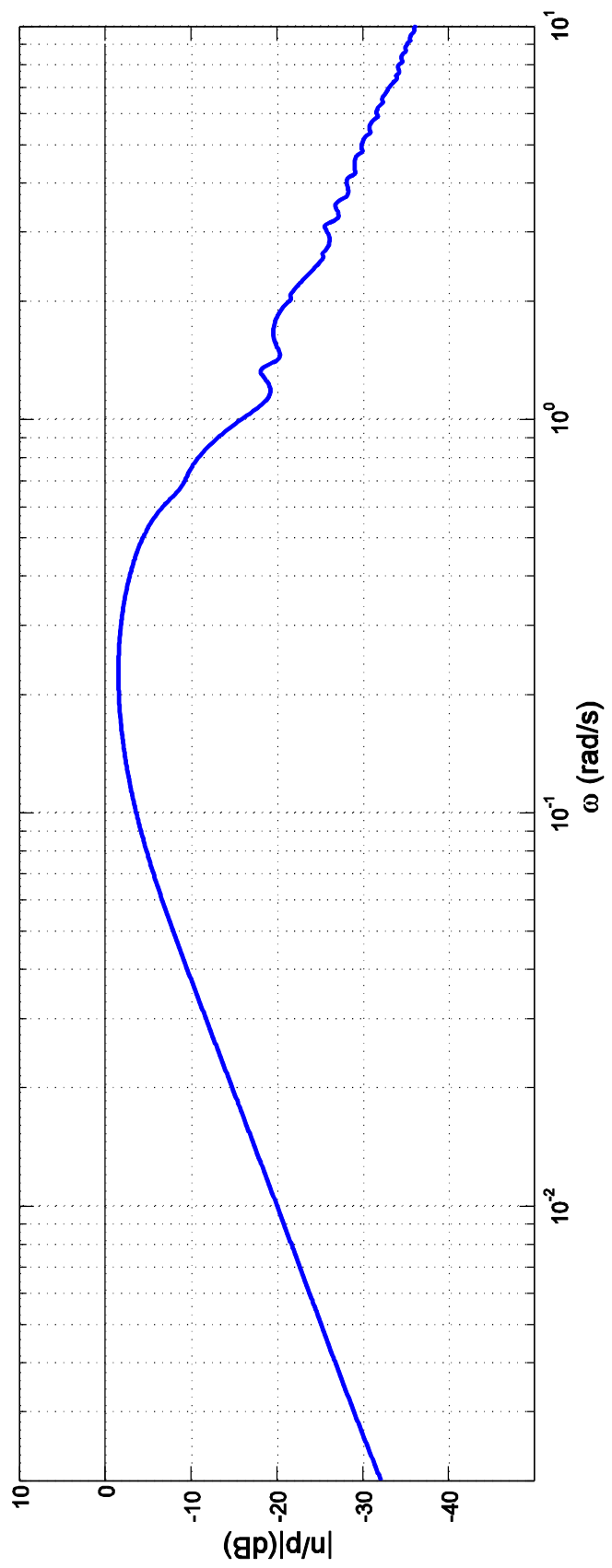


Figure 7.5